Search for the Kaonic Cluster ppK^-

Analysis of the reaction

$p + p \rightarrow p + K^+ + \Lambda$

of HADES and FOPI

Outline

- Introduction
- Exclusive Data Samples
- Phase Space Model Comparison
- Coherent Approach with Partial Wave Analysis
- Upper Limit of ppK^- Contribution
- Summary

K–N Interaction

Kaons in Medium

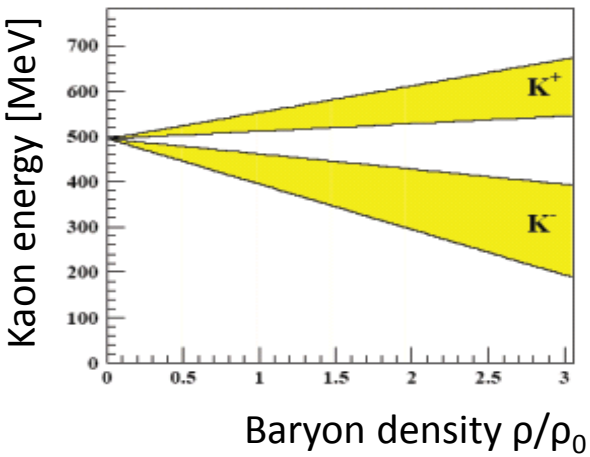

K^+ : Repulsive Interaction

K^- : Attractive Interaction

C. Sturm, Diss. TUD 2001

$\bar{K}$ Spectral Function

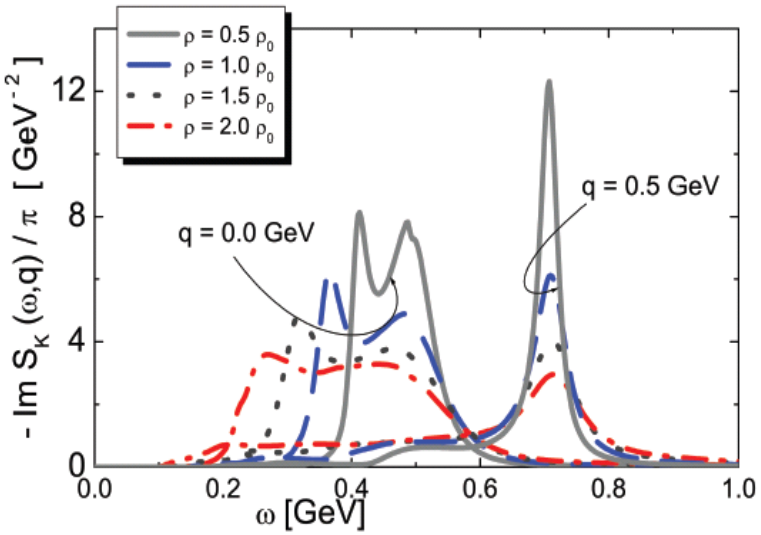

Lutz, Prog.Part.Nucl.Phys, 53 125-136

Coupling of $\bar{K}$ to Resonances

$$\Sigma + \pi \leftrightarrow \Lambda(1405) \leftrightarrow \bar{K} + N$$

$$\Lambda + \pi \leftrightarrow \Sigma(1385) \leftrightarrow \bar{K} + N$$

Resonances close to $\bar{K}$N threshold → Chiral Perturbation cannot be applied

Coupled Channel Calculation

Self Consistent Bethe-Salpeter Equation

$$T_{ij}(\sqrt{s}) = V_{ij}(\sqrt{s}) + V_{il}(\sqrt{s})G_l(\sqrt{s})T_{lj}(\sqrt{s})$$

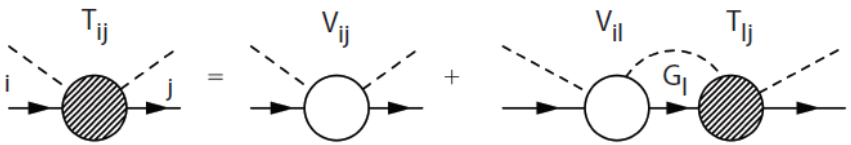

T.Hyodo,W.Weise,Phys.Rev.C77 (2008)

Chiral Potential

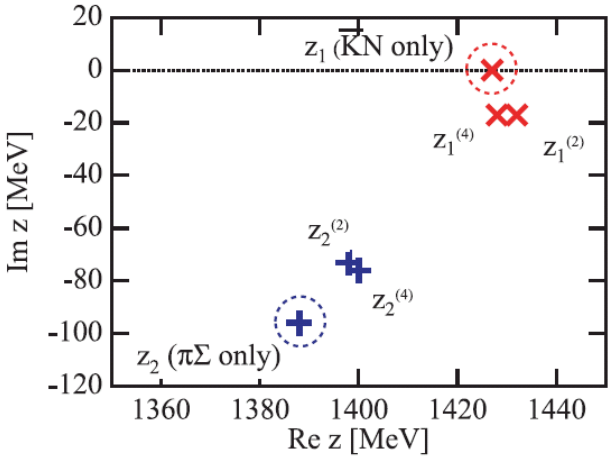

T.Hyodo,W.Weise,Phys.Rev.C77 (2008)

Phenomenological Potential

Quasi bound state of K^-p
via attractive I=0 interaction

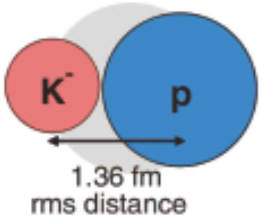

J. Esmaili, Y.Akaishi, T. Yamazaki Phys.Lett. B 686,23
J. Esmaili, Y.Akaishi, T. Yamazaki Phys.Rev. C 83

Kaonic Cluster

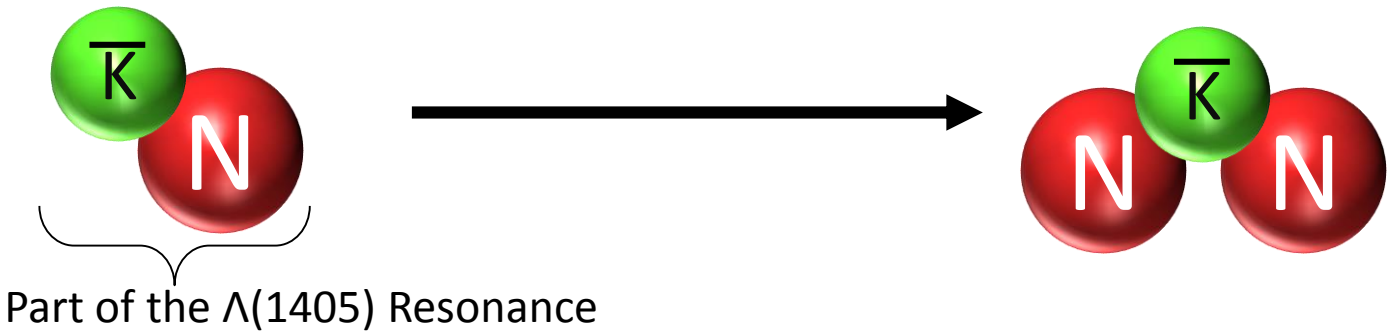

Part of the Λ(1405) Resonance

Kaonic Cluster

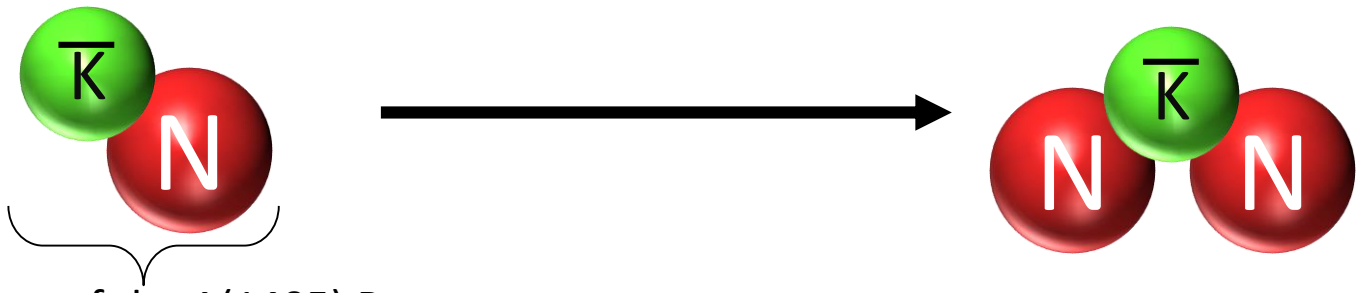

Part of the Λ(1405) Resonance

Theoretical Predictions

	Chiral, energy dependent				
	var. [DHW09, DHW08]	Fad. [BO12b, BO12a]	var. [BGL12]	Fad. [IKS10]	Fad. [RS14]
BE	17–23	26–35	16	9–16	32
Γ_m	40–70	50	41	34–46	49
Γ_{nm}	4–12	30			
	Non-chiral, static calculations				
	var. [YA02, AY02]	Fad. [SGM07, SGMR07]	Fad. [IS07, IS09]	var. [WG09]	var. [FIK+11]
BE	48	50–70	60–95	40–80	40
Γ_m	61	90–110	45–80	40–85	64–86
Γ_{nm}	12			~20	~21

Binding Energy (BE):
10-100 MeV
Mesonic Decay (Γ_m)
30-110 MeV
Non-Mesonic Decay (Γ_{nm})
4-30 MeV

Experimental Results on ppK$^-$

FINUDA

M(ppK$^-$) = 2.255 GeVc^{-2}
B(ppK$^-$) = 115 MeV
Γ(ppK$^-$) = 67 MeVc^{-2}

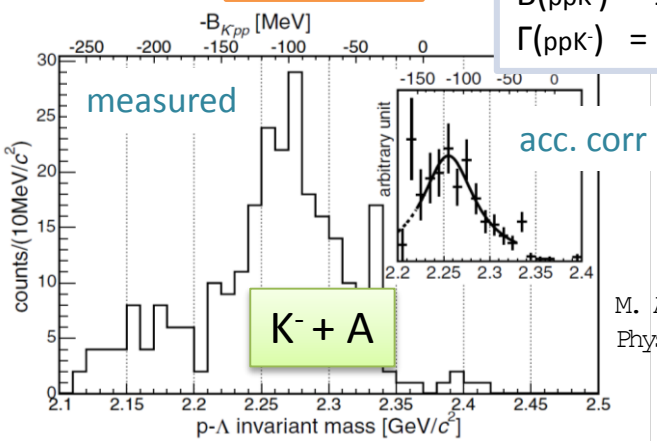

M. Agnello et al.
Phys.Rev.Lett.**94** (2005)

DISTO

M(ppK$^-$) = 2.267 GeVc^{-2}
B(ppK$^-$) = 103 MeV
Γ(ppK$^-$) = 118 MeVc^{-2}

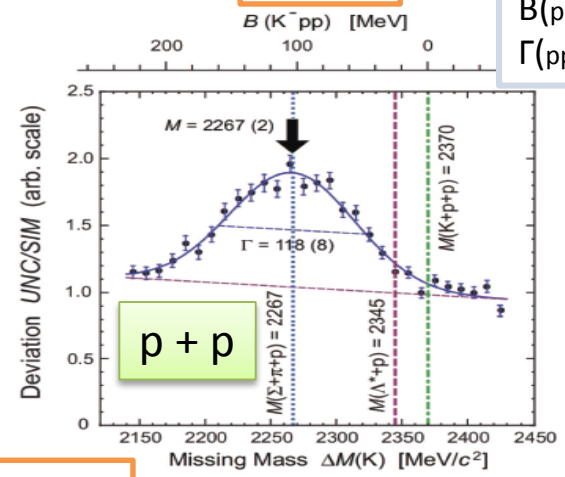

T. Yamazaki et al.
Phys.Rev.Lett.**104**, (2010)

LEPS/ SPRING8

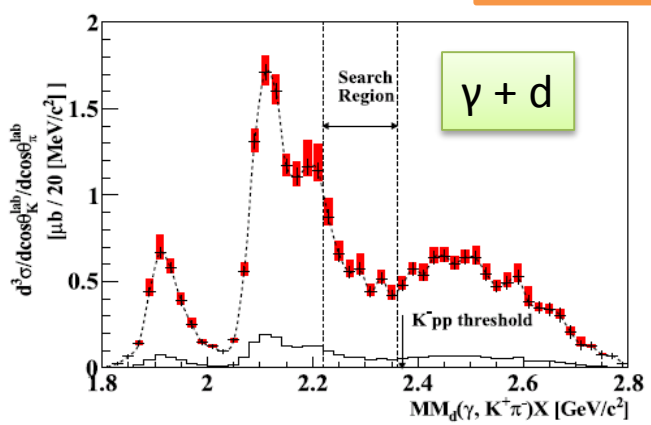

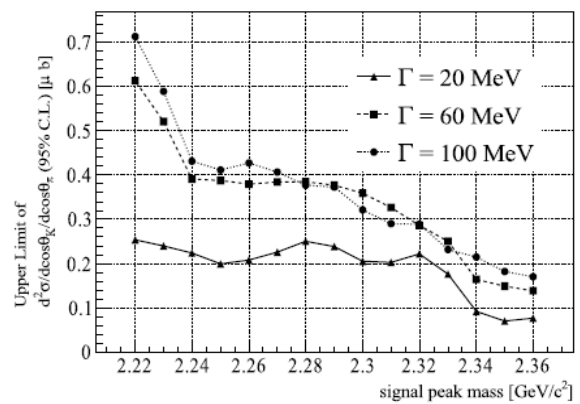

A.O. Tokayasu et al.
Phys.Lett. B728, (2014)

Kaonic Cluster

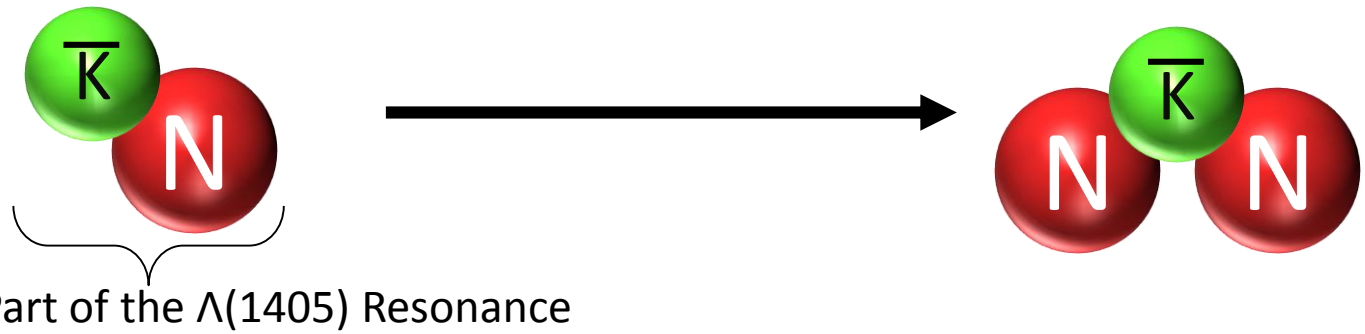

$$p + p \longrightarrow \underbrace{\Lambda(1405) + p}_{ppK^- \;+\; K^+} + K^+$$

$$ppK^- \longrightarrow \Lambda + p$$

J. Beringer
Phys.Rev. D86 (2012)

Kaonic Cluster

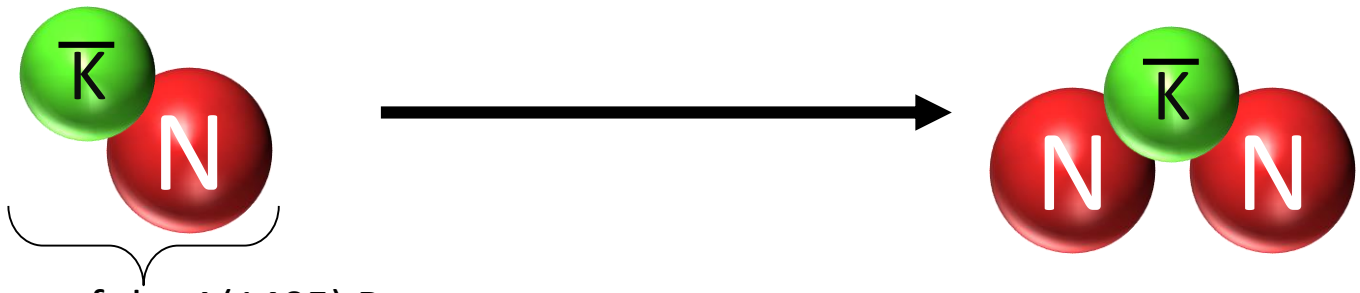

Part of the Λ(1405) Resonance

$p + p \longrightarrow \underbrace{\Lambda(1405) + p}_{ppK^- + K^+} + K^+$

$ppK^- + K^+ \longrightarrow \Lambda + p$

Physical Background:

$p + p \longrightarrow \Lambda + p + K^+$

$p + p \longrightarrow N^{*+} + p$

$N^{*+} \longrightarrow \Lambda + K^+$

N^{*+} - Resonances

Resonance	J^P	Mass (GeV/c^2)	Width (GeV/c^2)
$N^*(1650)$	$\frac{1}{2}^-$	1.655	0.150
$N^*(1710)$	$\frac{1}{2}^+$	1.170	0.100
$N^*(1720)$	$\frac{3}{2}^+$	1.720	0.250
$N^*(1875)$	$\frac{3}{2}^-$	1.875	0.220
$N^*(1880)$	$\frac{1}{2}^+$	1.870	0.235
$N^*(1895)$	$\frac{1}{2}^-$	2.090	0.090
$N^*(1900)$	$\frac{3}{2}^+$	1.900	0.250

J. Beringer
Phys.Rev. D86 (2012)

Experimental Data

The FOPI Experiment

SIS18 GSI Darmstadt

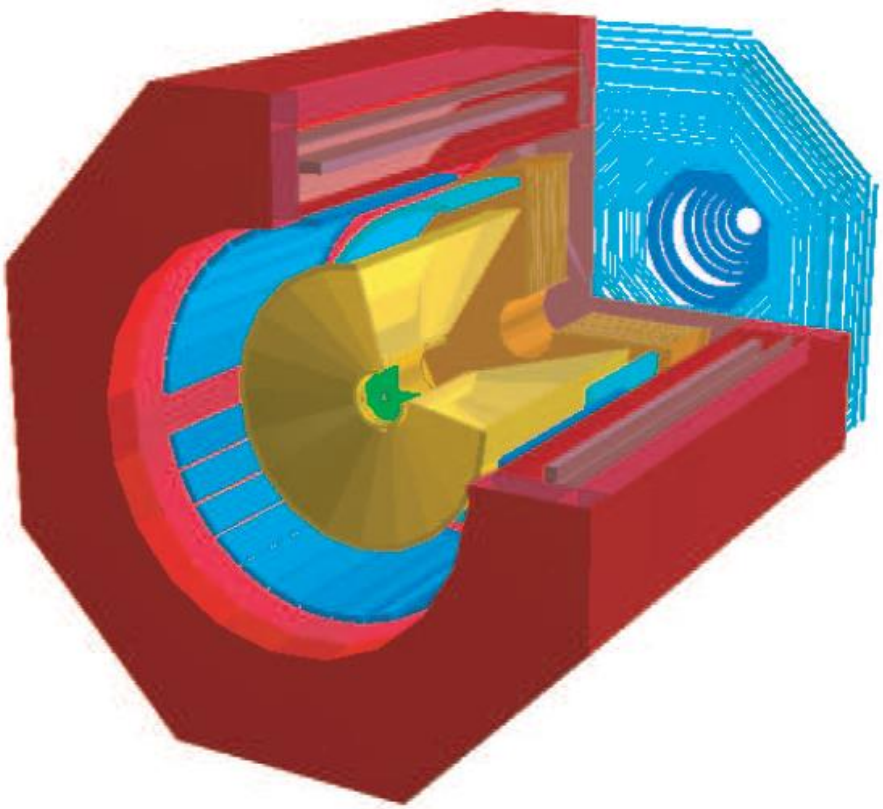

Beam Energy: 3.1 GeV

- Fixed-target Setup
- Full azimuthal coverage, 5˚- 110˚ in polar angle
- Momentum resolution ≈ 7% - 15 %
- Particle identification via dE/dx & ToF

Trigger Detector – SiΛViO:

Λ – Enhancement: $14.1 \pm 7.9(stat)^{+4.3}_{-0.6}$

Total Number of exclusive Events: 903

The HADES experiment

High **A**cceptance **D**i-electron **S**pectrometer
GSI, Darmstadt

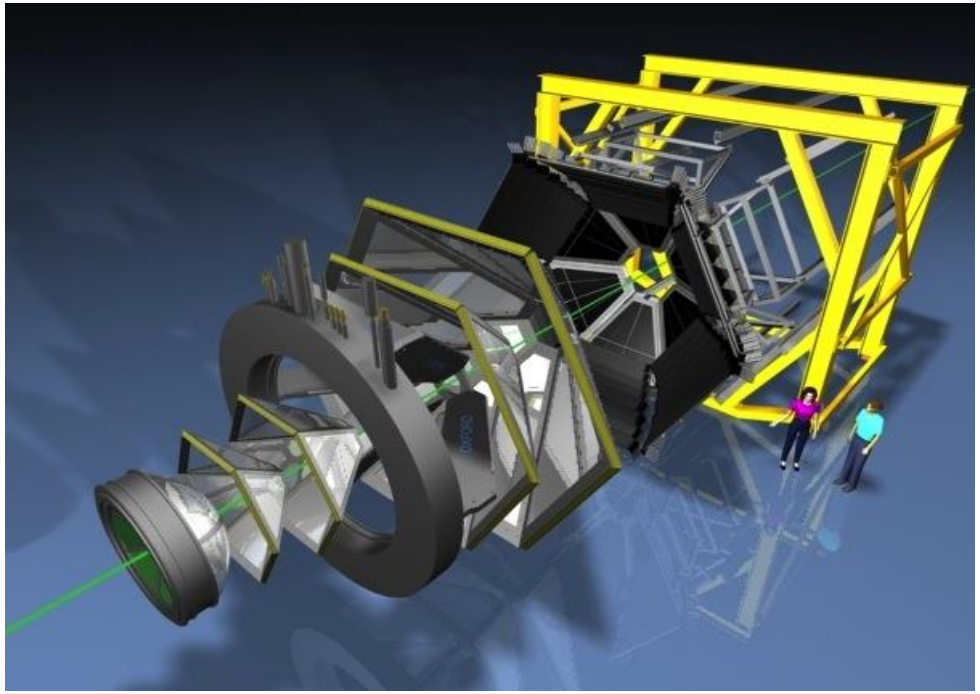

Beam Energy: 3.5 GeV

- Fixed-target Setup
- Full azimuthal coverage, 15˚- 185˚ in polar angle
- Momentum resolution ≈ 1% - 5 %
- Particle identification via dE/dx & ToF

HADES Coll. (G. Agakishiev et al.),
Eur. Phys. **J. A41** (2009)

Total Number of exclusive Events: 21000

The HADES Data Sample

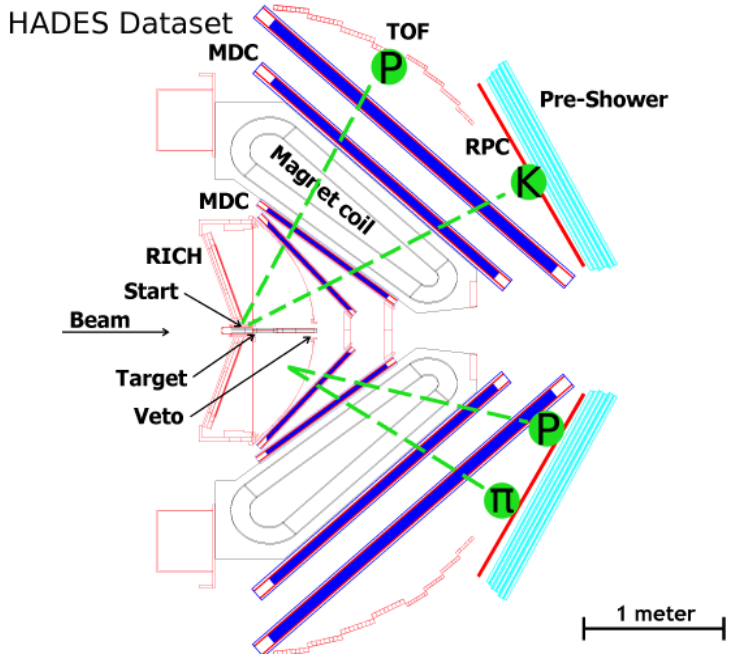

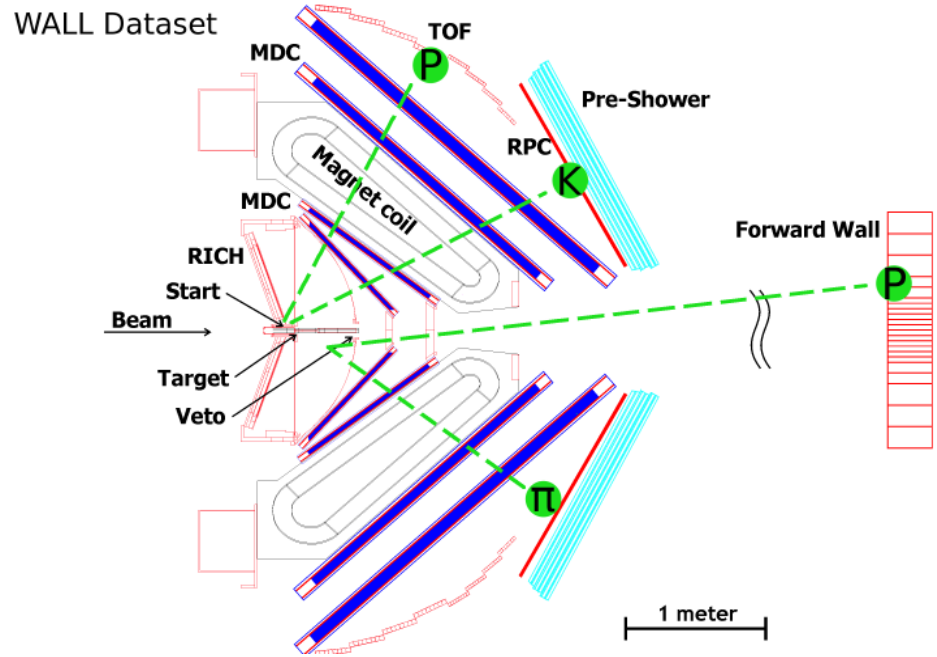

HADES data

13,000 events of $pK^+\Lambda$

Background from wrong PID ≈6%

Background from $pK^+\Sigma^0$ ≈1%

WALL data

8000 events of $pK^+\Lambda$

Background from wrong PID ≈11.7%

Background from $pK^+\Sigma^0$ ≈ 3%

Total Data Set

Hades Data E_{beam}=3.5 GeV

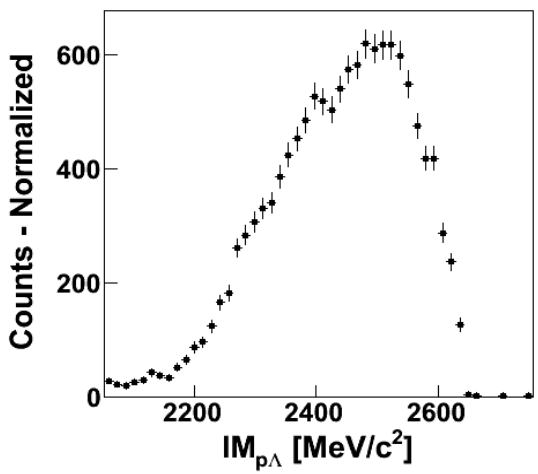

Had. Wall Data E_{beam}=3.5 GeV

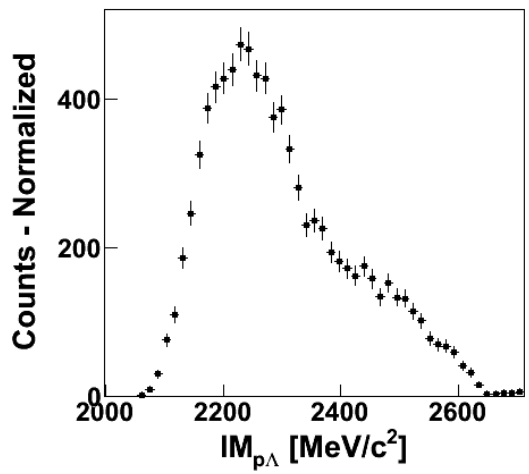

FOPI Data E_{beam}=3.1 GeV

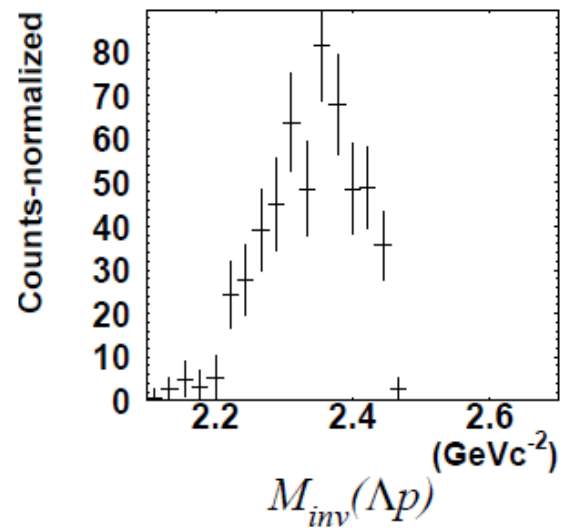

R. Münzer, PhD Thesis, TUM 2014
E. Epple, PhD Thesis, TUM 2014

Total Data Set

Hades Data E_{beam}=3.5 GeV

Had. Wall Data E_{beam}=3.5 GeV

FOPI Data E_{beam}=3.1 GeV

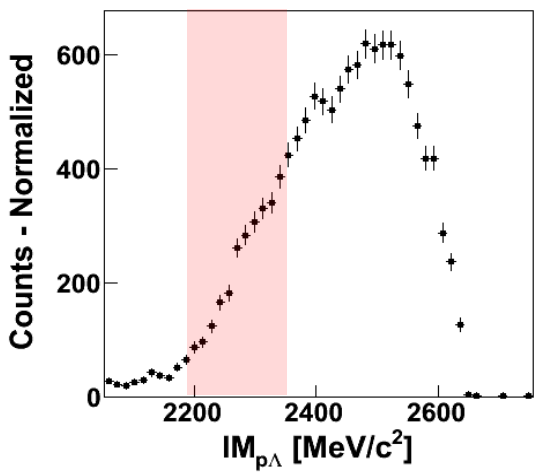

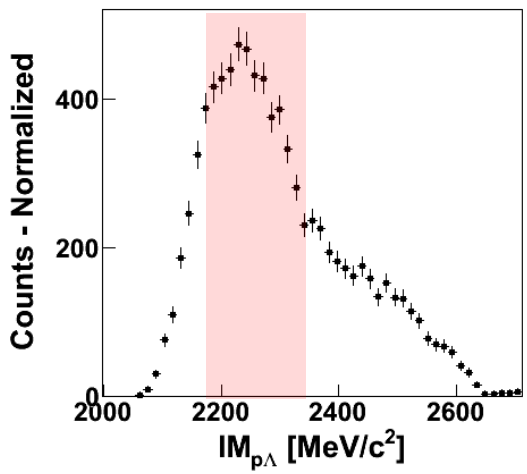

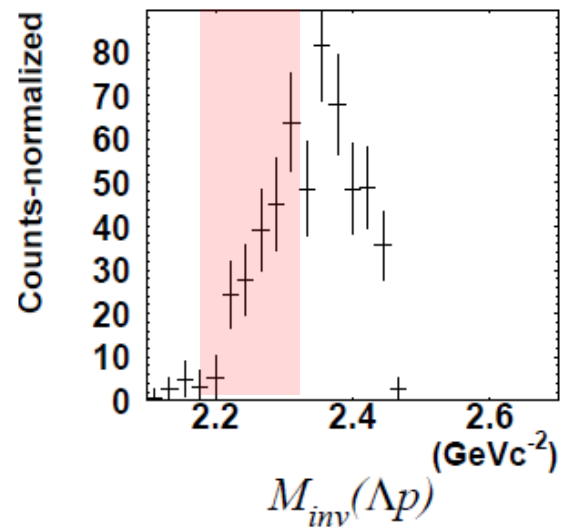

No Peak Visible
No Signal?

R. Münzer, PhD Thesis, TUM 2014
E. Epple, PhD Thesis, TUM 2014

Model Comparison

Phase Space Simulation

Partial Wave Analysis

Phase Space Simulation

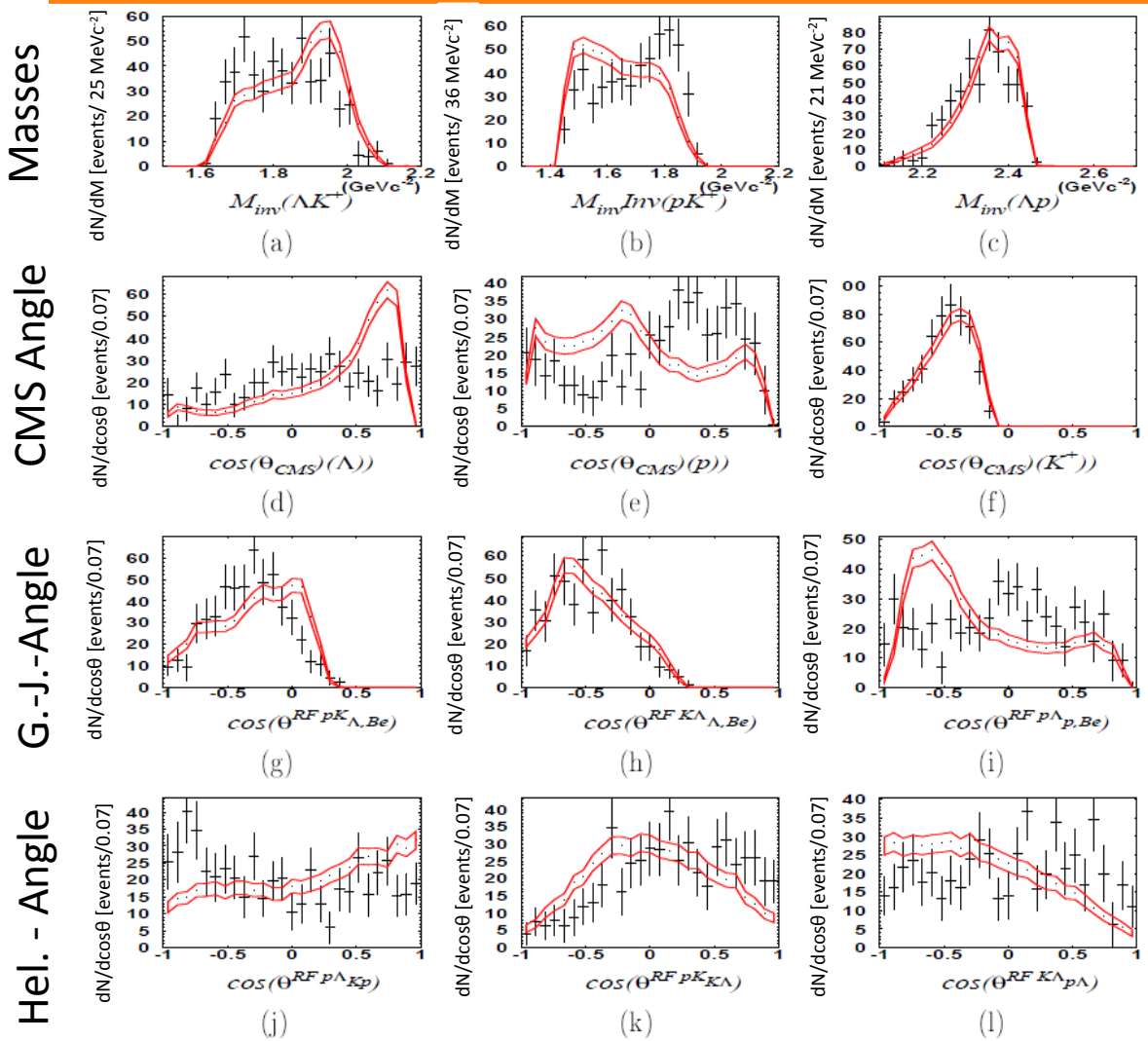

✚ Experimental Data

pp→ p K^+ Λ Phase Space

Phase Space Model

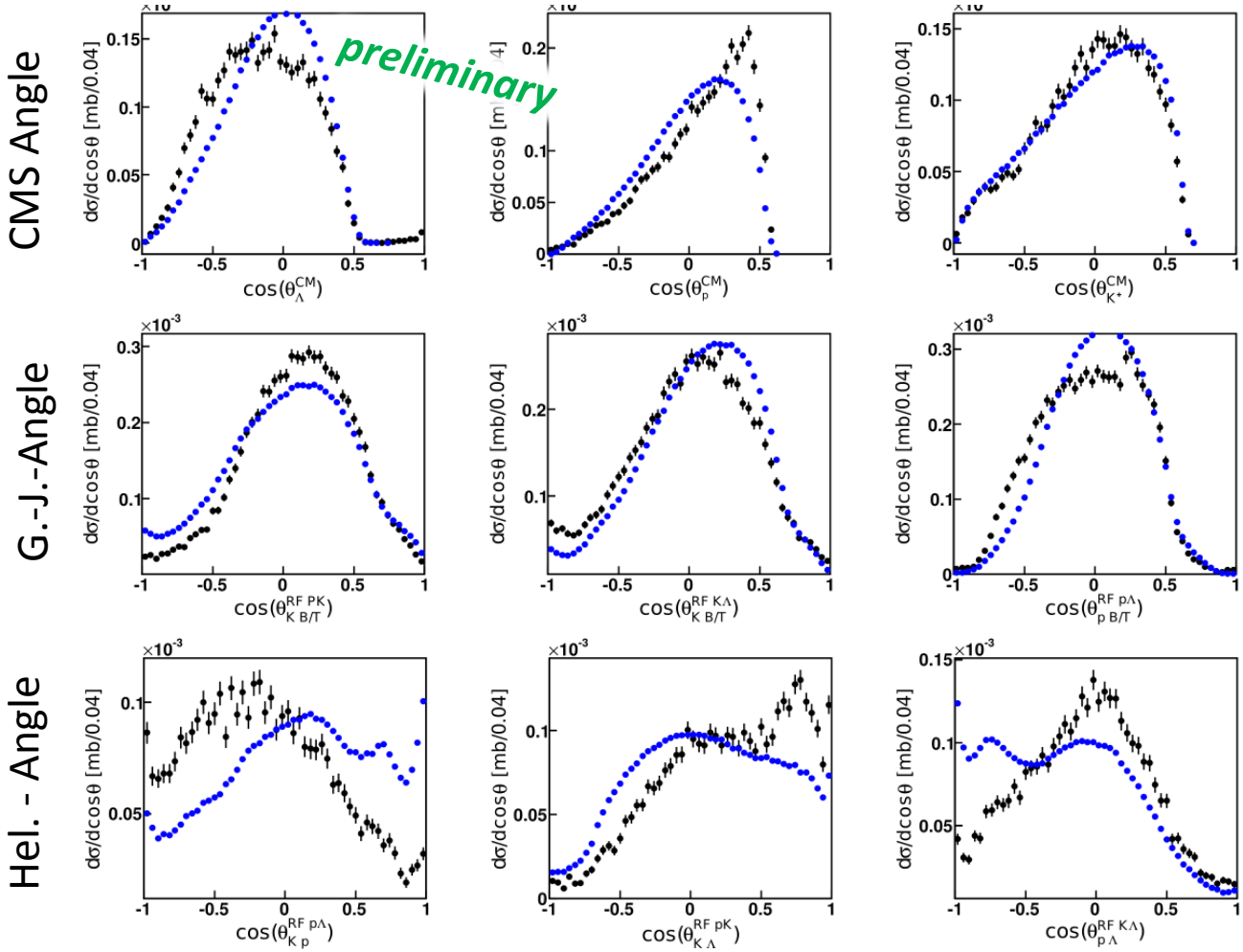

Inside HADES acceptance

- Experimental Data
- pp→p K^+ Λ Phase Space

Partial Wave Analysis

Bonn-Gatchina PWA Framework

A. Sarantsev et.al., Eur.Phys J A 25 2005

Cross-section Decomposition

$$d\sigma = \frac{(2\pi)^4 |A|^2}{4|\boldsymbol{k}|\sqrt{s}} d\Phi_3(P, q_1, q_2, q_3) \ , \qquad P = k_1 + k_2$$

A : reaction amplitude $A \propto A_{tr}^{\alpha}(s)$ (Transition amplitude of wave α)
k : 3-momentum of the initial particle in the CM
$s - P^2 : (k_1+k_2)^2$
$d\Phi_3(P,q_1,q_2,q_3)$: invariant three-particle phase space

Parameterization of the Transition

$$A_{\mathrm{tr}}^{\alpha}(s) = \left(a_1^{\alpha} + a_3^{\alpha}\sqrt{s}\right) exp\left(\mathrm{i}a_2^{\alpha}\right)$$

a_1^{α} Constant amplitude

a_2^{α} Phase

a_3^{α} Energy dependent amp.

Systematical Analysis

Systematical Scan over different p-p Initial Systems and different inclusion of N* Resonances

Initial System

J^P	$S_{tot} = 0$	$S_{tot} = 1$
L=0	0^+	
L=1		$0^-, 1^-, 2^-$
L=2	2^+	
L=3		$2^-, 3^-, 4^-$

Resonance in final State

Resonance	J^P	Mass (GeV/c^2)	Width (GeV/c^2)
$N^*(1650)$	$\frac{1}{2}^-$	1.655	0.150
$N^*(1710)$	$\frac{1}{2}^+$	1.710	0.100
$N^*(1720)$	$\frac{3}{2}^+$	1.720	0.250
$N^*(1875)$	$\frac{3}{2}^-$	1.875	0.220
$N^*(1880)$	$\frac{1}{2}^+$	1.870	0.235
$N^*(1895)$	$\frac{1}{2}^-$	2.090	0.090
$N^*(1900)$	$\frac{3}{2}^+$	1.900	0.250

J. Beringer
Phys.Rev. D86 (2012)

Four Best PWA Solutions

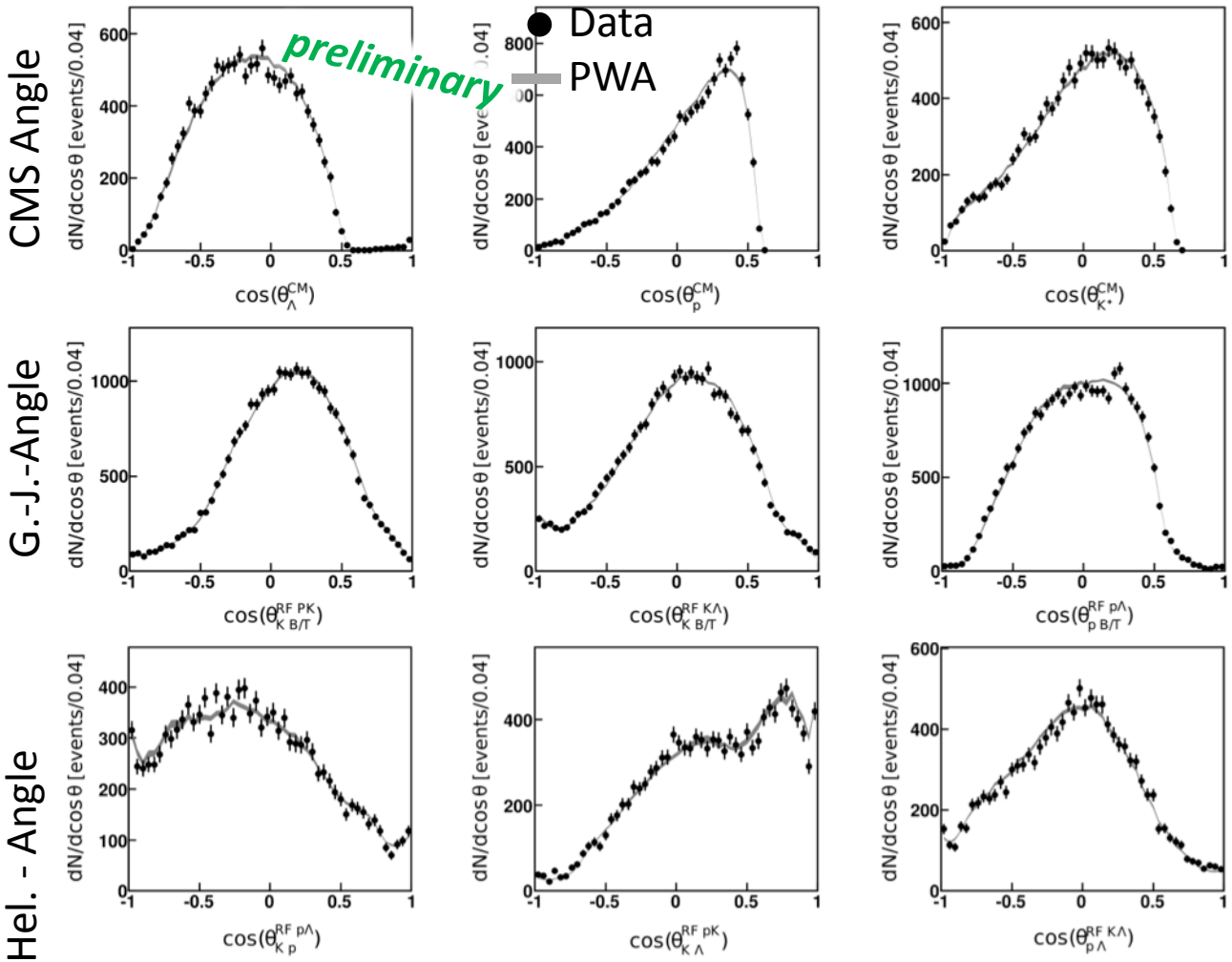

Inside HADES acceptance

Measured Data

PWA solutions

PWA Results

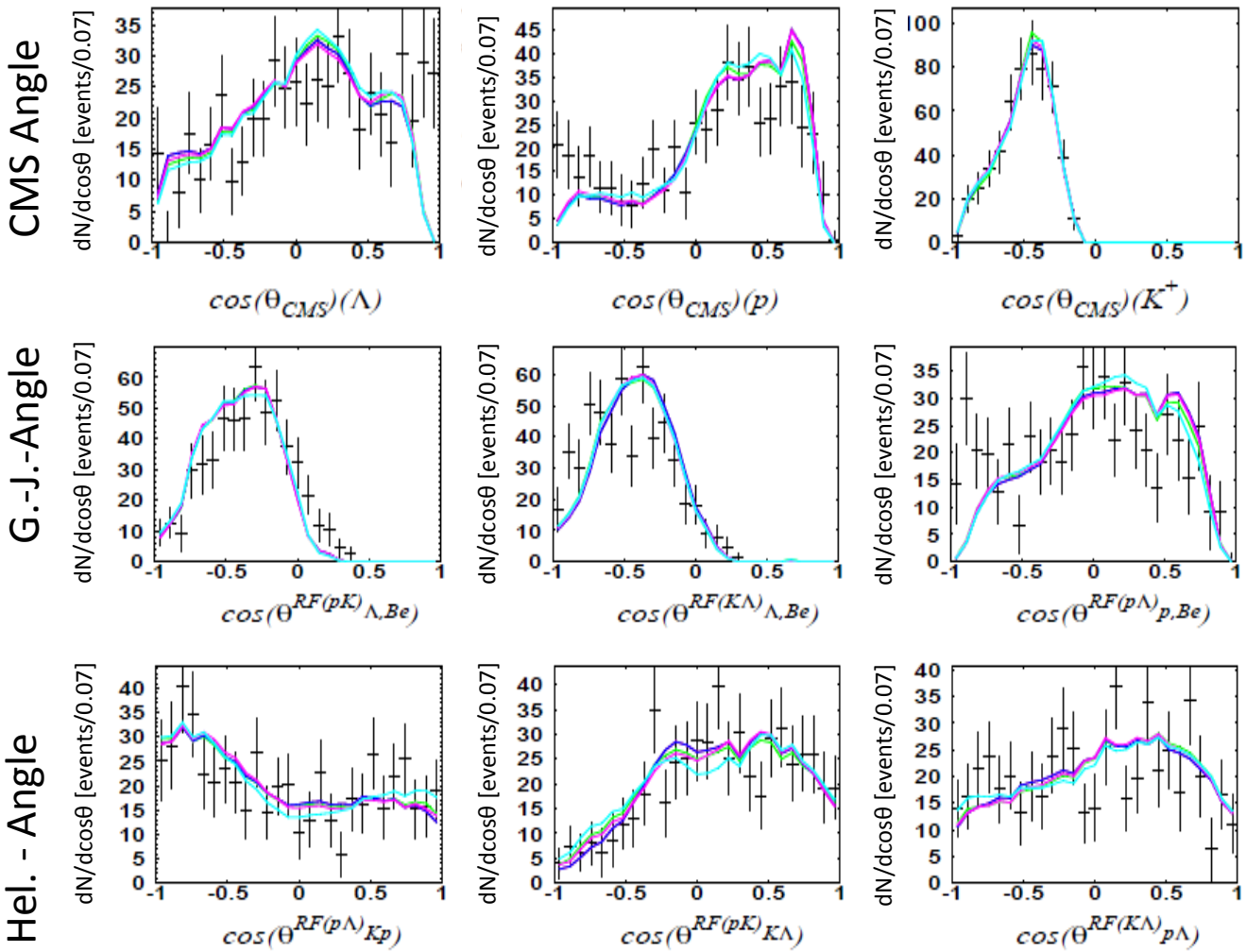

✚ Experimental Data

Solution A
Solution B
Solution C
Solution D
Solution E

Four Best PWA Solutions

FOPI

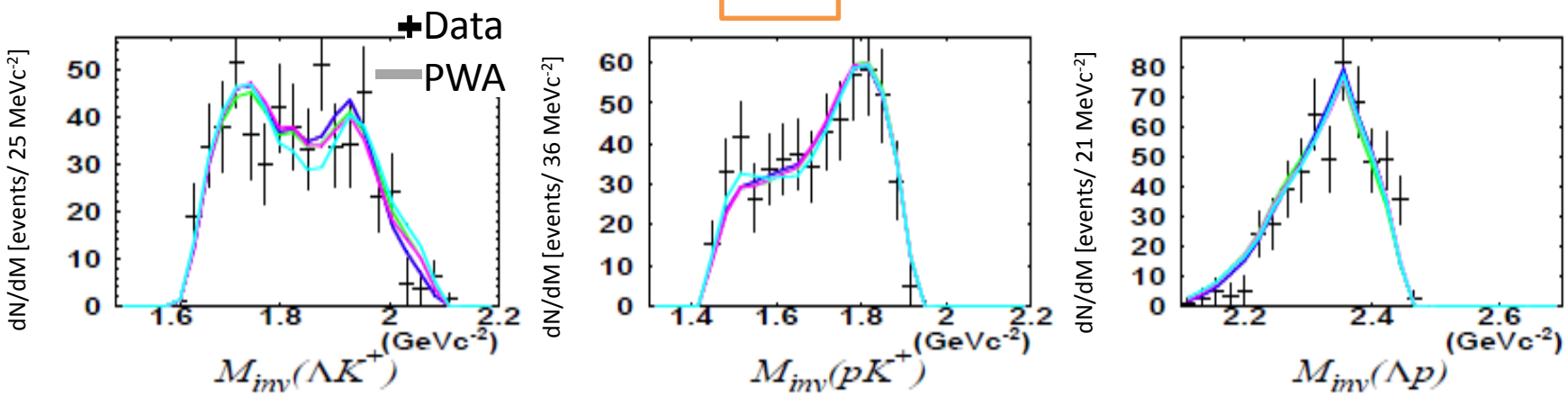

HADES

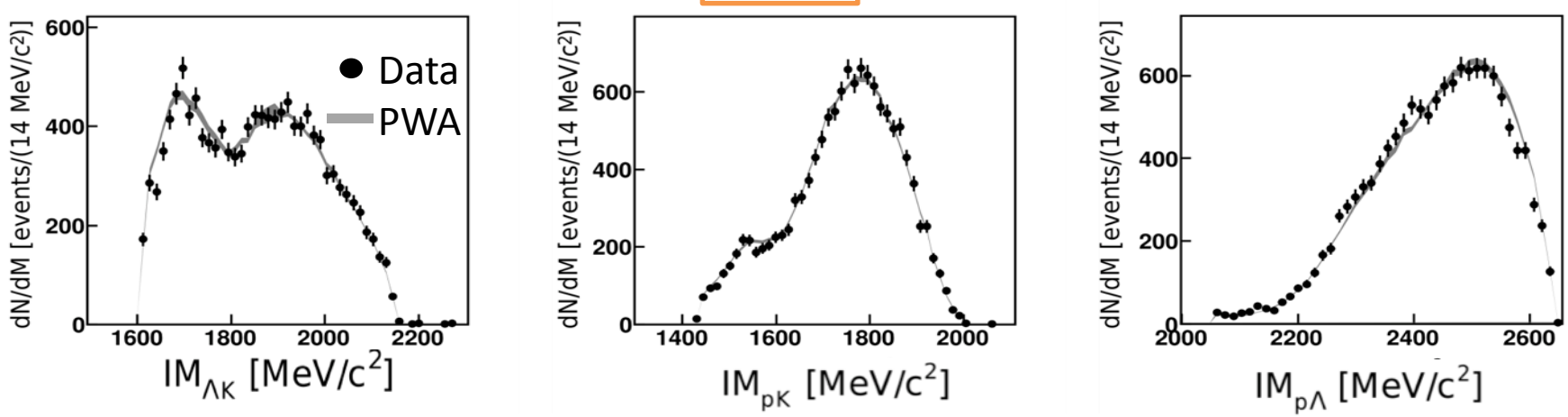

Contribution of Production Channels

PWA Results – Relative Contribution

Sol.	X^2 / ndf	Direct $pK^+\Lambda$	N^{*+} (1650)	N^{*+} (1710)	N^{*+} (1720)	N^{*+} (1875)	N^{*+} (1880)	N^{*+} (1895)	N^{*+} (1900)
A	1.09	0 %	11.3 %	52.4 %	11.8 %	6.3 %	10.9 %	0 %	7.3 %
B	1.09	16.6 %	9.4 %	42.3 %	14.1 %	0 %	9.7 %	0 %	7.9 %
C	1.10	0 %	11.1 %	49.5 %	7.5 %	0 %	14.1 %	9.3 %	8.5 %
D	1.12	13.9 %	6.8 %	43.8 %	11.9 %	5.3 %	9.4 %	0 %	8.9 %
E	1.15	21.1 %	8.6 %	41.9 %	17.6 %	0 %	0 %	0 %	10.8 %

PWA Results – Relative Contribution

Sol.	X^2 / ndf	Direct $pK^+\Lambda$	N^{*+} (1650)	N^{*+} (1710)	N^{*+} (1720)	N^{*+} (1875)	N^{*+} (1880)	N^{*+} (1895)	N^{*+} (1900)
A	1.09	0 %	11.3 %	52.4 %	11.8 %	6.3 %	10.9 %	0 %	7.3 %
B	1.09	16.6 %	9.4 %	42.3 %	14.1 %	0 %	9.7 %	0 %	7.9 %
C	1.10	0 %	11.1 %	49.5 %	7.5 %	0 %	14.1 %	9.3 %	8.5 %
D	1.12	13.9 %	6.8 %	43.8 %	11.9 %	5.3 %	9.4 %	0 %	8.9 %
E	1.15	21.1 %	8.6 %	41.9 %	17.6 %	0 %	0 %	0 %	10.8 %

PWA Results – Relative Contribution

Sol.	X^2 / ndf	Direct $pK^+\Lambda$	N^{*+} (1650)	N^{*+} (1710)	N^{*+} (1720)	N^{*+} (1875)	N^{*+} (1880)	N^{*+} (1895)	N^{*+} (1900)
A	1.09	0 %	11.3 %	52.4 %	11.8 %	6.3 %	10.9 %	0 %	7.3 %
B	1.09	16.6 %	9.4 %	42.3 %	14.1 %				
C	1.10	0 %	11.1 %	49.5 %	7.5 %				
D	1.12	13.9 %	6.8 %	43.8 %	11.9 %				
E	1.15	21.1 %	8.6 %	41.9 %	17.6 %				

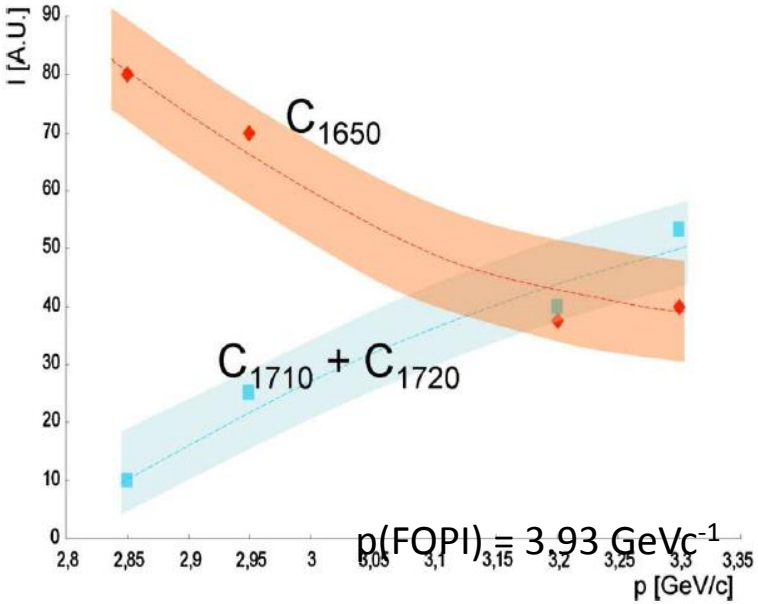

p(FOPI) = 3.93 $GeVc^{-1}$

S. Abd El-Samad et al.
Phys.Lett B688 (2010)

PWA Results – Relative Contribution

Sol.	X^2 / ndf	Direct $pK^+\Lambda$	N^{*+} (1650)	N^{*+} (1710)	N^{*+} (1720)	N^{*+} (1875)	N^{*+} (1880)	N^{*+} (1895)	N^{*+} (1900)
A	1.09	0 %	11.3 %	52.4 %	11.8 %	6.3 %	10.9 %	0 %	7.3 %
B	1.09	16.6 %	9.4 %	42.3 %	14.1 %	0 %	9.7 %	0 %	7.9 %
C	1.10	0 %	11.1 %	49.5 %	7.5 %	0 %	14.1 %	9.3 %	8.5 %
D	1.12	13.9 %	6.8 %	43.8 %	11.9 %	5.3 %	9.4 %	0 %	8.9 %
E	1.15	21.1 %	8.6 %	41.9 %	17.6 %	0 %	0 %	0 %	10.8 %

PWA Results – Relative Contribution

Sol.	X^2 / ndf	Direct $pK^+\Lambda$	N^{*+} (1650)	N^{*+} (1710)	N^{*+} (1720)	N^{*+} (1875)	N^{*+} (1880)	N^{*+} (1895)	N^{*+} (1900)
A	1.09	0 %	11.3 %	52.4 %	11.8 %	6.3 %	10.9 %	0 %	7.3 %
B	1.09	16.6 %	9.4 %	42.3 %	14.1 %	0 %	9.7 %	0 %	7.9 %
C	1.10	0 %	11.1 %	49.5 %	7.5 %	0 %	14.1 %	9.3 %	8.5 %
D	1.12	13.9 %	6.8 %	43.8 %	11.9 %	5.3 %	9.4 %	0 %	8.9 %
E	1.15	21.1 %	8.6 %	41.9 %	17.6 %	0 %	0 %	0 %	10.8 %

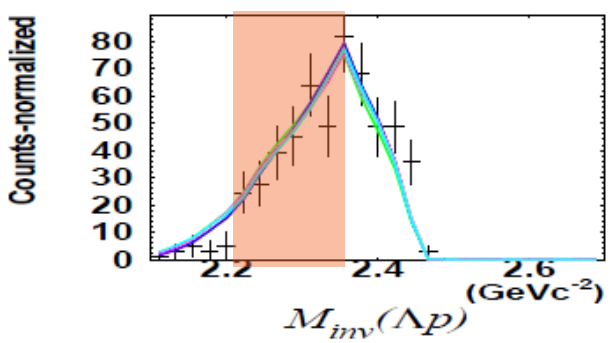

Experimental Data can be described by known sources

Upper Limit of ppK^- Contribution

ppK^- Upper Limit Determination

-> ppK^- Waves include in BG-PWA

-> Mass and Width fixed

-> Background for 5 best solution without ppK^-

-> Stepwise increase of Amplitude (a_1)

-> Phase Parameter free (a_2)
=> Optimal amount of Interference

Exclusion limit:
Confidence Level (95%) (CL_s)

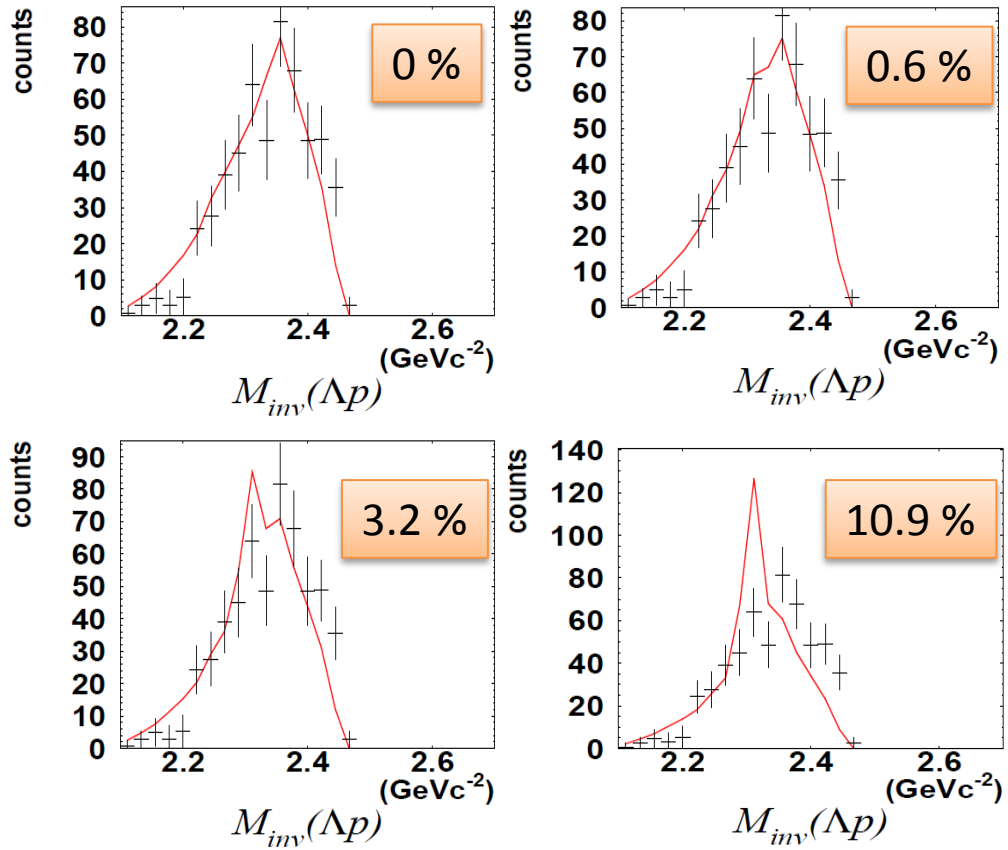

$M(ppK^-) = 2.305\ GeVc^{-2}$ $\Gamma(ppK^-)=20\ MeVc^{-2}$

ppK$^-$ Upper Limit Determination

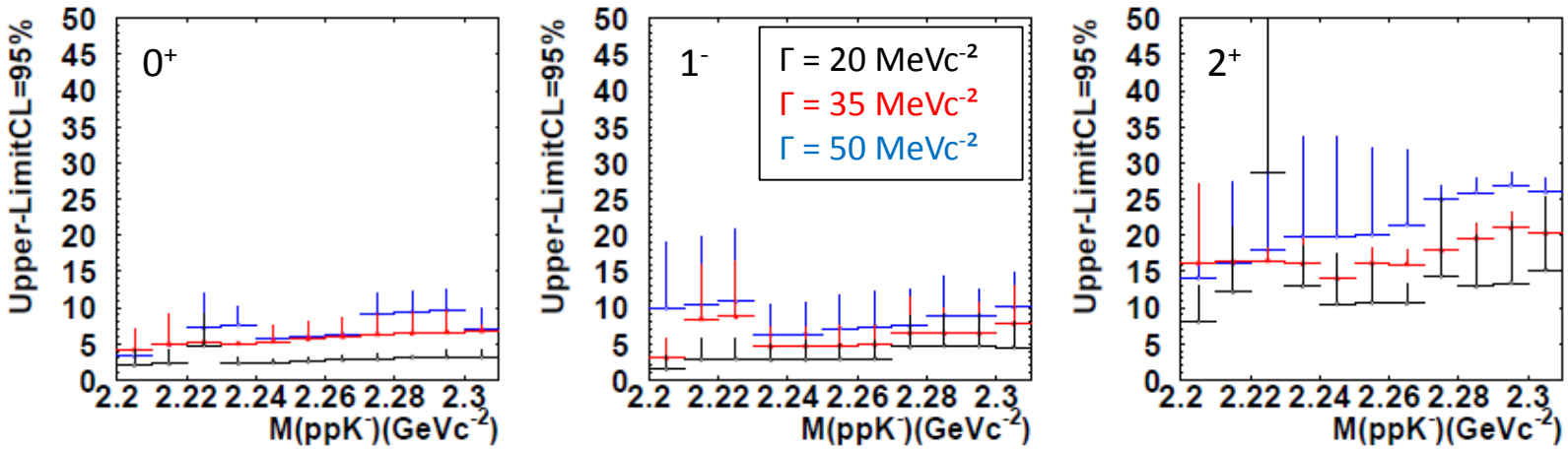

p + p -> p + K$^+$ + Λ
Total Cross Section

$$\sigma_{pK^+\Lambda} = 41.0 \pm 12.8 \mu b$$

Interpolated from literature

Upper Limit Cross Section

Γ (MeVc^{-2})	Cross Section (µb)
20	$7.6 \pm 1.2^{-3.5}$ - $22.4 \pm 3.6^{-10.7}$
35	$6.3 \pm 1.7^{-0.6}$ - $9.5 \pm 2.6^{-0.9}$
50	$10.2 \pm 1.8^{-4.5}$ - $11.6 \pm 3.4^{-0.6}$
60	$11.2 \pm 1.9^{-5.0}$ - $33.8 \pm 5.2^{-16.9}$
80	$11.4 \pm 2.7^{-3.8}$ - $35.9 \pm 5.7^{-17.4}$

Upper Limit

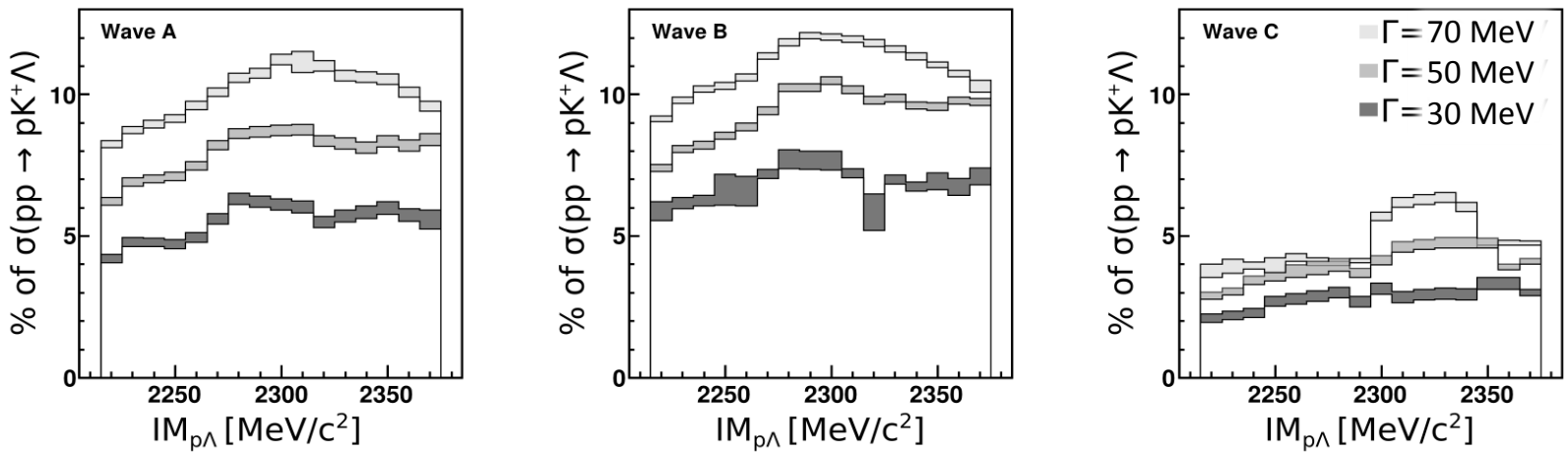

Measured total cross-section: $\sigma_{pK^+\Lambda} = 38.12 \pm 0.43^{+3.55}_{-2.83} \pm 2.67(p+p\text{-}error) - 2.9(background)\ \mu b$

Upper limit of ppK⁻ Cross Section:

Γ (MeVc⁻²)	Cross Section (μb)
0^+	1.9 – 3.9
1^-	2.1 – 4.2
2^+	0.7 – 2.1

Production Cross Section Λ(1405)

$9.2 \pm 0.9 \pm 0.7\ ^{+3.3}_{-1.0}\ \mu b$

HADES coll. (G. Agakishiev et al.)
Phys. Rev. **C 87,** 025201 (2013)

Summary

- 13000 (HADES) + 8000 (WALL) + 903 (FOPI) exclusive events $p + p \rightarrow p + K^+ + \Lambda$ reconstructed

- Experimental data cannot be reproduced by Phase Space

- Good explanation by Bonn-Gatchina PWA framework:

  Strong contribution of N^{*+} resonances

  No Additional Signal needed

- Determination of upper limit of the kaonic cluster between 7.4 and 35.9 µb (FOPI) and 0.7 – 4.2 µb (HADES) .

- Important effect of Interference => No Peak in final spectrum

Future Perspectives

- Combined analysis of results from different experiments at different energies and polarization observables => Application to the DFG accepted

experiment	$\sqrt{s}$ (GeV)	$\epsilon_{pK^+\Lambda}$	ϵ_{ppK^-}	statistics	polar.
COSY-TOF [AS+06a]	2.63	84.87	-231.40	791	N
COSY-TOF [AS+06a]	2.66	114.91	-201.35	1037	N
COSY-TOF [Rit13]	2.67	121.56	-194.71	160000	?
COSY-TOF [AS+06a]	2.72	171.05	-145.22	4323	N
DISTO [M+10, Mag01]	2.75	200.44	-115.83	121000	Y
COSY-TOF [M.R11]	2.75	203.69	-112.58	43662	Y
COSY-TOF [AES+10]	2.75	203.69	-112.58	7228	N
COSY-TOF [AES+10]	2.75	203.69	-112.58	15372	N
COSY-TOF [AB+10]	2.79	238.95	-77.32	89684	N
COSY-TOF [AESBB+13]	2.79	245.70	-70.57	30000	N
COSY-TOF [AB+10]	2.83	284.06	-32.21	3322	N
COSY-TOF [AES+10]	2.83	284.06	-32.21	5791	N
COSY-TOF [AES+10]	2.87	318.86	2.60	6263	N
DISTO [M+10, Mag01]	2.87	318.86	2.60	304000	Y
DISTO [M+10, Mag01, B+99]	2.98	430.48	114.21	424000	Y
FOPI	3.06	508.97	192.70	903	N
HADES	3.18	629.33	313.06	20000	N

AES+10: S. Abd El-Samad et al. Phys.Lett B688 (2010)
AB+10: M. Abdel-Bary et al., Eur.Phys.J A46(2010)
AESBB+13: S. Abd El-Samad et al., Eur.Phys.J A49(2013)
Rit13: J.Ritmann, private communication (2013)
AS+06a : S. Abd El-Samad et al. Phys.Lett B632 (2006)
M+10: M. Maggiora et al. Nucl.Phys. A385 (2010)
Mag01: M. Maggiora Nucl. Phys. A691 (2001)
B+99: F. Balestra et al., Phys.Rev.Lett 83 (1999)
Epp14: E.Epple, Diss. TUM 2014

Outlook – Combined Analysis

HADES

Very Preliminary

FOPI

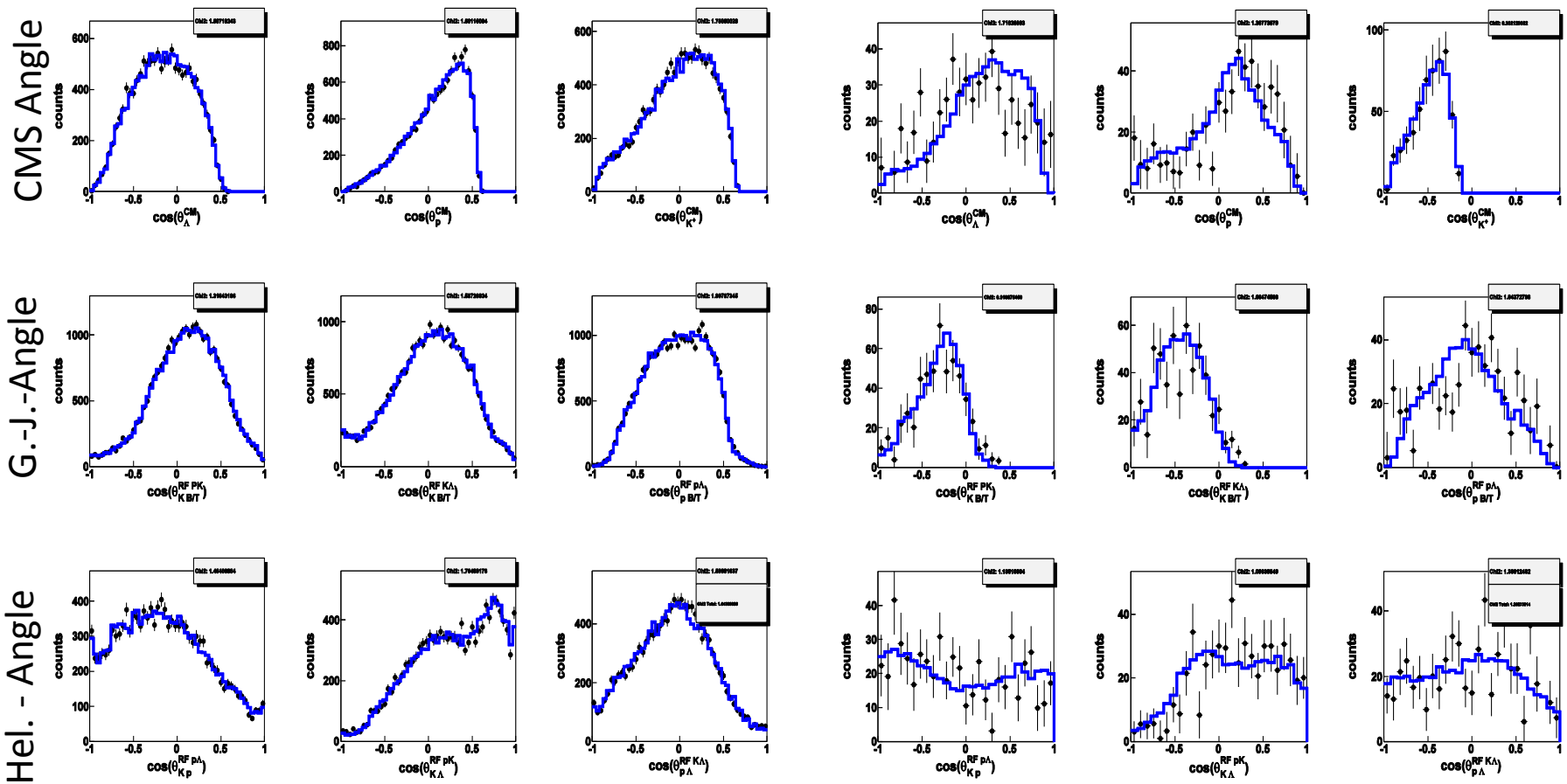

Thank You

HADES Collaboration

FOPI Collaboration

Backup

The Smallest Cluster

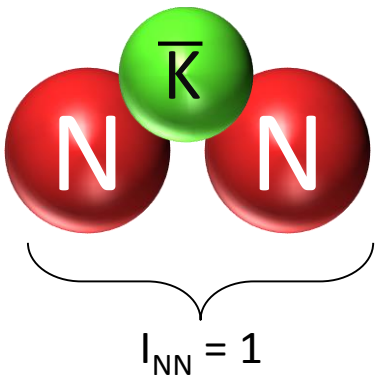

Property	Value
charge	+1
strangeness	-1
participants	ppK^-, $pn\bar{K}^0$
J^P	0^-

$\bar{K}NN$

- $\Sigma + N + \pi$, $\Lambda + N + \pi$ } Γ_m
- $\Sigma + N$, $\Lambda + N$ } Γ_{nm}

	Chiral, energy dependent				
	var. [DHW09, DHW08]	Fad. [BO12b, BO12a]	var. [BGL12]	Fad. [IKS10]	Fad. [RS14]
BE	17–23	26–35	16	9–16	32
Γ_m	40–70	50	41	34–46	49
Γ_{nm}	4–12	30			
	Non-chiral, static calculations				
	var. [YA02, AY02]	Fad. [SGM07, SGMR07]	Fad. [IS07, IS09]	var. [WG09]	var. [FIK+11]
BE	48	50–70	60–95	40–80	40
Γ_m	61	90–110	45–80	40–85	64–86
Γ_{nm}	12			~20	~21

Binding Energy (BE):
10-100 MeV
Mesonic Decay (Γ_m)
30-110 MeV
Non-Mesonic Decay (Γ_{nm})
4-30 MeV

Trigger Detector - SiΛViO

Silicon Λ-Vertexing and **I**dentification **O**nline

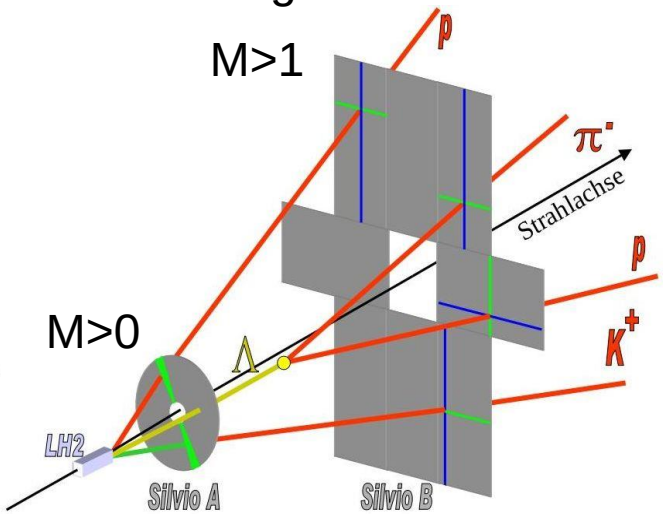

Trigger conditions:

LVL1 : Multiplicty(ToF) > 1

LVL2 : LVL1 + SiΛViO

Inclusive Λ Reconstruction

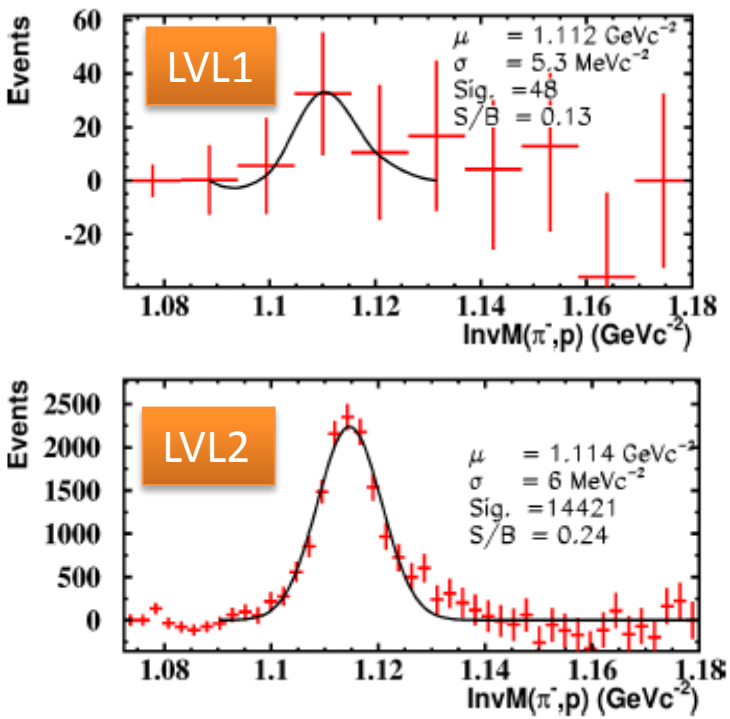

Λ – Enhancement: $14.1 \pm 7.9(stat)^{+4.3}_{-0.6}$

R. Münzer et. al. NIM A 745 (2014) 38-49

Reconstruction of exclusive Reactions

$p + p \rightarrow p + K^{+} + \Lambda$

Inclusive Reconstruction

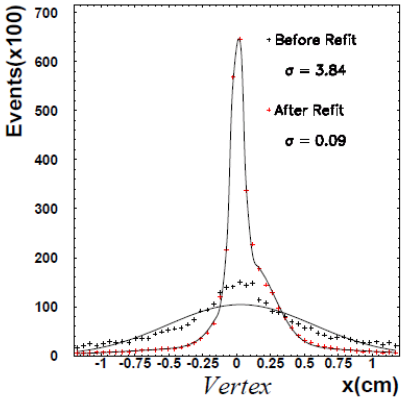

(a)

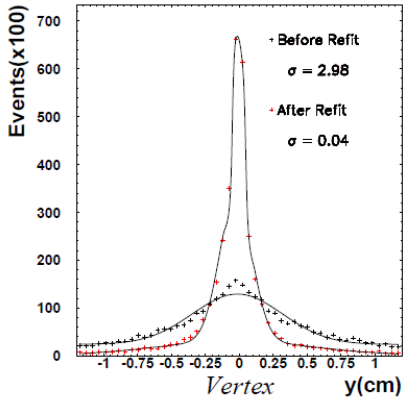

(b)

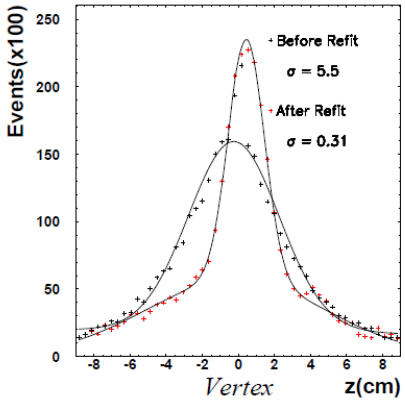

	Before Refit [cm]	After Refit [cm]
σ_x	3.84	0.09
σ_y	2.98	0.04
σ_z	5.50	0.31

Exclusive Data Sample

Primary K^+ Selection

Kaon Candidates in RPC and CDC

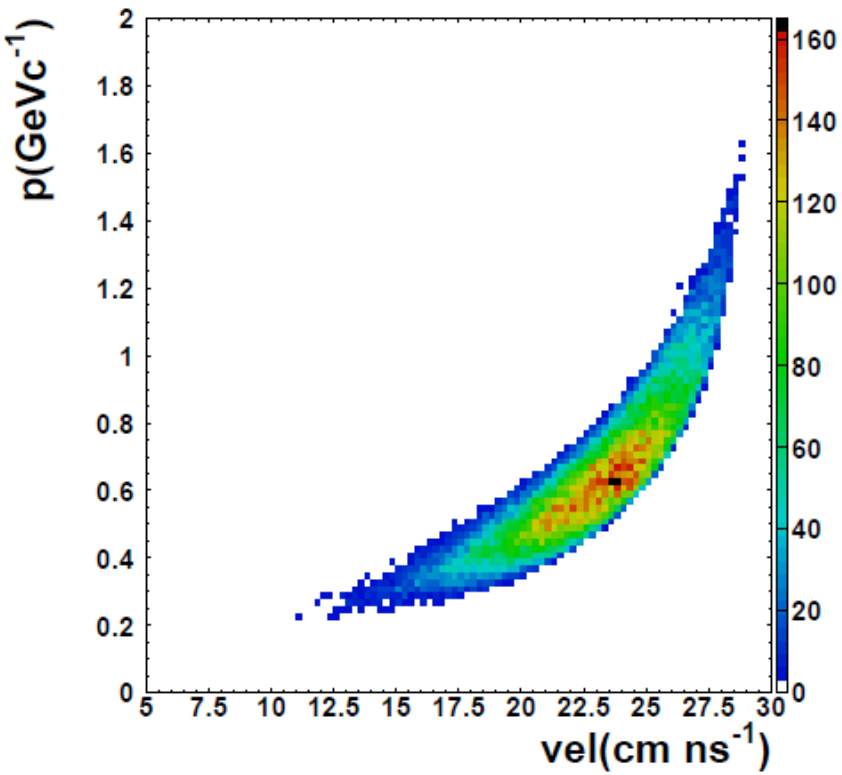

Exclusive Data Sample

Primary K^+ Selection

↓

Λ Selection

Λ Candidates in all sub detector Combinations

$\Lambda \rightarrow p + \pi^-$

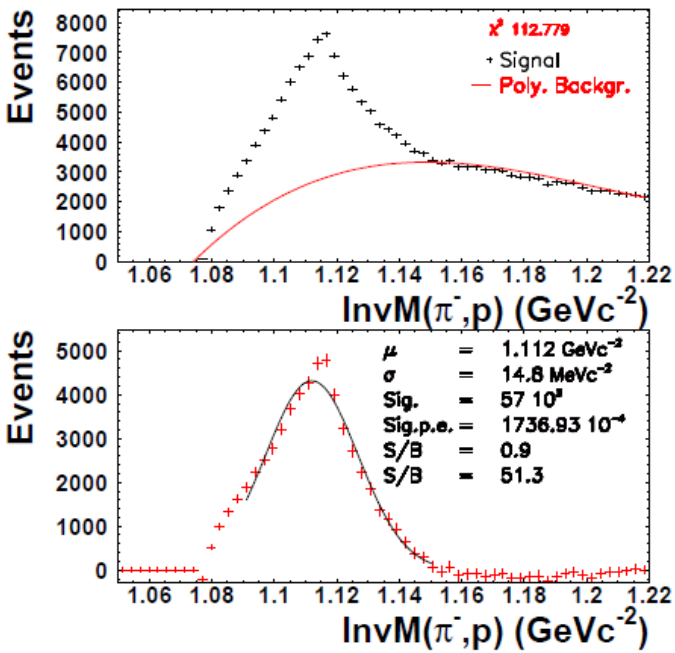

Exclusive Reconstruction

$$p + p \xrightarrow{3.1GeV} \Lambda + p + K^+$$
$$\Lambda \rightarrow p + \pi^-$$

Primary K^+ Selection

Λ Identification

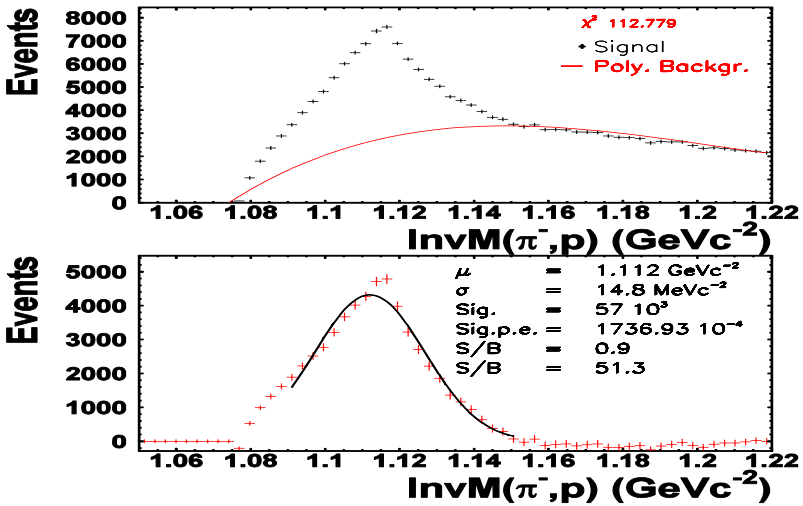

Exclusive Reconstruction

$$p + p \xrightarrow{3.1GeV} \Lambda + p + K^+$$
$$\hookrightarrow p + \pi^-$$

Primary K⁺ Selection

↓

Λ Identification

↓

Exclusive Selection by Kinematical Refit

↓

Secondary K⁺ Selection Sideband Analysis

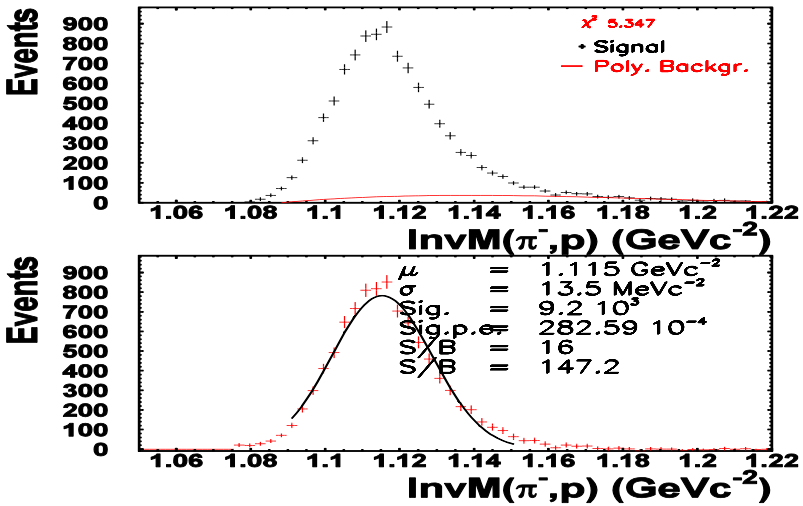

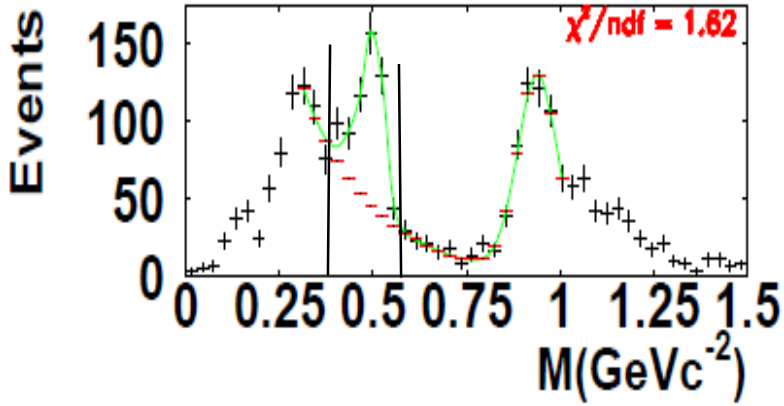

Exclusive Data Sample

Primary K^+ Selection

↓

Λ Selection

↓

Exclusive Selection by kinemetical refit

Kinematical Refit

Variation of Track parameters with error

$$\chi^2 = (\vec{\alpha} - \vec{\alpha}_0)^T V_{\vec{\alpha}_0}^{-1} (\vec{\alpha} - \vec{\alpha}_0)$$

$$pvalue = \int_{\chi^2_{fit}}^{\infty} f_\nu(\chi^2) d\chi^2.$$

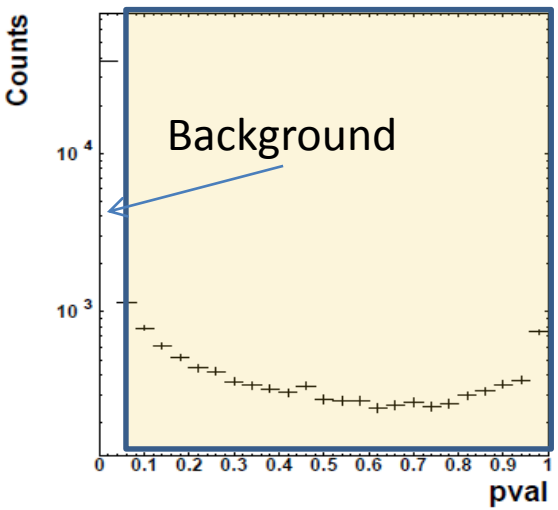

Different Kaon selection

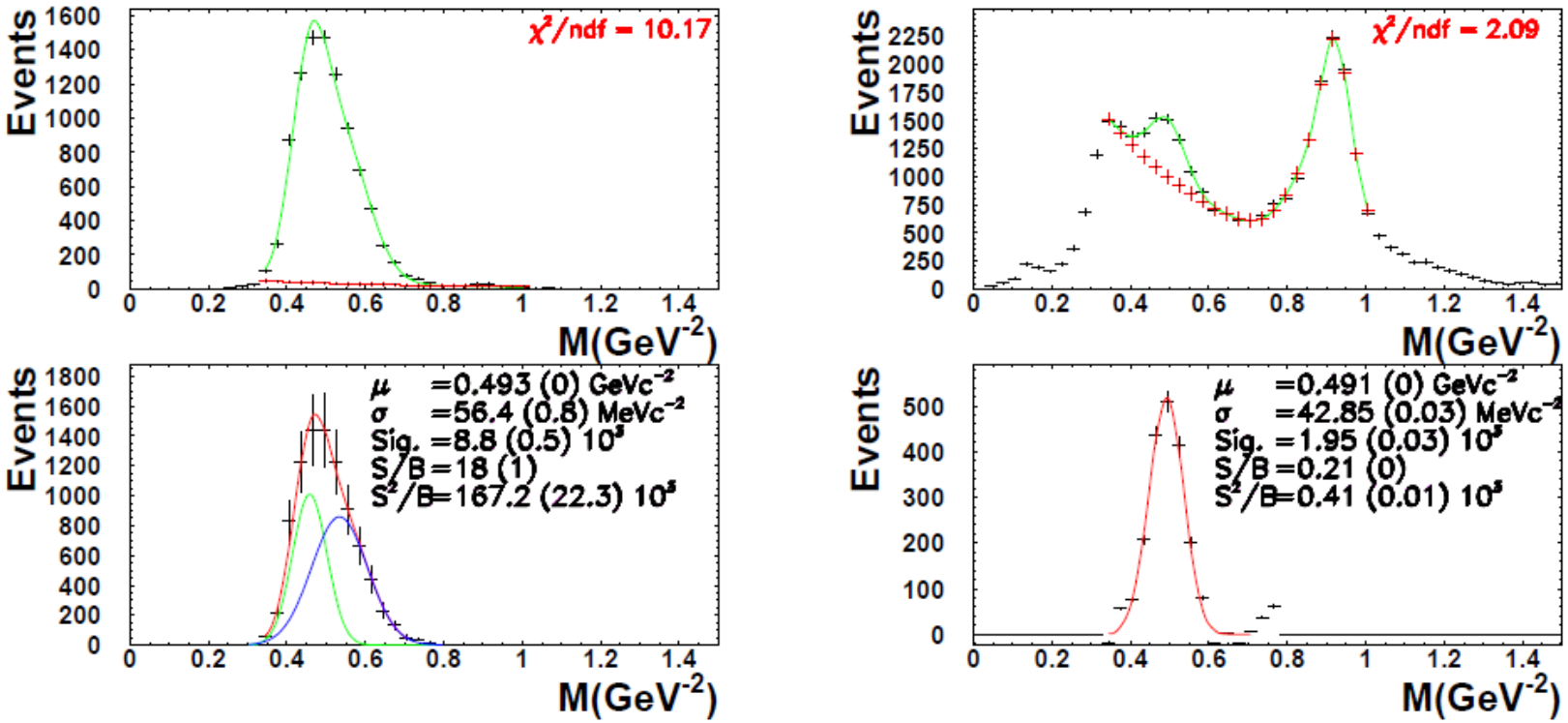

Backup

p < 0.5 GeV/c

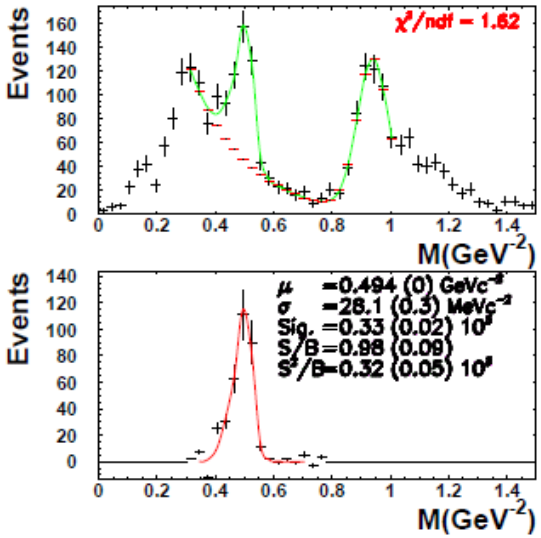

0.5 GeV/c < p < 0.6 GeV/c

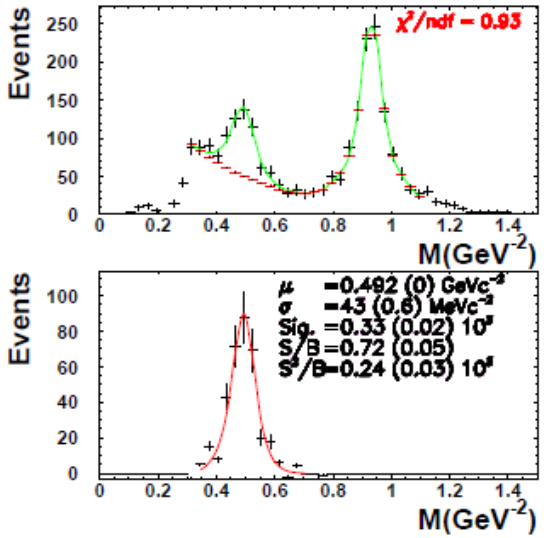

p > 0.6 GeV/c

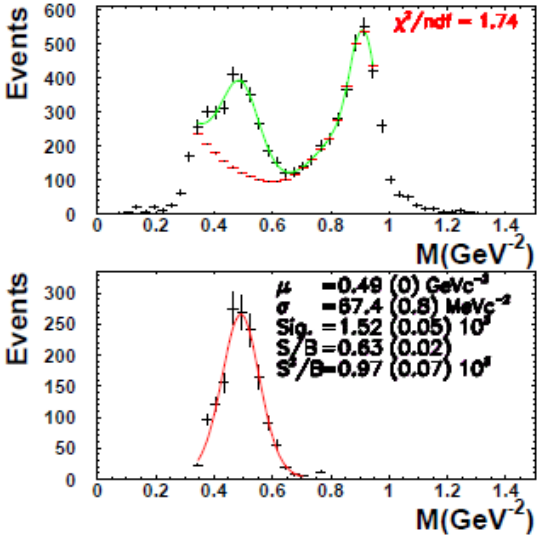

Sideband Analysis

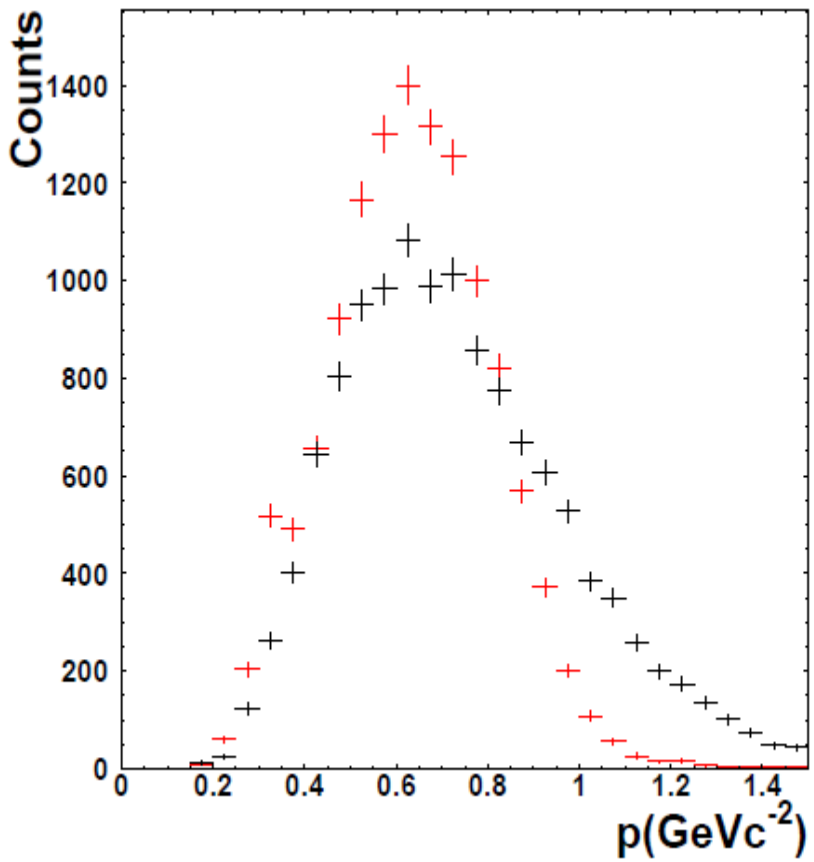

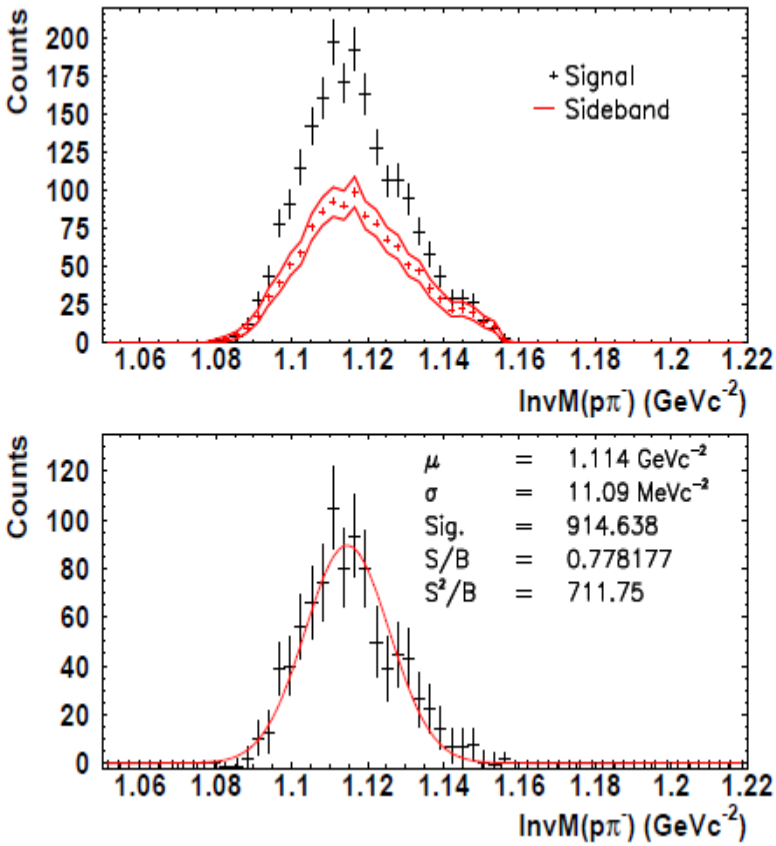

Λ / Σ Separation

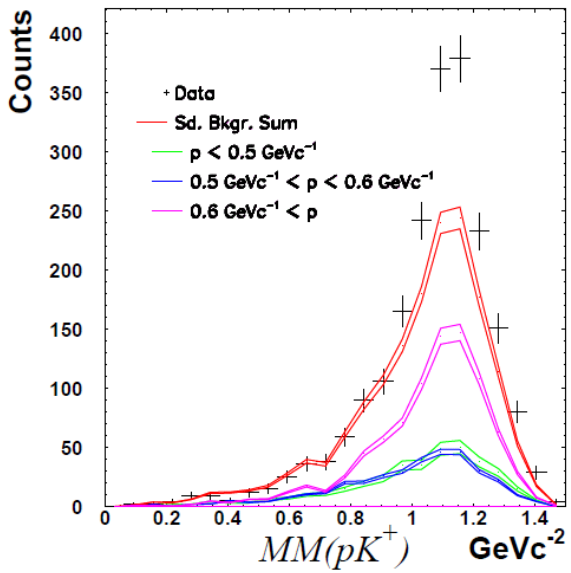

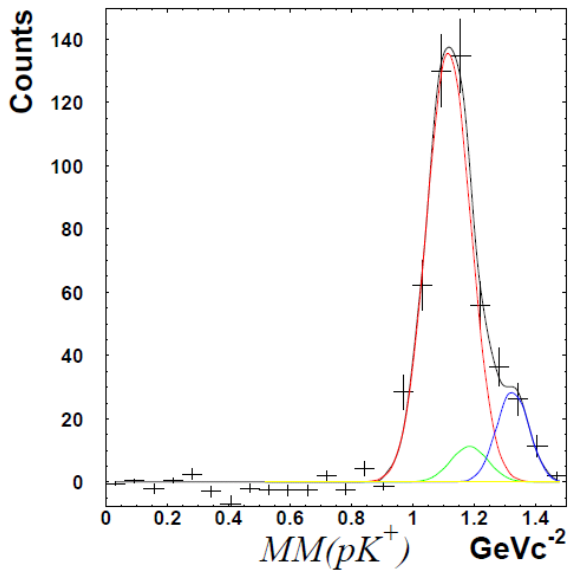

Remaining Background

$1/14.8.$

Particle	Mass	Fit μ	Fit σ	Fit Amplitude
Λ	1115.8	1.1171	0.07	136.35
Σ^0	1192.1	1.185	0.06	11.277
higher Resonance contribution		1.32	0.05	28.8

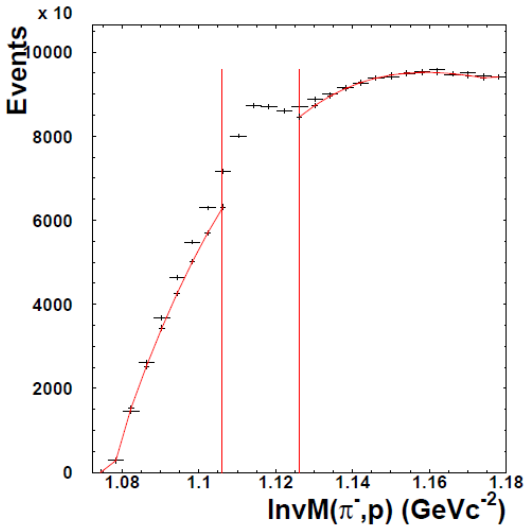

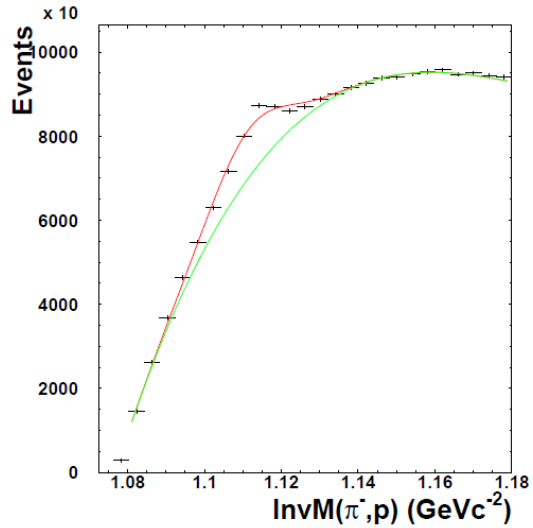

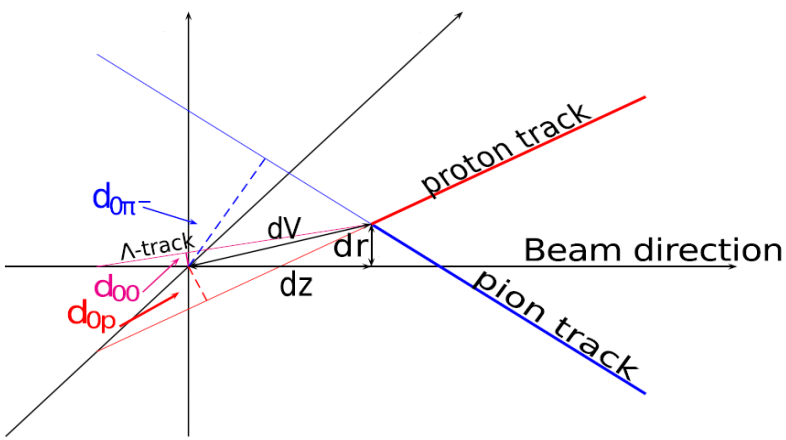

value	minimal value [cm]	maximal value [cm]
$primvertex_x$	-1.0	1.0
$primvertex_y$	-1.0	1.0
$primvertex_z$	-2.0	2.0
dr	3.0	∞

Exclusive Data Sample

Sideband Background

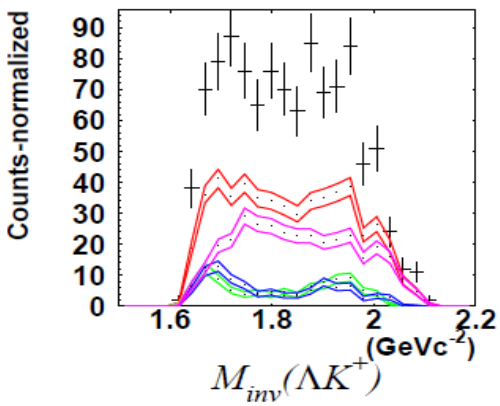

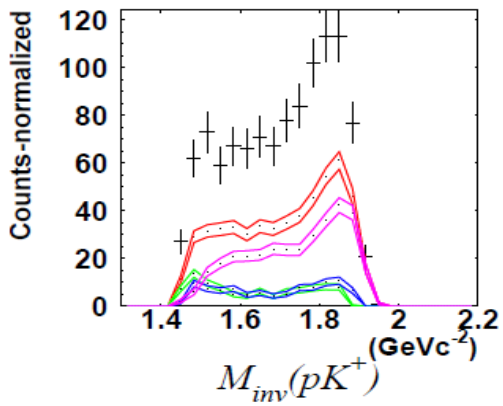

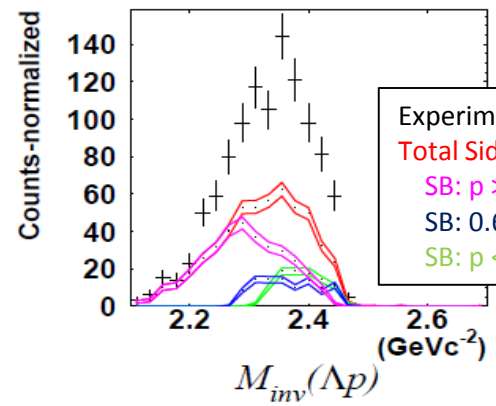

Experimental Data
Total Sideband Background
SB: p > 0.6 GeVc^{-1}
SB: 0.6 GeVc^{-1}> p > 0.5 GeVc^{-1}
SB: p < 0.5 GeVc^{-1}

Background Subtracted

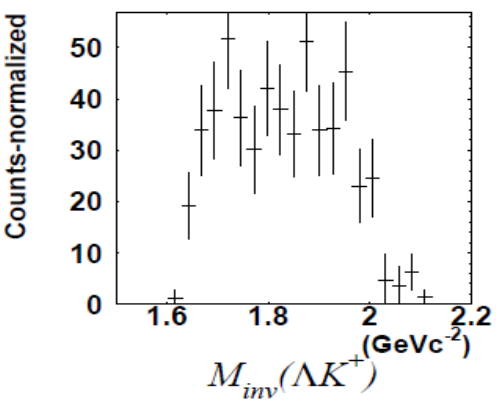

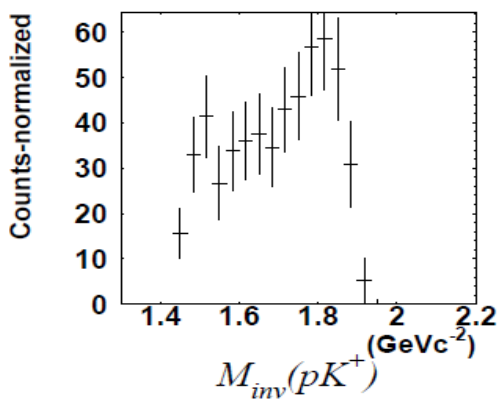

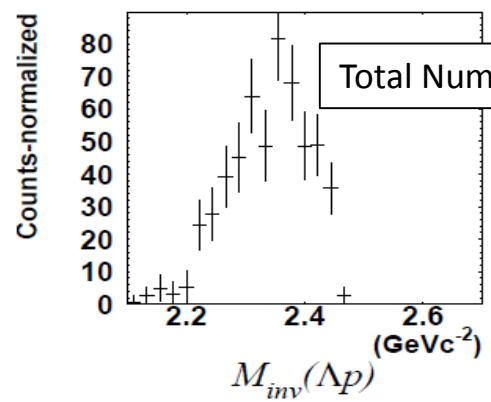

Total Number of Events: 903

Exclusive Data Sample

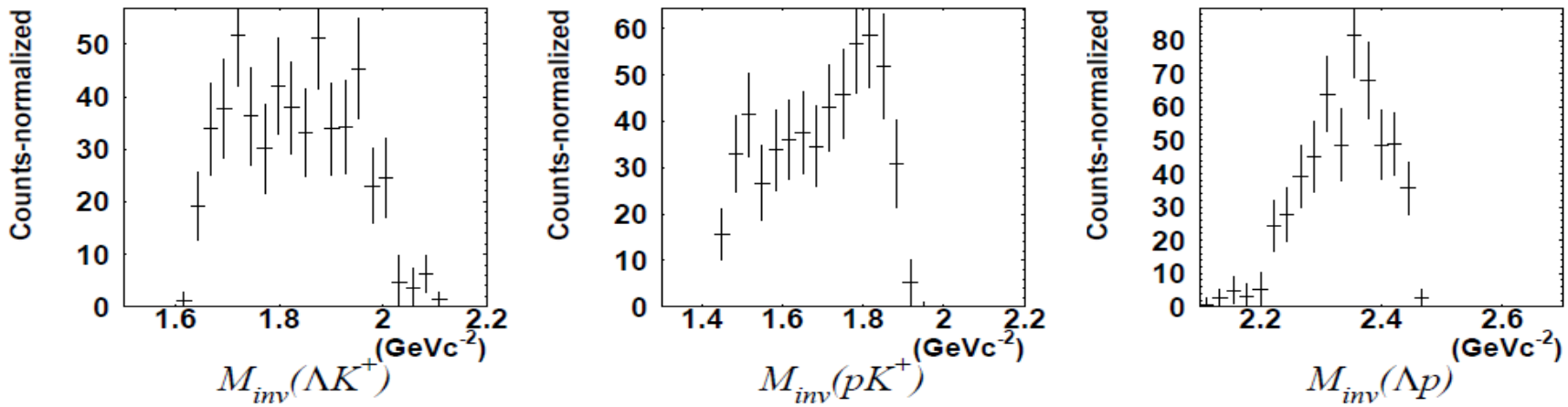

Momentum Region	Signal Events	Background Events
0.0 - 0.5 GeV/c	177	146
0.5 - 0.6 GeV/c	150	136
0.6 - GeV/c	577	577
Total	903	859

Angular Distributions

Center-of-mass angle

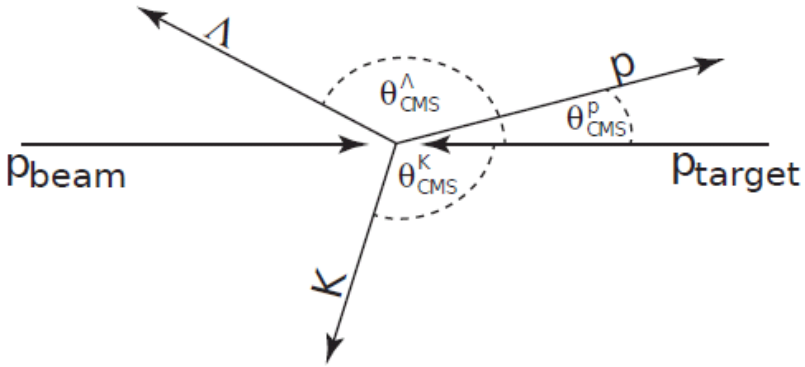

Gottfried-Jackson Angle

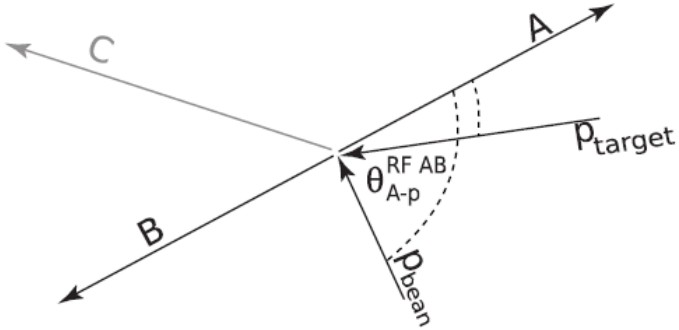

Helicity Angle

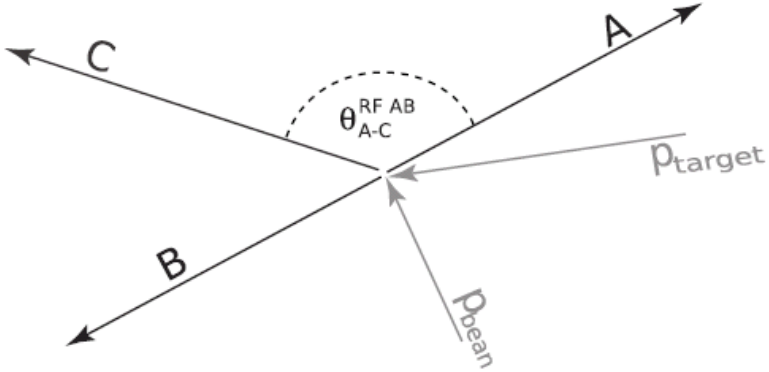

Simulation Packages

Phase Space Simulation

Incoherent Cocktail

$$p + p \rightarrow p + K^+ + \Lambda$$

$$p + p \rightarrow p + N^{+*}(\rightarrow K^+ + \Lambda)$$

Angular Distribution

Fröhlich et al.
PoS ACAT2007 (2007)

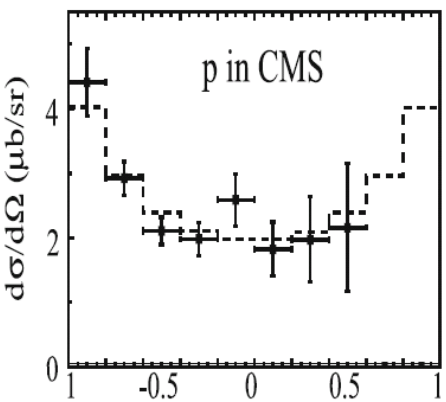

M. Abdel-Bary et al.,
Eur.Phys.J A46(2010)

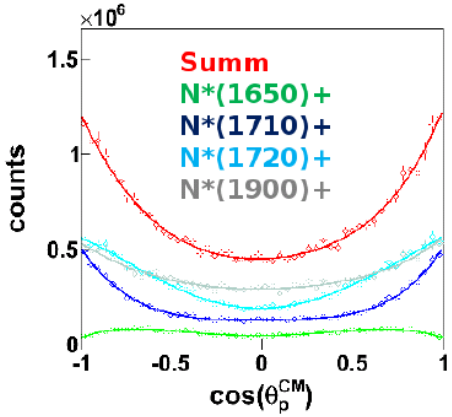

E. Epple,
Diss. TUM (2014)

Transport Modell - UrQMD

Quantum Molecular Dynamics

Description of all particle correlations

Production of p K^+ Λ via Resonances (N^{+*})

The UrQMD Model,
http://urqmd.org/ 2013

Phase Space Simulation

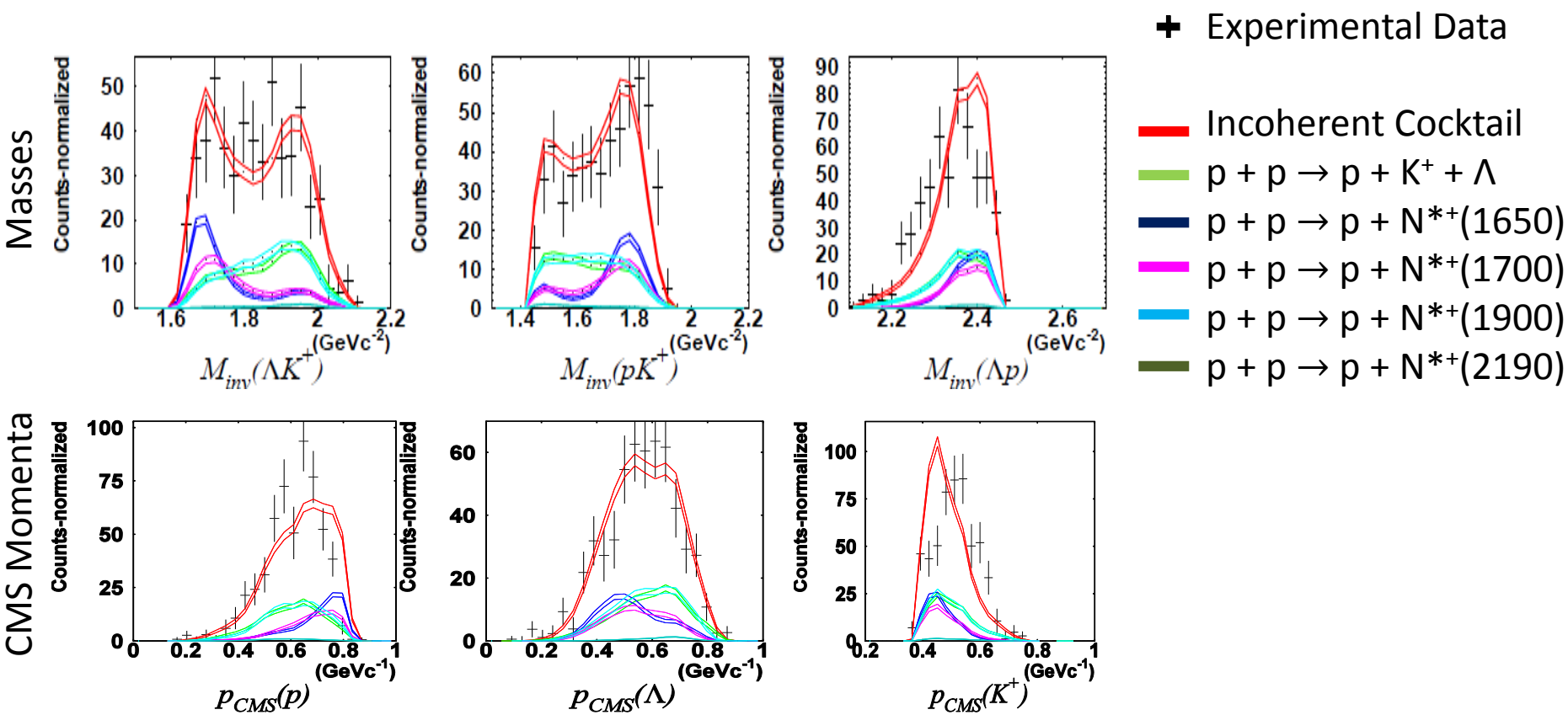

Phase Space Simulation

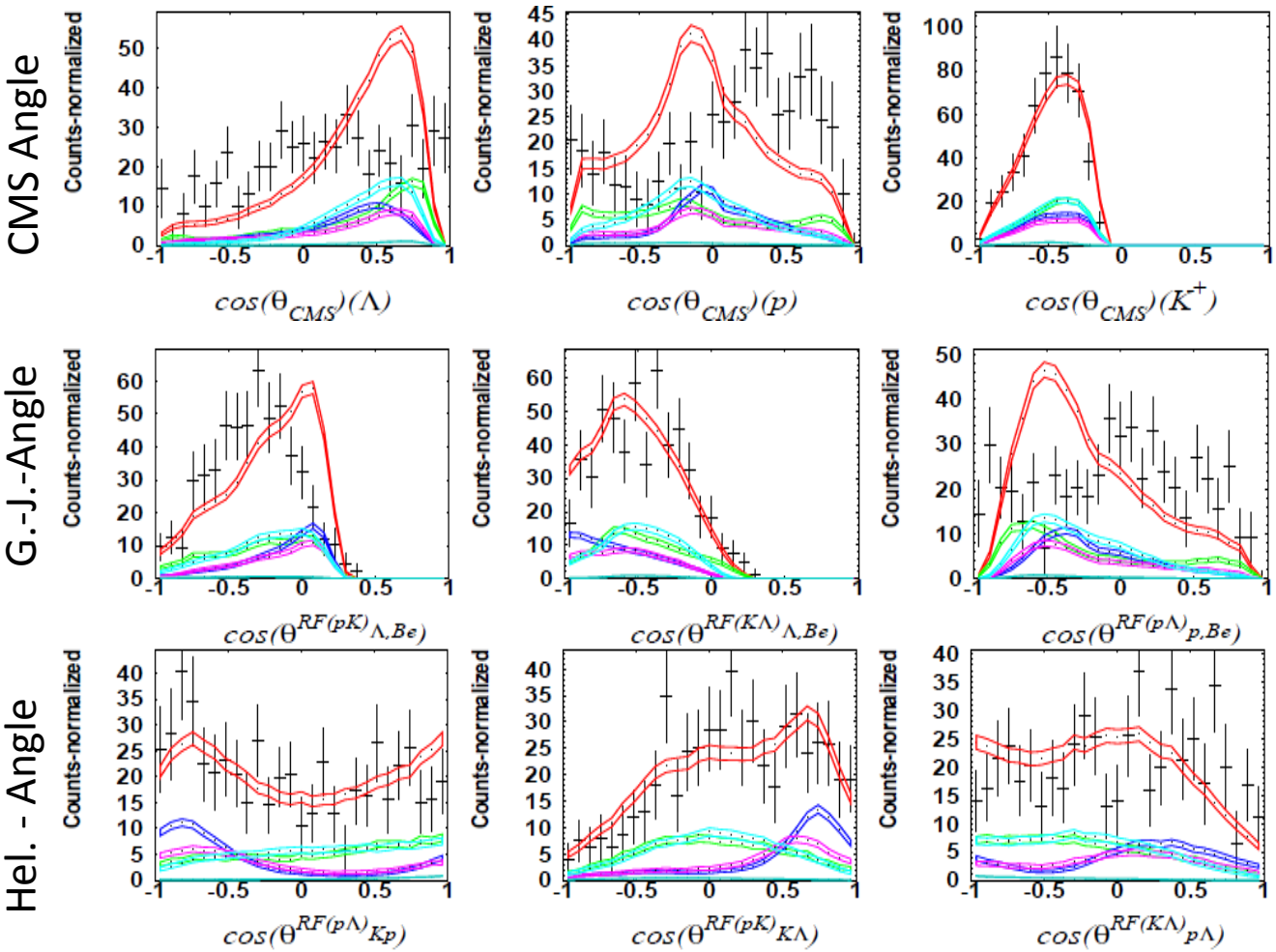

✚ Experimental Data

Incoherent Cocktail

$p + p \rightarrow p + K^+ + \Lambda$

$p + p \rightarrow p + N^{*+}(1650)$

$p + p \rightarrow p + N^{*+}(1700)$

$p + p \rightarrow p + N^{*+}(1900)$

$p + p \rightarrow p + N^{*+}(2190)$

Phase Space Simulation

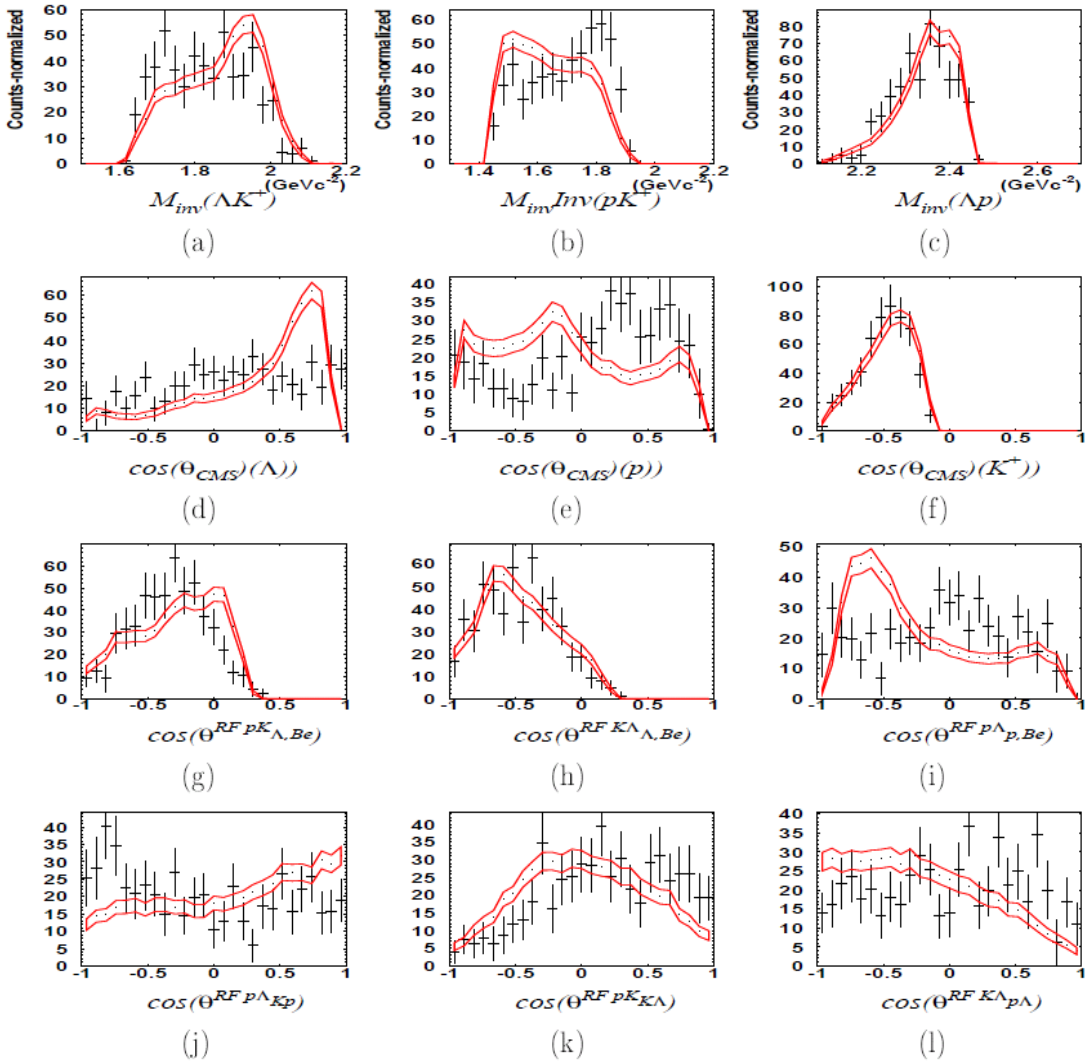

✚ Experimental Data

pp -> p K^+ Λ Phase Space Simulation

Phase Space Simulation

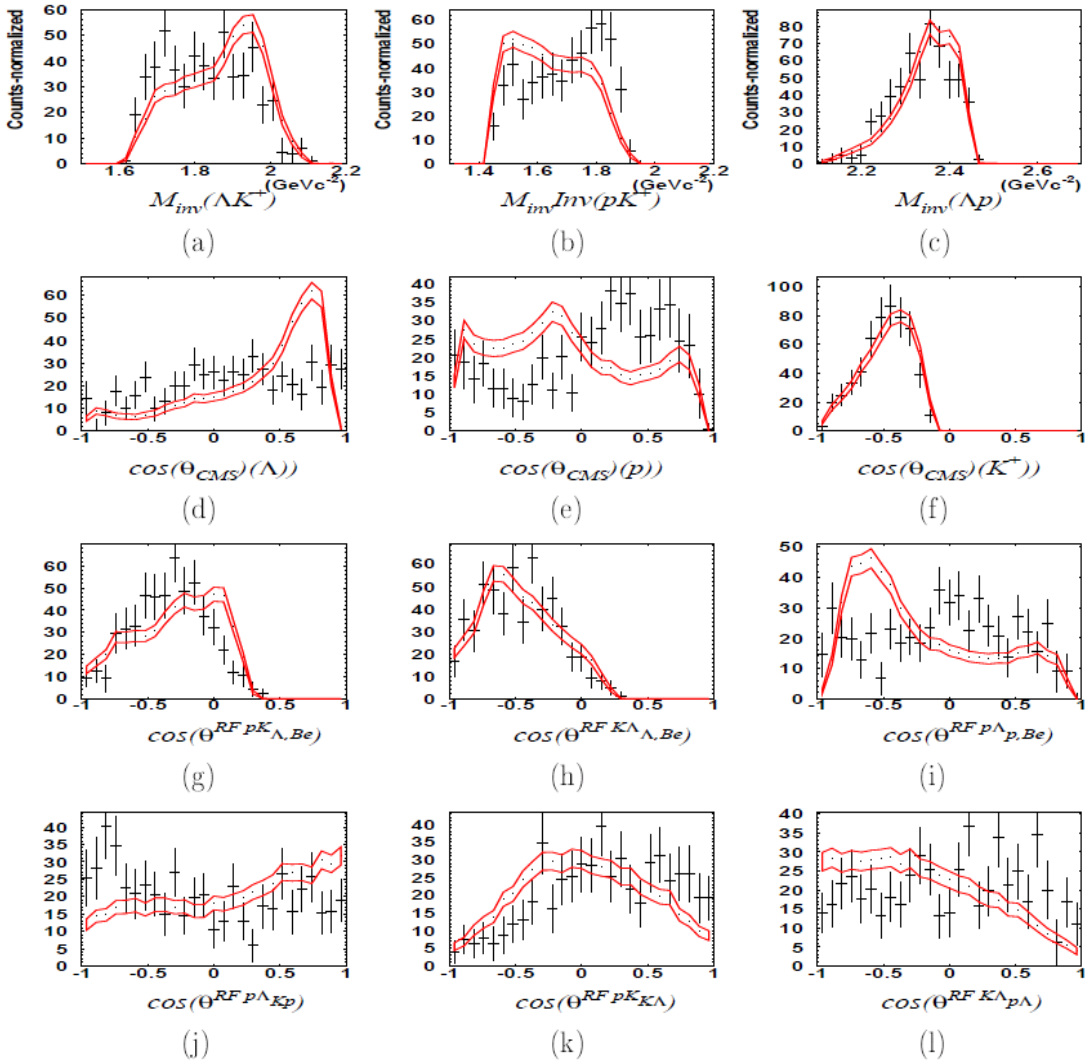

✚ Experimental Data

pp -> p K^+ Λ Phase Space Simulation

Phase Space Simulation

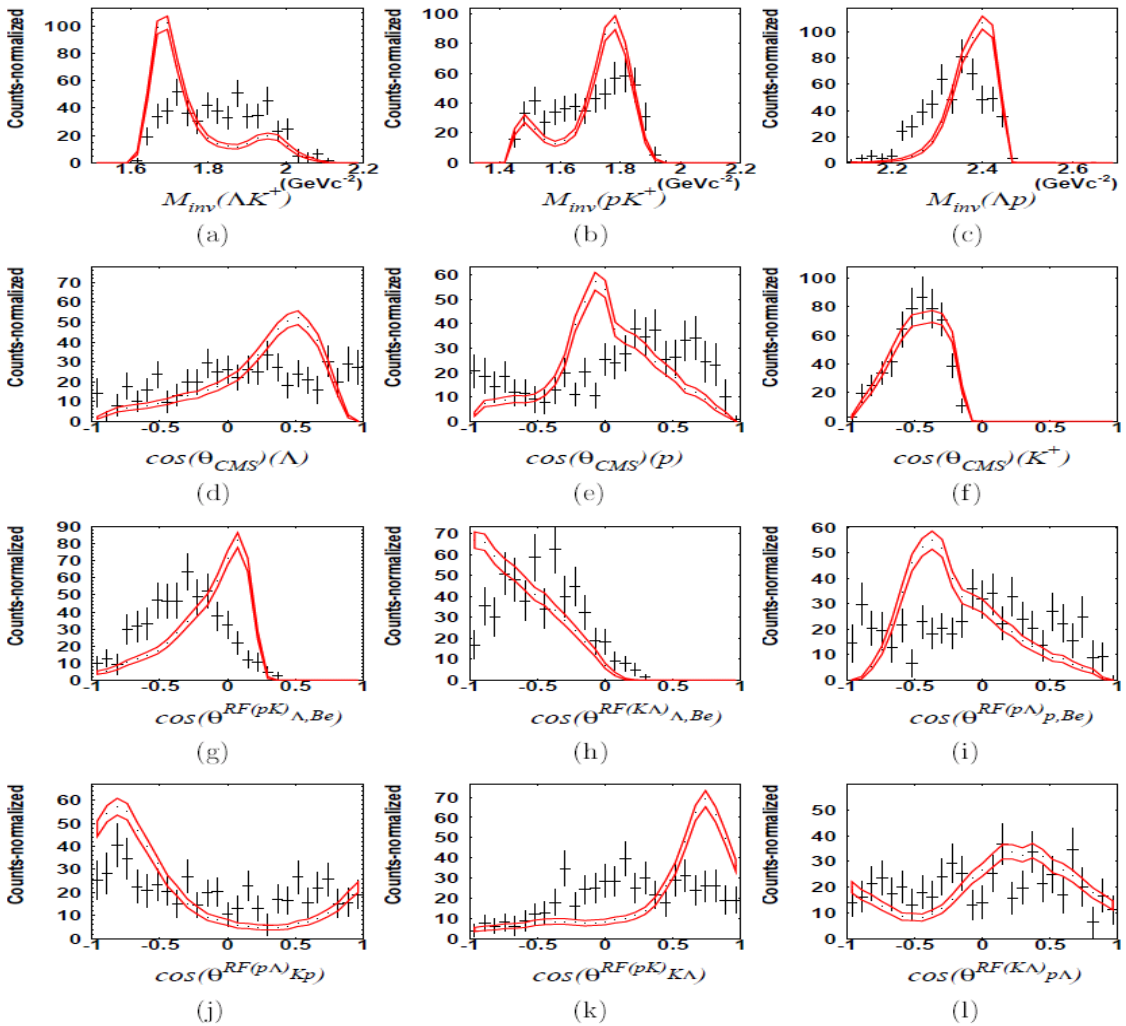

- ✚ Experimental Data
- ▬ pp -> p N*$^+$(1650) Phase Space Simulation

Phase Space Simulation

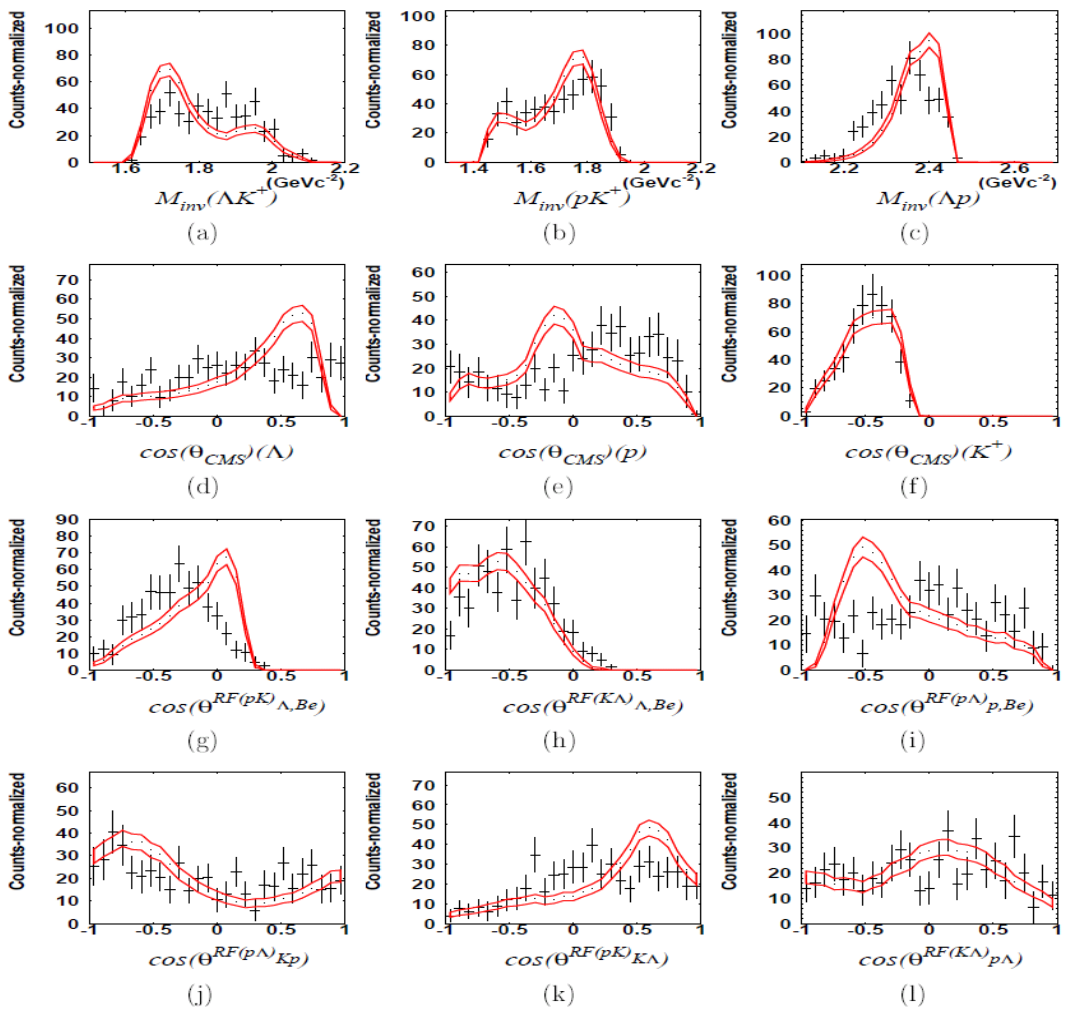

- ✚ Experimental Data
- pp -> p N*$^+$(1700) Phase Space Simulation

Phase Space Simulation

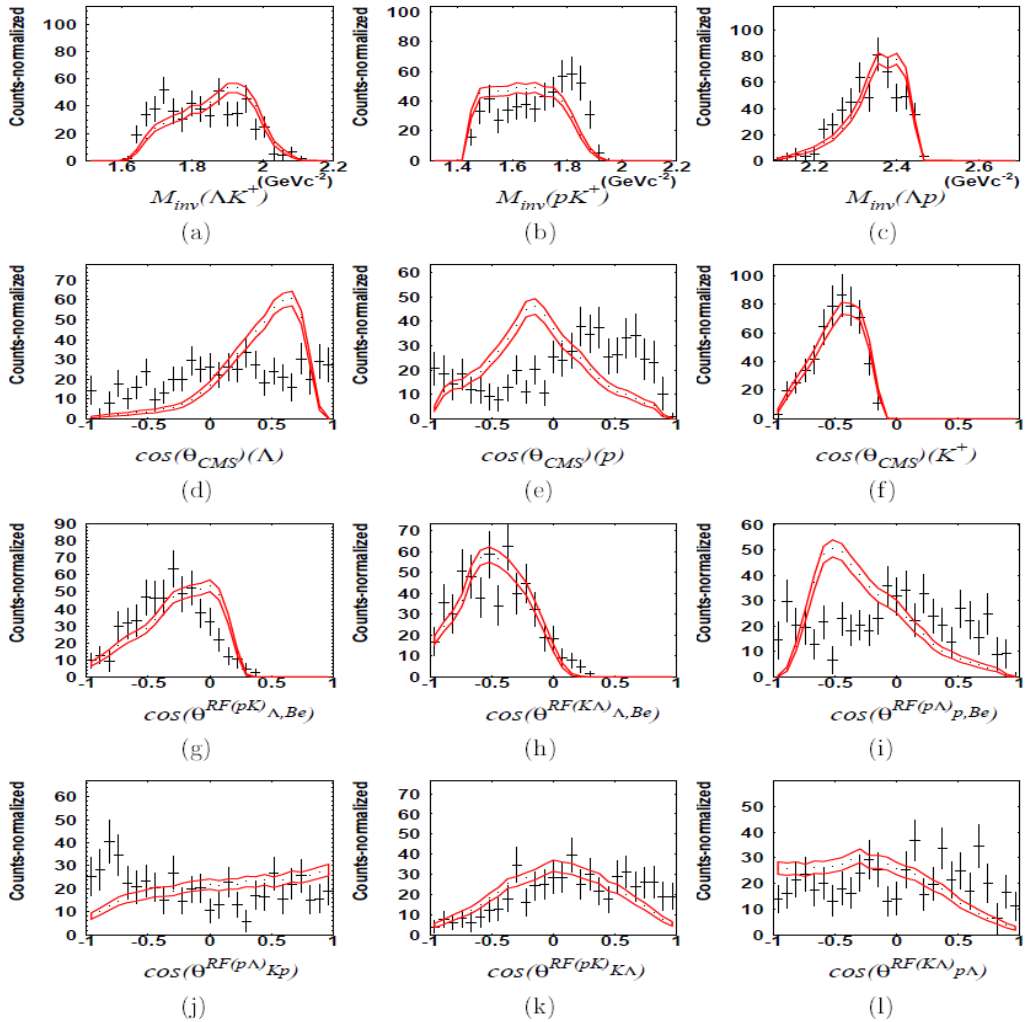

- Experimental Data
- pp -> p N*$^+$(1900) Phase Space Simulation

Phase Space Simulation

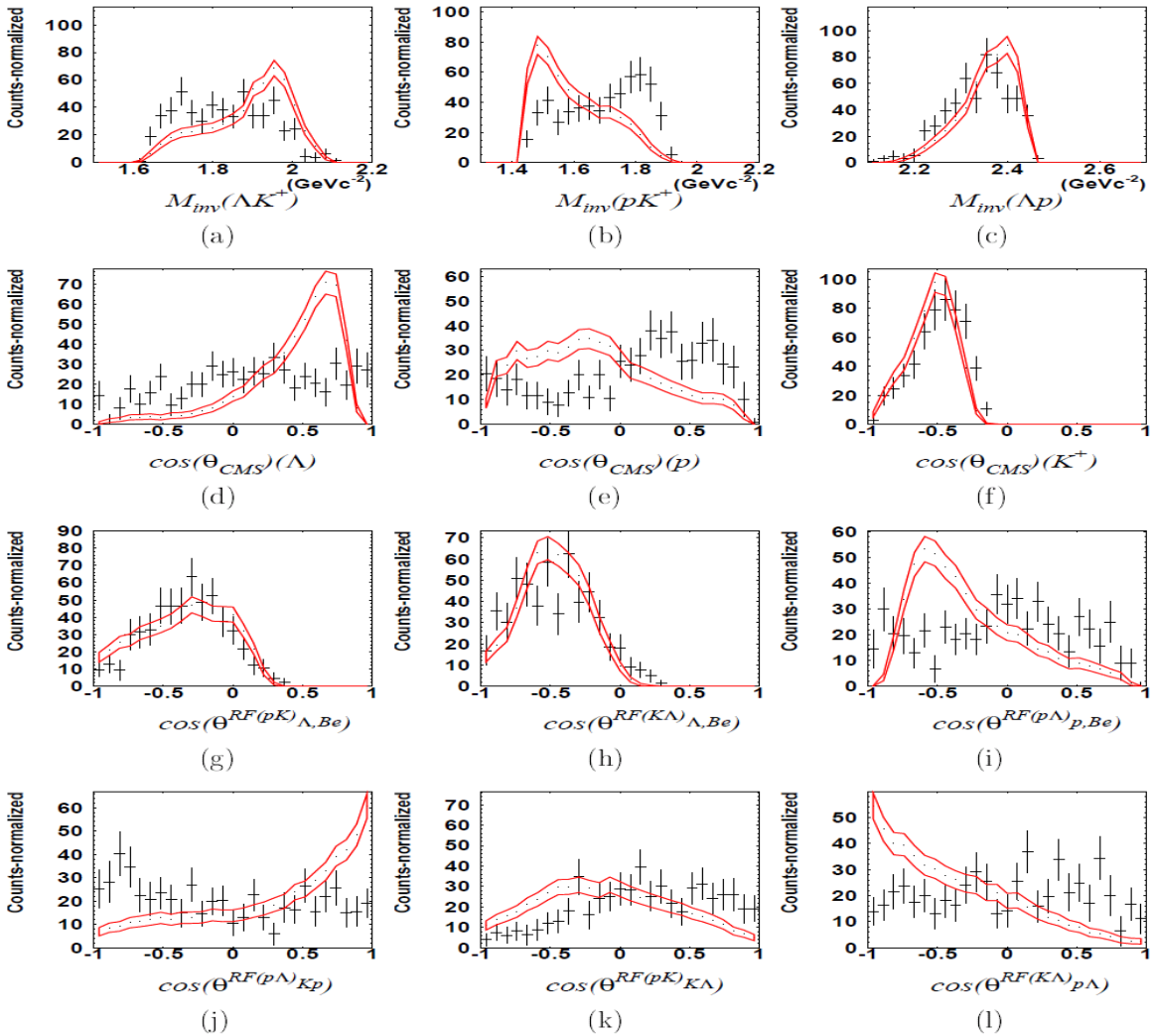

- ✚ Experimental Data
- pp -> p N*$^+$(2190) Phase Space Simulation

UrQMD Simulation

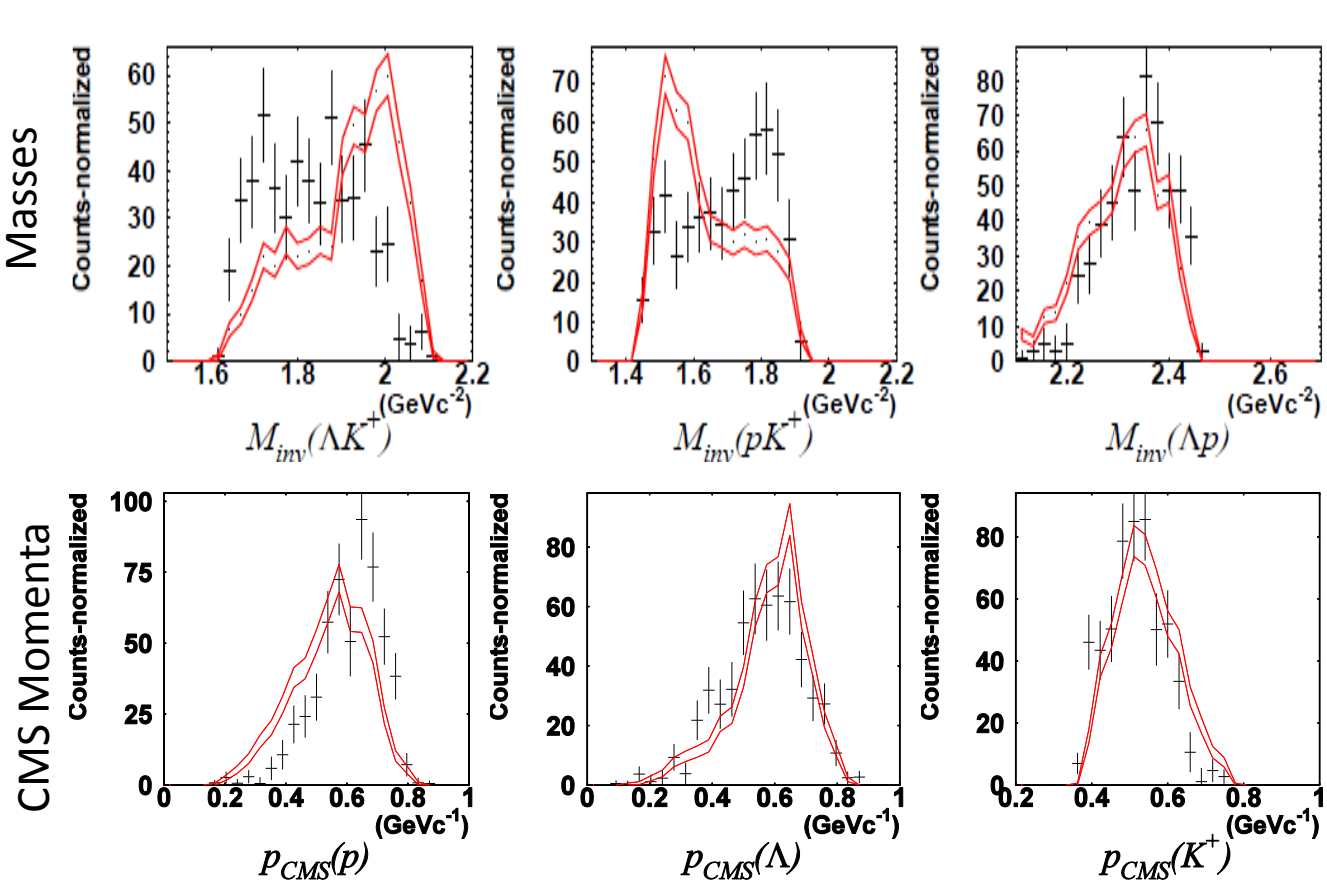

✚ Experimental Data

UrQMD Simulations

UrQMD Simulation

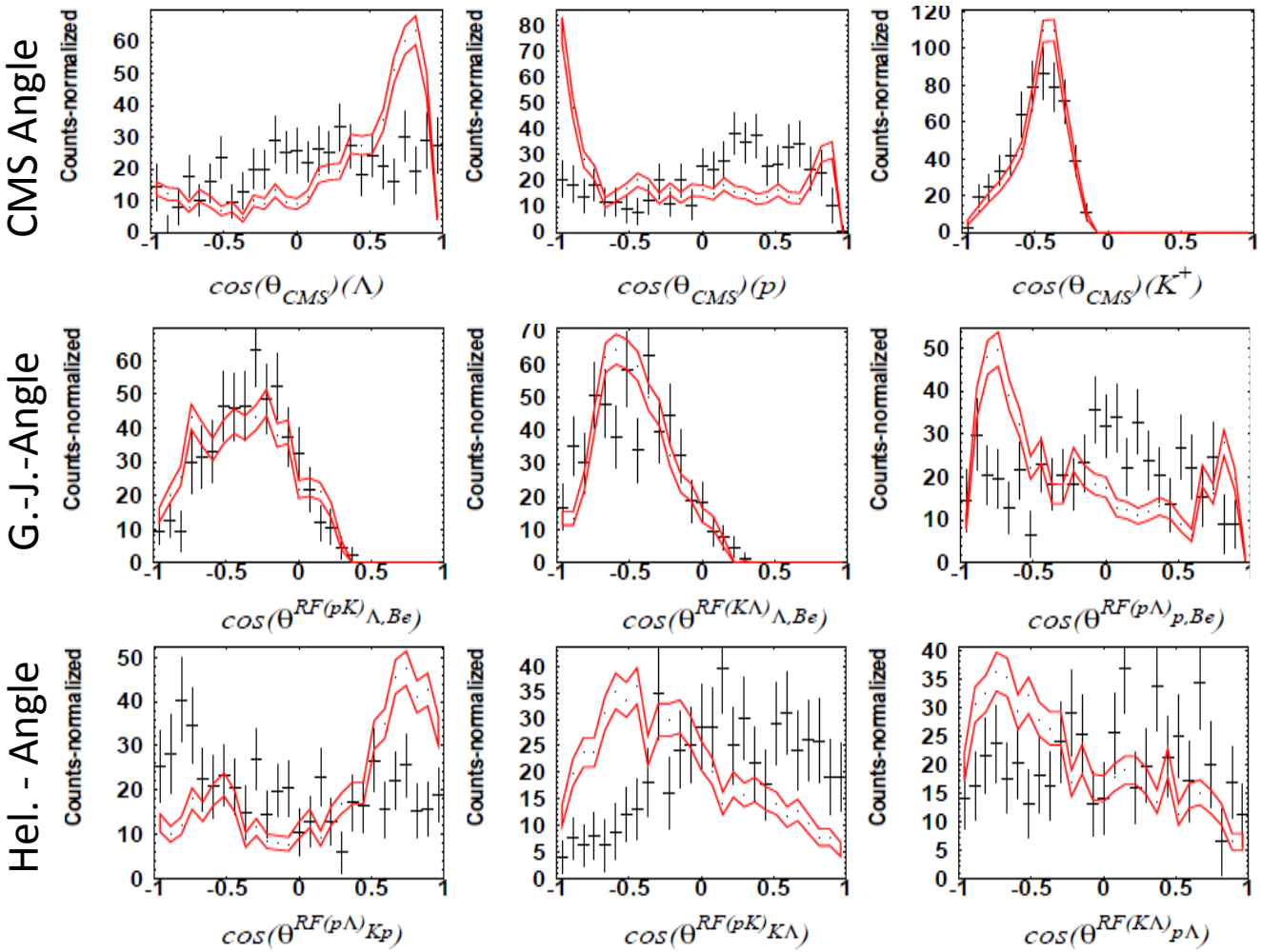

✚ Experimental Data

UrQMD Simulations

$A =$ N^* (1875) waves enabled (1) / disabled (0)

$B =$ N^* (1880) waves enabled (1) / disabled (0)

$C =$ N^* (1895) waves enabled (1) / disabled (0)

$D =$ N^* (1900) waves enabled (1) / disabled (0)

$E =$ $pK^+\Lambda$ non resonant waves enabled (1) / disabled (0)

$F = 5$ Initial proton states: ${}^1S_0, {}^1D_2, {}^3P_0, {}^3P_1, {}^3P_2, {}^3F_3$

$= 4$ Initial proton states: ${}^1S_0, {}^1D_2, {}^3P_0, {}^3P_1, {}^3P_2$

$= 3$ Initial proton states: ${}^1S_0, {}^1D_2, {}^3P_0, {}^3P_1$

$= 2$ Initial proton states: ${}^1S_0, {}^1D_2, {}^3P_0$

$= 1$ Initial proton states: ${}^1S_0, {}^1D_2$

$= 0$ Initial proton states: ${}^1S_0$

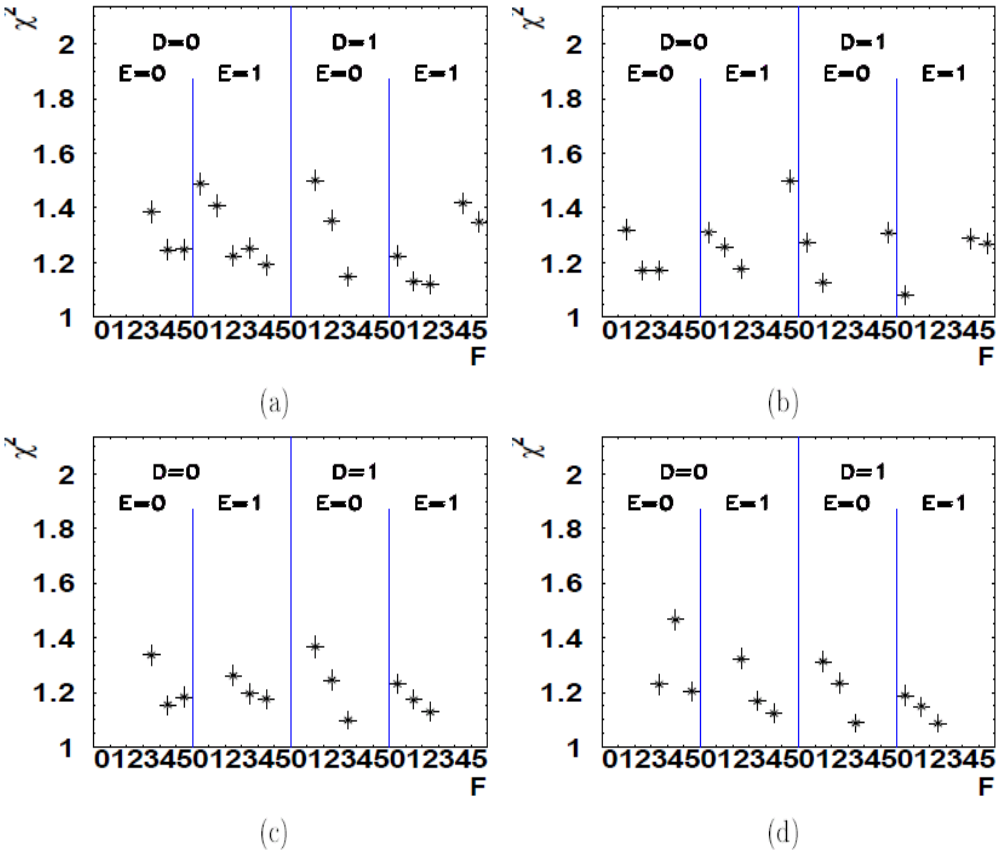

PWA Results in 4π

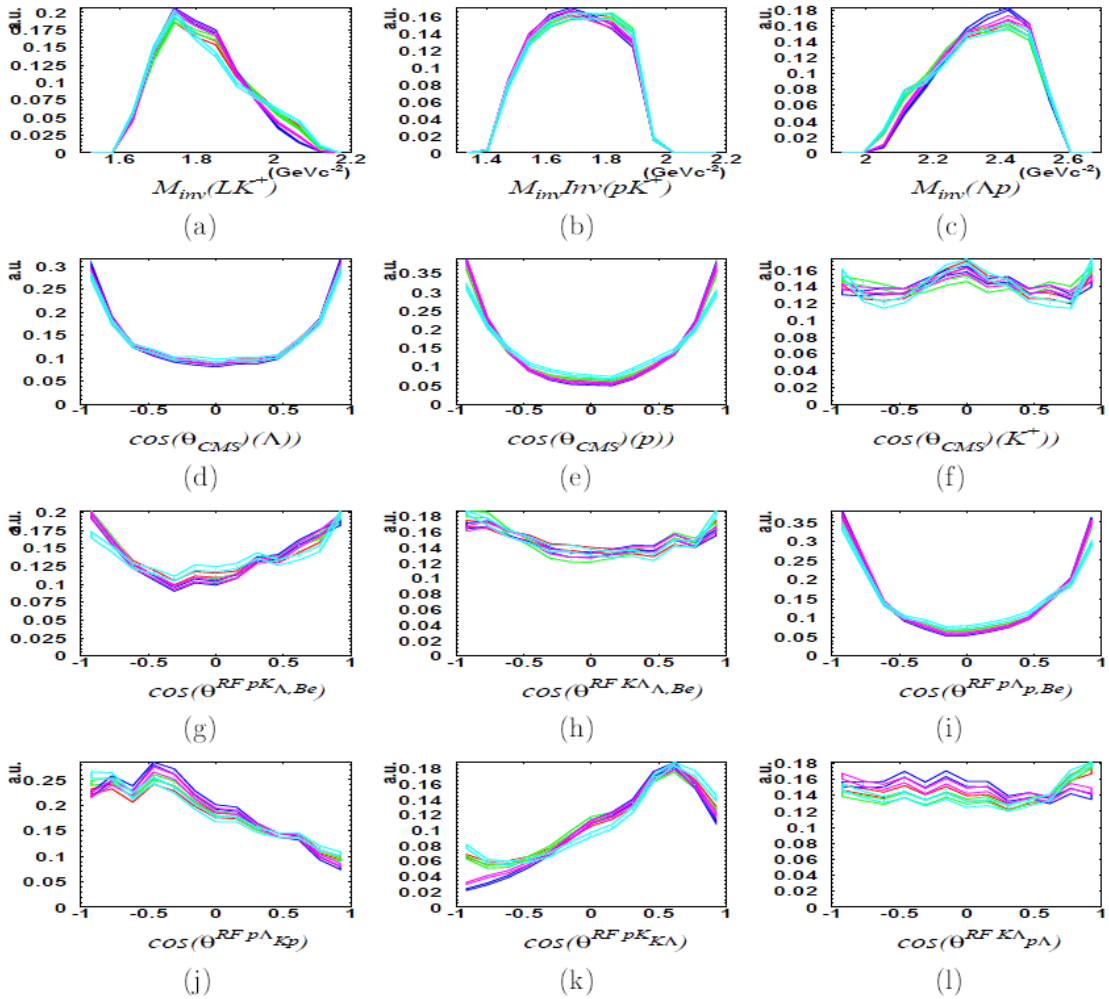

ppK$^-$ Upper Limit Determination

Exclusion limit:

$$p_\mu > \alpha\,(1 - p_0)$$

$$p_\mu = \int_{\chi^2_{signal}}^{\infty} f_\nu(\chi^2)\,d\chi^2$$

Scan of different mass and width
M(ppK$^-$) = 2.205-2.305 GeV/c²
Γ(ppK$^-$) = 20-80 MeV/c²
And 5 best solution of PWA w/o ppK$^-$

Background Solution: 000113

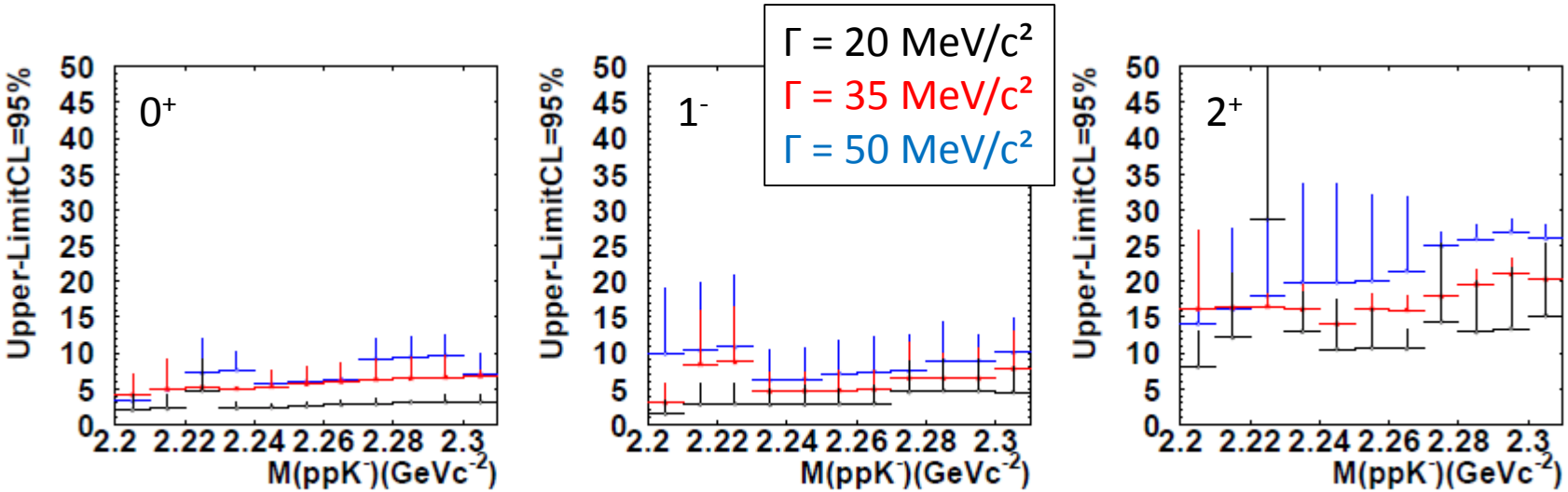

Bonn-Gatchina PWA

Cross Section for the production of three particles out of a collision of two particle

$$d\sigma = \frac{(2\pi)^4 |A|^2}{4|\boldsymbol{k}|\sqrt{s}} d\Phi_3(P, q_1, q_2, q_3) \ , \qquad P = k_1 + k_2$$

http://pwa.hiskp.uni-bonn.de/

A.V. Anisovich, V.V. Anisovich, E. Klempt, V.A. Nikonov and A.V. Sarantsev
Eur. Phys. J. A 34, 129152 (2007)

A - reaction amplitude
k – 3-momentum of the initial particle in the CM
s – $P^2=(k_1+k_2)^2$
$d\Phi_3(P,q_1,q_2,q_3)$ – invariant three-particles phase space

The decomposition of the scattering amplitude into partial waves can be written as follows:

$$A = \sum A^{\alpha}_{tr}(s) Q^{in}_{\mu_1 \ldots \mu_J}(SLJ) A_{2b}(i, S_2 L_2 J_2)(s_i) \times \ Q^{fin}_{\mu_1 \ldots \mu_J}(i, S_2 L_2 J_2 S' L' J) \ . \quad (2)$$

S,L,J – spin, orbital mom. and total angular momentum of the pp system
S_2,L_2,J_2 – spin, orbital mom. and total angular momentum of the two particle system in fin. state
S',L' – spin, orbital mom. between the two particle system and the third particle with four mom. q_i
multiindex α – possible combinations of the S, L,J, S_2, L_2, J_2, S', L' and i
A_{tr}^{α} (s) - transition Amplitude
A_{2b}^{α} (i,S_2,L_2,J_2) – rescattering process in he final two-particle channel (e.g. production of Δ)

Fitting Procedure

The transition Amplitude is parameterized as follows

$$A_{tr}^{\alpha}(s) = \left(a_1^{\alpha} + a_3^{\alpha}\sqrt{s}\right) e^{i a_2^{\alpha}}$$

This is a log-likelihood minimization on an event-by-event base

What we included to model the $PK^+\Lambda$ process:

N* Resonances in the PDG with measured decay into $K^+\Lambda$

Notation in PDG	Old notation	Mass [GeV/c^2]	Width [GeV/c^2]	$\Gamma_{\Lambda K}/\Gamma_{All}$ %
N(1650) $\frac{1}{2}^-$	N(1650)S_{11}	1.655	0.150	3-11
N(1710) $\frac{1}{2}^+$	N(1710)P_{11}	1.710	0.200	5-25
N(1720) $\frac{3}{2}^+$	N(1720)D_{13}	1.720	0.250	1-15
N(1875) $\frac{3}{2}^-$	N(1875)D_{13}	1.875	0.220	4± 2
N(1880) $\frac{1}{2}^+$	N(1880)P_{11}	1.870	0.235	2± 1
N(1895) $\frac{1}{2}^-$	N(1895)S_{11}	1.895	0.090	18± 5
N(1900) $\frac{3}{2}^+$	N(1900)P_{13}	1.900	0.250	0-10

And the production of $pK^+\Lambda$ via non resonant waves

Systematic

N* content

No.	Combination
0	N(1650), N(1710), N(1720)
1	N(1650), N(1710), N(1720), N(1900)
2	N(1650), N(1710), N(1720), N(1895)
3	N(1650), N(1710), N(1720), N(1880)
4	N(1650), N(1710), N(1720), N(1875)
5	N(1650), N(1710), N(1720), N(1900), N(1880)
6	N(1650), N(1710), N(1720), N(1900), N(1895)
7	N(1650), N(1710), N(1720), N(1900), N(1875)
8	N(1650), N(1710), N(1720), N(1895), N(1880)
9	N(1650), N(1710), N(1720), N(1895), N(1875)
10	N(1650), N(1710), N(1720), N(1880), N(1875)

non-resonant content

No.	Combination
0	no non-resonant waves
1	$(pL)(^1S_0) - K$
2	previous wave + $(pL)(^3S_1) - K$
3	previous waves + $(pL)(^1P_1) - K$
4	previous waves + $(pL)(^3P_0) - K$
5	previous waves + $(pL)(^3P_1) - K$
6	previous waves + $(pL)(^3P_2) - K$
7	previous waves + $(pL)(^1D_2) - K$
8	previous waves + $(pL)(^3D_1) - K$
9	previous waves + $(pL)(^3D_2) - K$

Best Solutions

No. of N* combination	No. of non-res. waves	Log-likelih.
0	7	-2415.74
1	**8**	**-2708.49**
2	8	-2524.59
3	**8**	**-2712.49**
4	4	-2671.05
5	8	-2310.4
6	**9**	**-2754.37**
7	8	-2657.77
8	**8**	**-2734.97**
9	6	-2698.86
10	4	-2642.58

Solution inside WALL acceptance

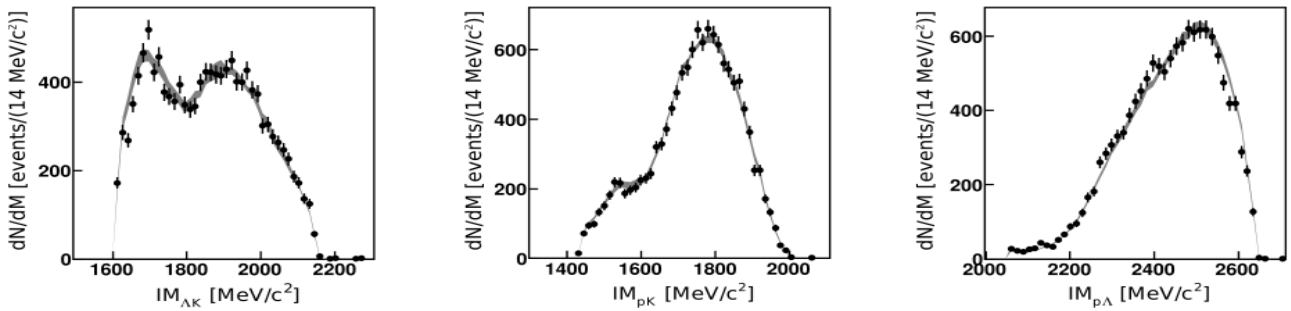

Figure 2.18: Two-particle masses for the **HADES data set** (black points) shown with the **four best PWA solutions** (gray band), obtained by a ?t to the HADES and WALL data.

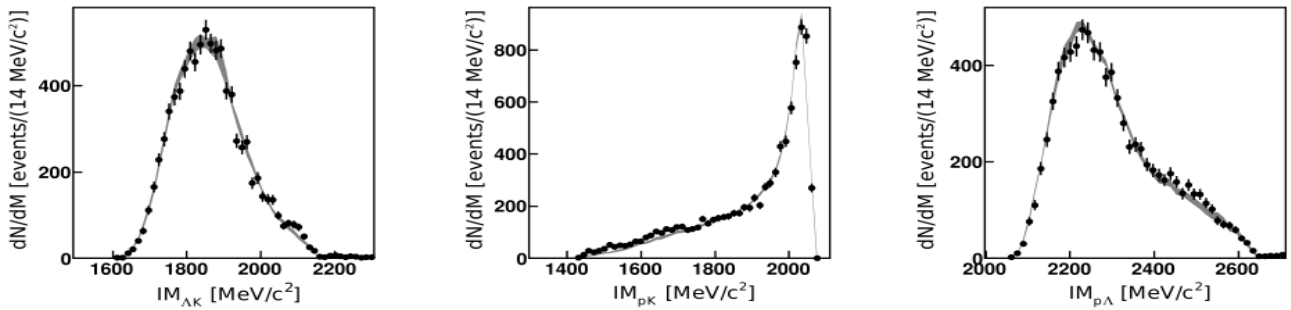

Figure 2.19: Two-particle masses for the **WALL data set** (black points) shown with the **four best PWA solutions** (gray band), obtained by a ?t to the HADES and WALL data.

PWA Results

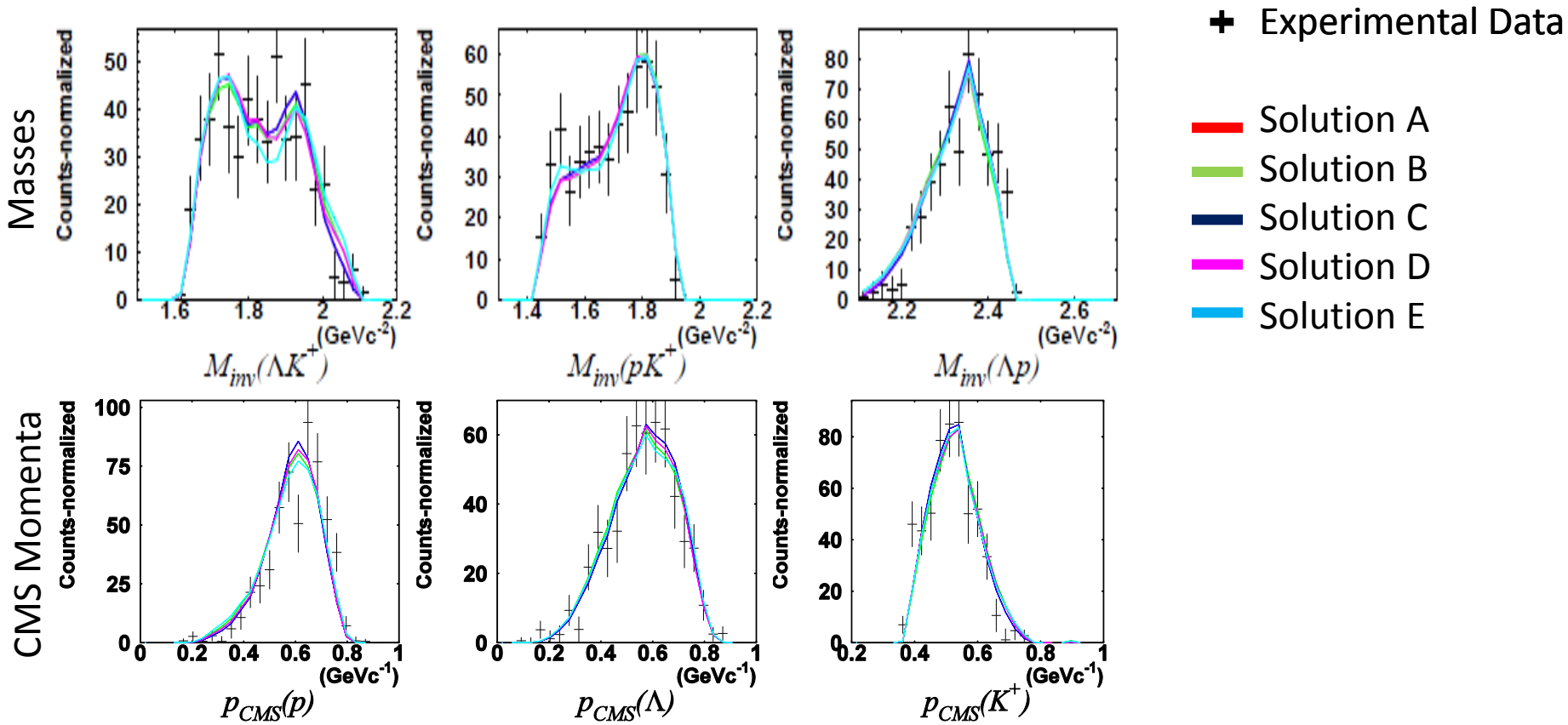
Masses
CMS Momenta
Counts-normalized
(GeVc^{-2})
(GeVc^{-1})
$M_{inv}(\Lambda K^+)$
$M_{inv}(pK^+)$
$M_{inv}(\Lambda p)$
$p_{CMS}(p)$
$p_{CMS}(\Lambda)$
$p_{CMS}(K^+)$
Experimental Data
Solution A
Solution B
Solution C
Solution D
Solution E

PWA Results

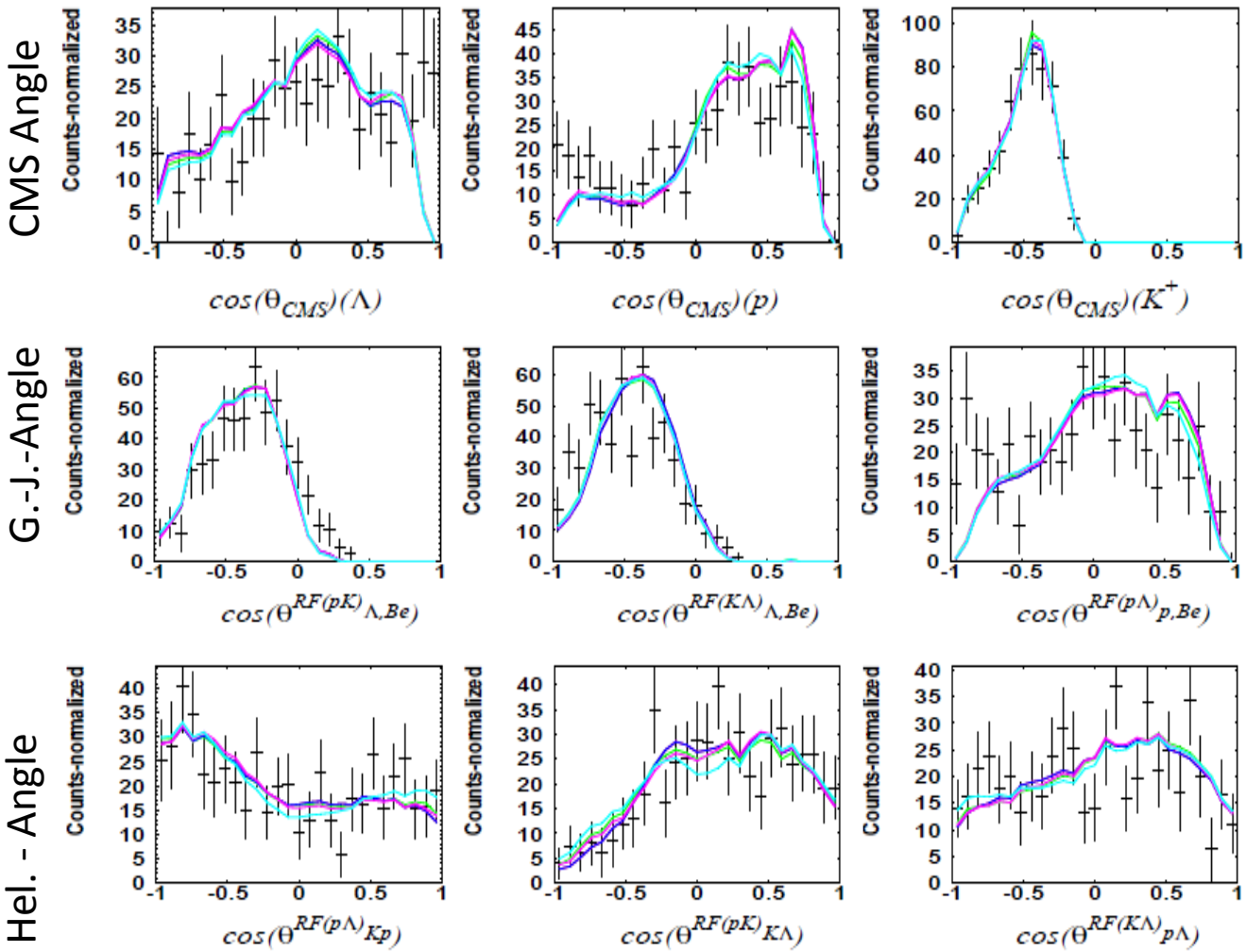

✚ Experimental Data

Solution A
Solution B
Solution C
Solution D
Solution E

Solution inside WALL acceptance

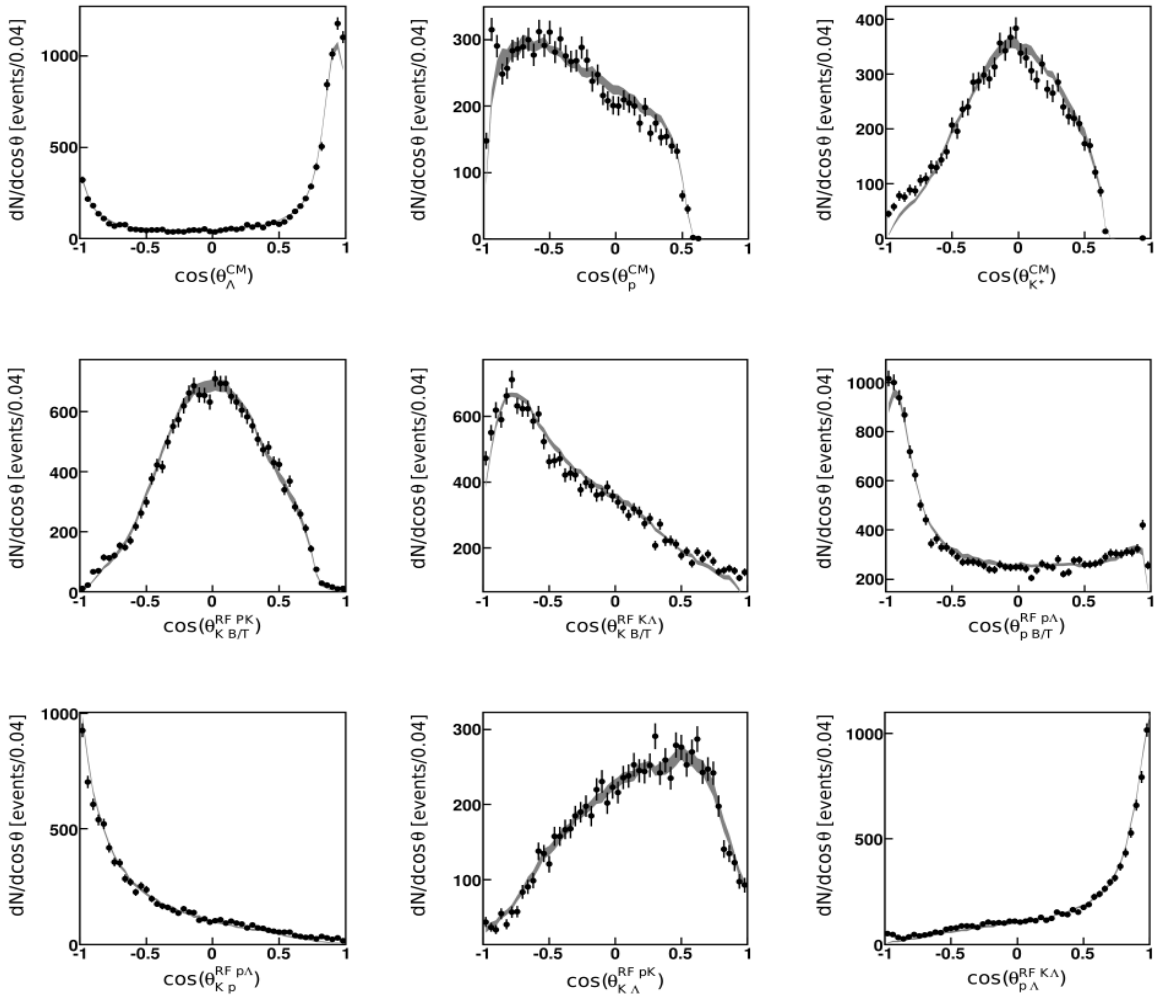

ppK^- Upper Limit

$p + p \rightarrow p + K^+ + \Lambda$
Total Cross Section

$$\sigma(\epsilon) = a\left(1 - \frac{s_0}{(\sqrt{s_0}+\epsilon)^2}\right)^b \left(\frac{s_0}{(\sqrt{s_0}+\epsilon)^2}\right)^c$$

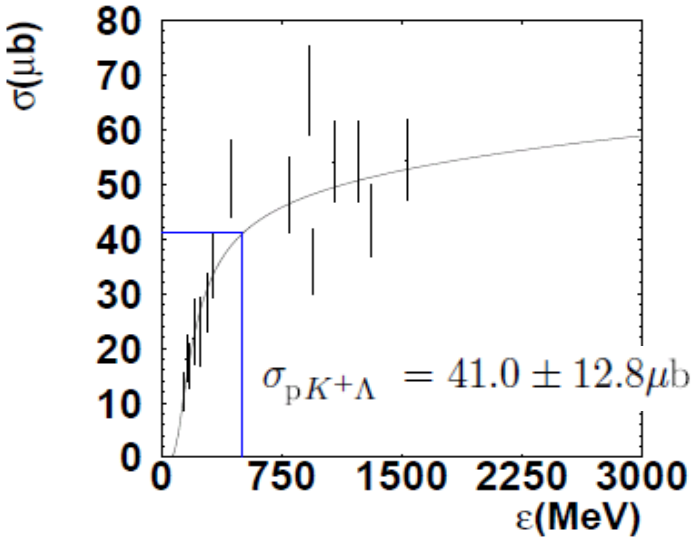

S. Abd El-Samad et al. Phys.Lett B688 (2010)
S. Abd El-Samad et al. Phys.Lett B632 (2007)
M. Abdel-Bary et al., Eur.Phys.J A46(2010)
S. Abd El-Samad et al., Eur.Phys.J A49(2013)
K.Fuchs et al., Springer Verlag 1985

Upper Limit Cross Section

Γ ($MeVc^{-2}$)	Cross Section (μb)
20	$7.6 \pm 1.2^{-3.5}$ - $22.4 \pm 3.6^{-10.7}$
35	$6.3 \pm 1.7^{-0.6}$ - $9.5 \pm 2.6^{-0.9}$
50	$10.2 \pm 1.8^{-4.5}$ - $11.6 \pm 3.4^{-0.6}$
60	$11.2 \pm 1.9^{-5.0}$ - $33.8 \pm 5.2^{-16.9}$
80	$11.4 \pm 2.7^{-3.8}$ - $35.9 \pm 5.7^{-17.4}$

High production cross section
even though no peak is visible

Peak structure suppressed
due to interference

Cross Check

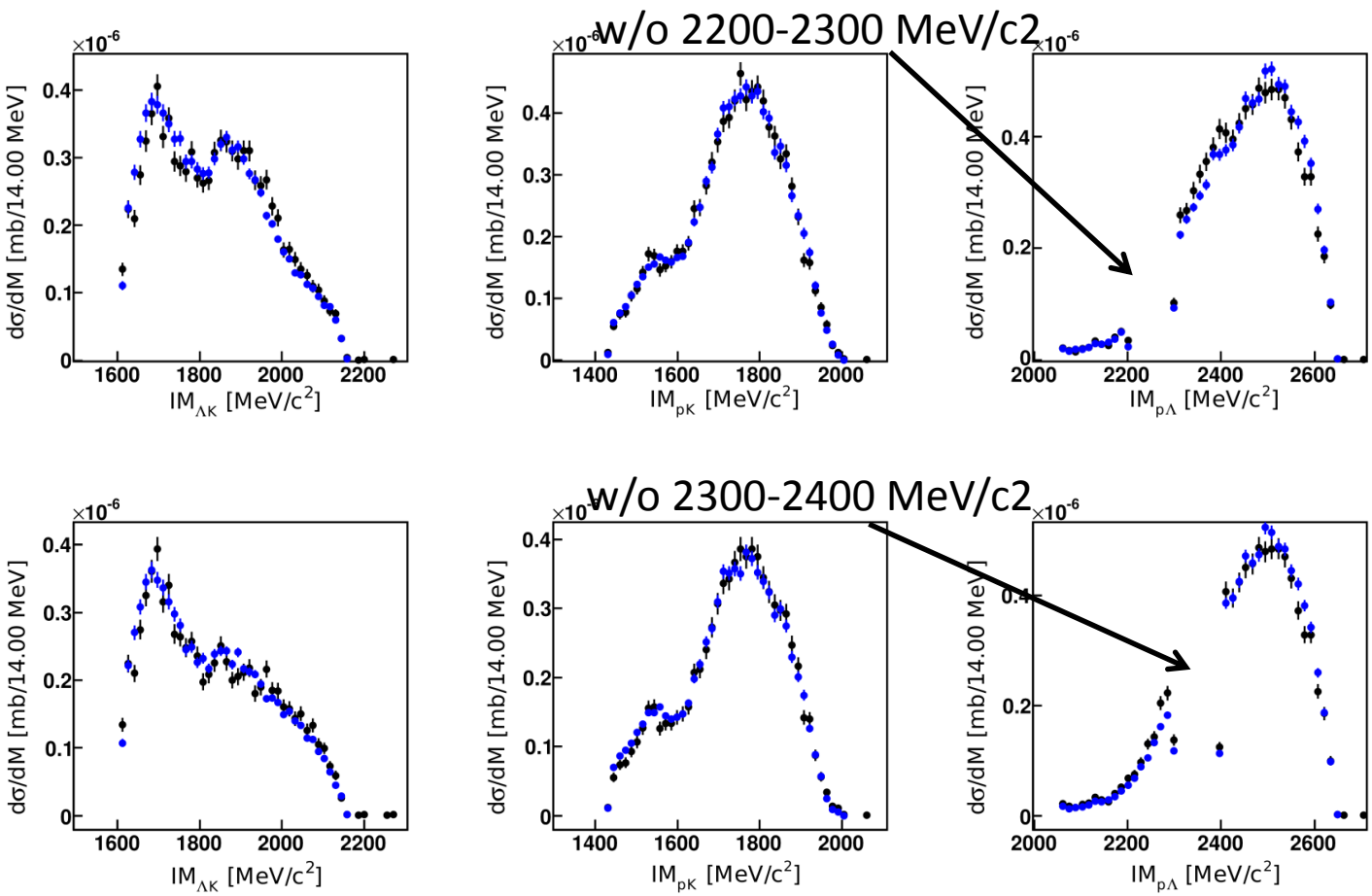
w/o 2200-2300 MeV/c2
w/o 2300-2400 MeV/c2
dσ/dM [mb/14.00 MeV]
IM$_{\Lambda K}$ [MeV/c^2]
IM$_{pK}$ [MeV/c^2]
IM$_{p\Lambda}$ [MeV/c^2]
×10^{-6}

Cross Check

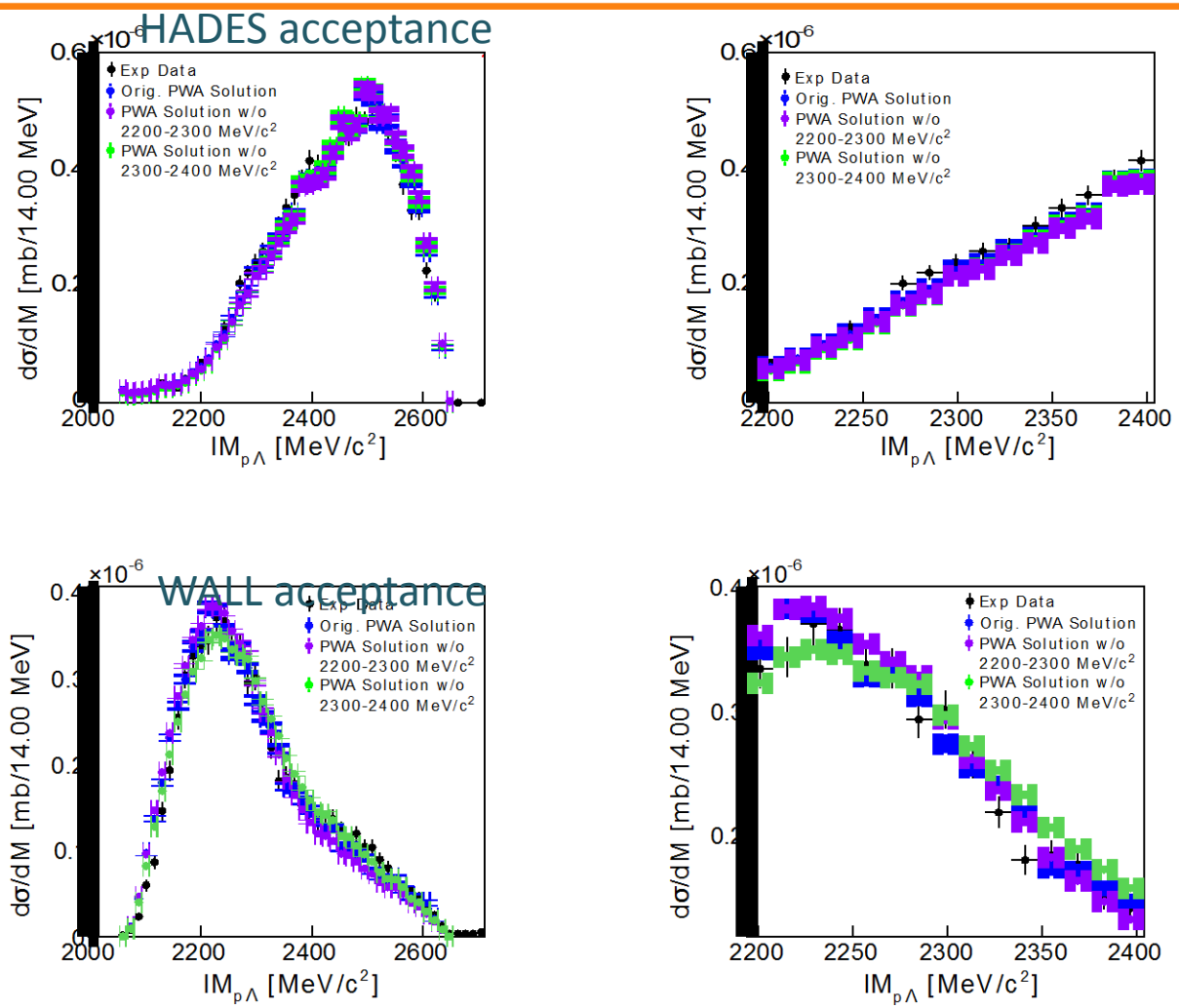

Good consistency among the results.
The solution is not biased by a possible signal in the excluded mass range

Result

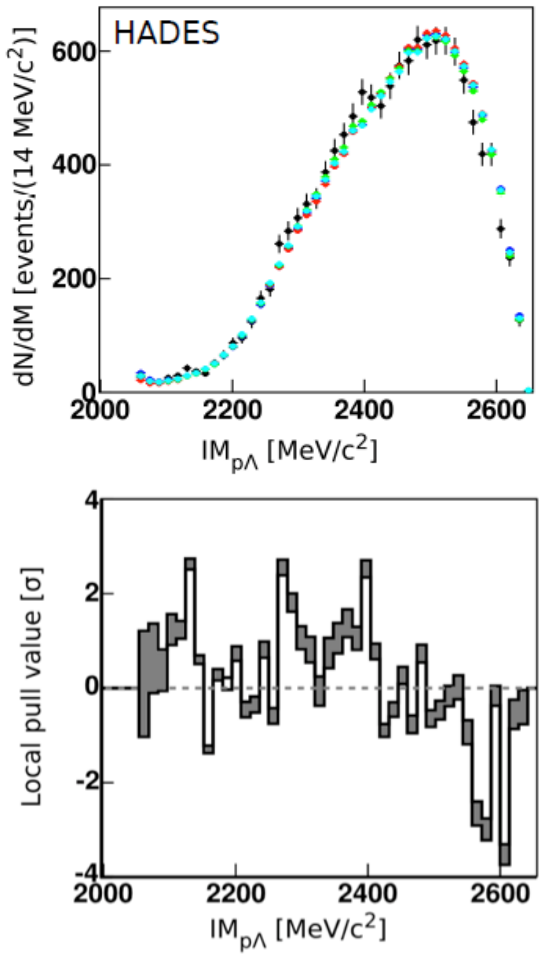

$$pull = \sum_{i=1}^{N_b} \frac{(m_i - \lambda_i)}{\lambda_i}$$

m_i are the number of measured events in the bin i
λ_i number of expected events in the bin according to the model
N_b is the number of bins

The best solution

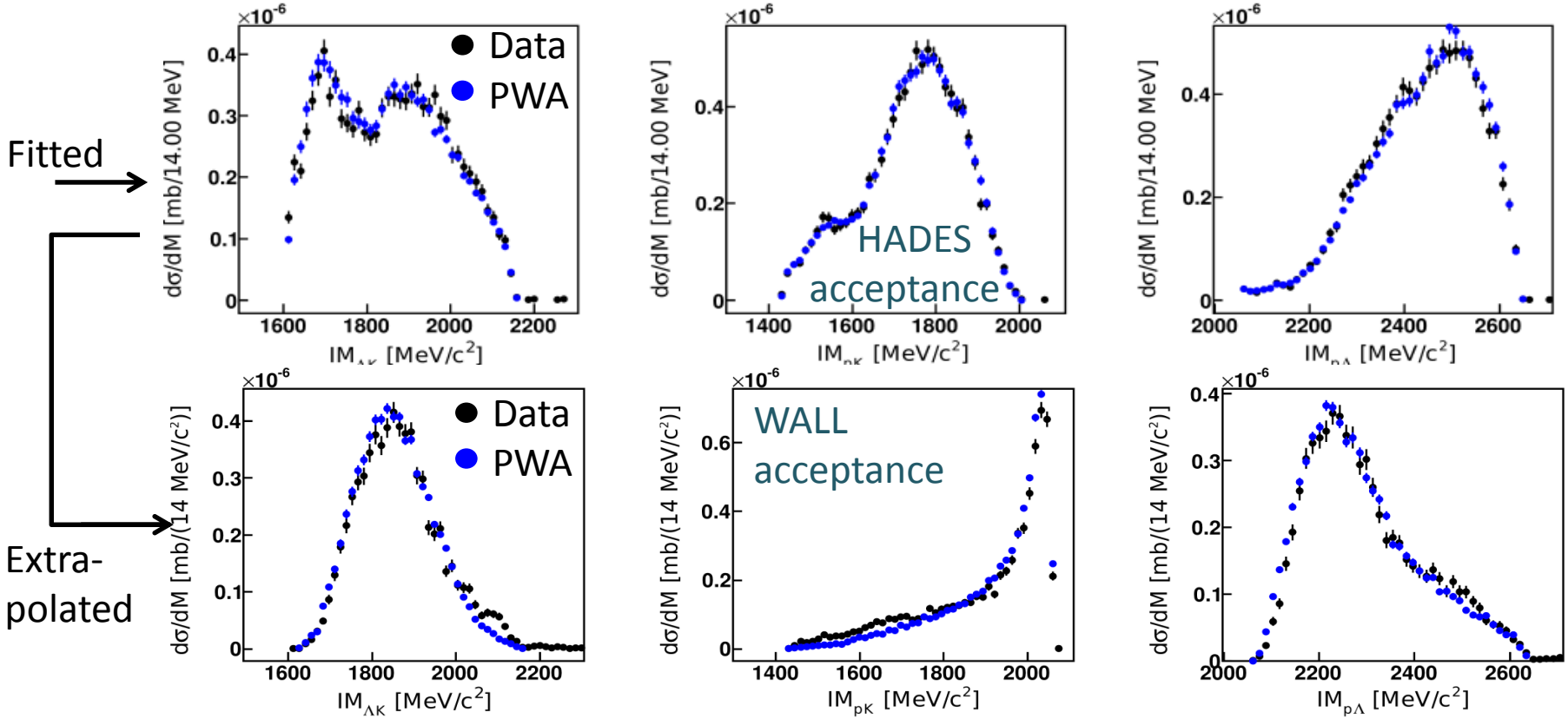

included resonances: N(1650), N(1710), N(1720), N(1900), N(1895)

Non-resonant waves:

$(pL)(^1S_0) - K$ $(pL)(^3S_1) - K$ $(pL)(^1P_1) - K$

$(pL)(^3P_0) - K$ $(pL)(^3P_2) - K$ $(pL)(^3P_1) - K$

$(pL)(^3D_1) - K$ $(pL)(^1D_2) - K$ $(pL)(^3D_2) - K$

Four Best PWA Solutions

Inside HADES acceptance

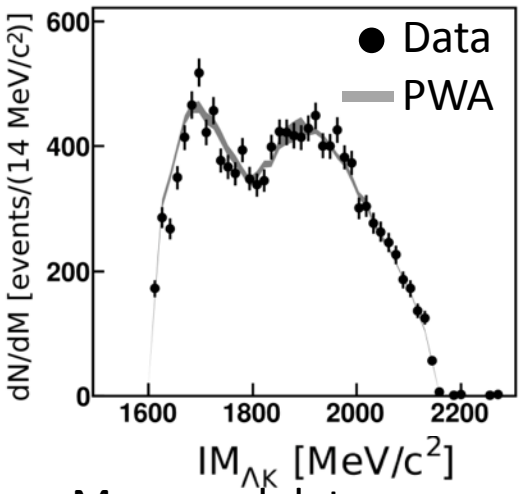

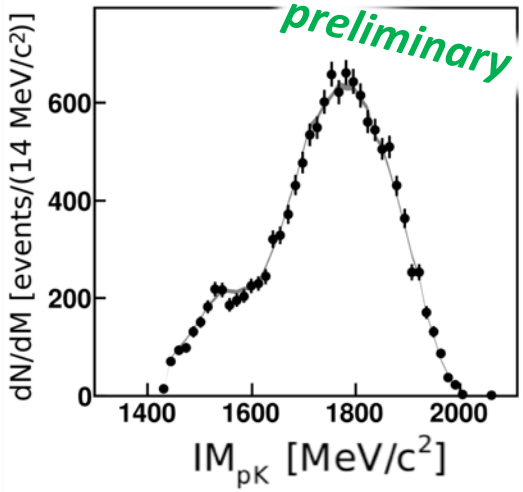

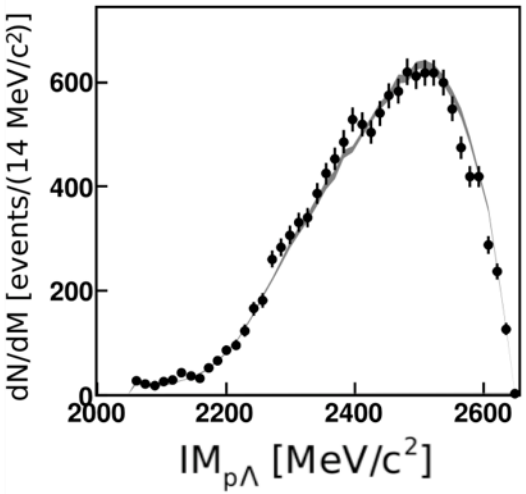

Measured data

PWA solutions

Name	N* combination
1/8	N(1650), N(1710), N(1720), N(1900)
3/8	N(1650), N(1710), N(1720), N(1880)
6/9	N(1650), N(1710), N(1720), N(1900), N(1895)
8/8	N(1650), N(1710), N(1720), N(1895), N(1880)

Test of the Null Hypothesis

Test of the Null Hypothesis

preliminary

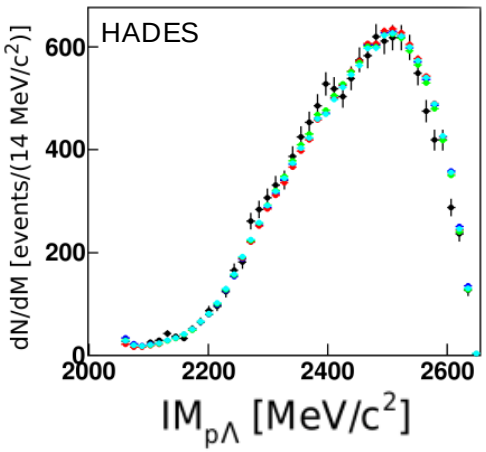

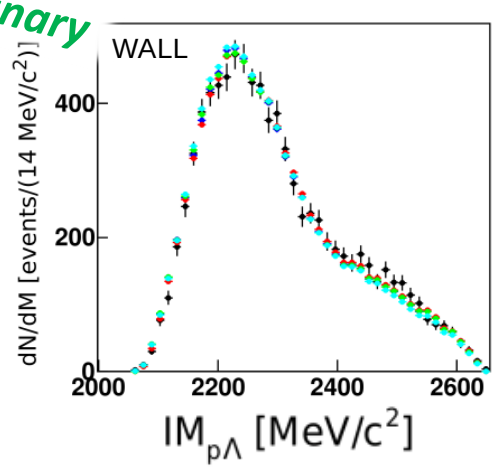

$$\chi^2_P = \frac{(m - \lambda)^2}{\lambda}$$

$$p - value = \int_{\chi^2_{P,d}}^{\infty} P(\chi^2, Ndf)\, d\chi^2$$

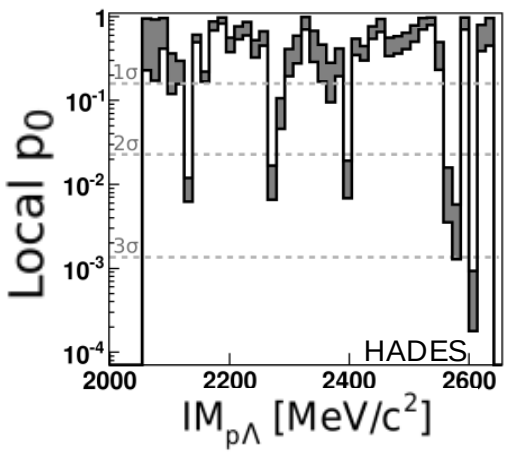

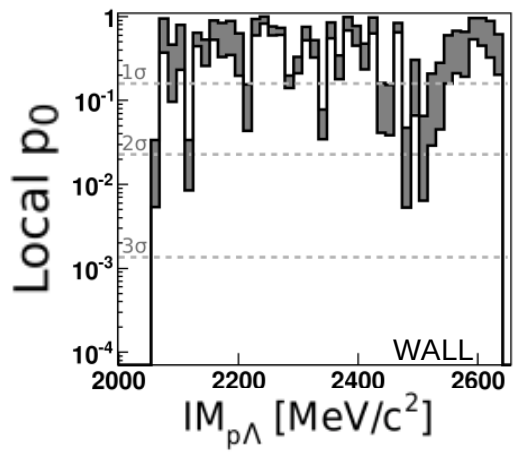

m_i measured events in bin i

λ_i expected events in bin i according to the model

Test of the Null Hypothesis

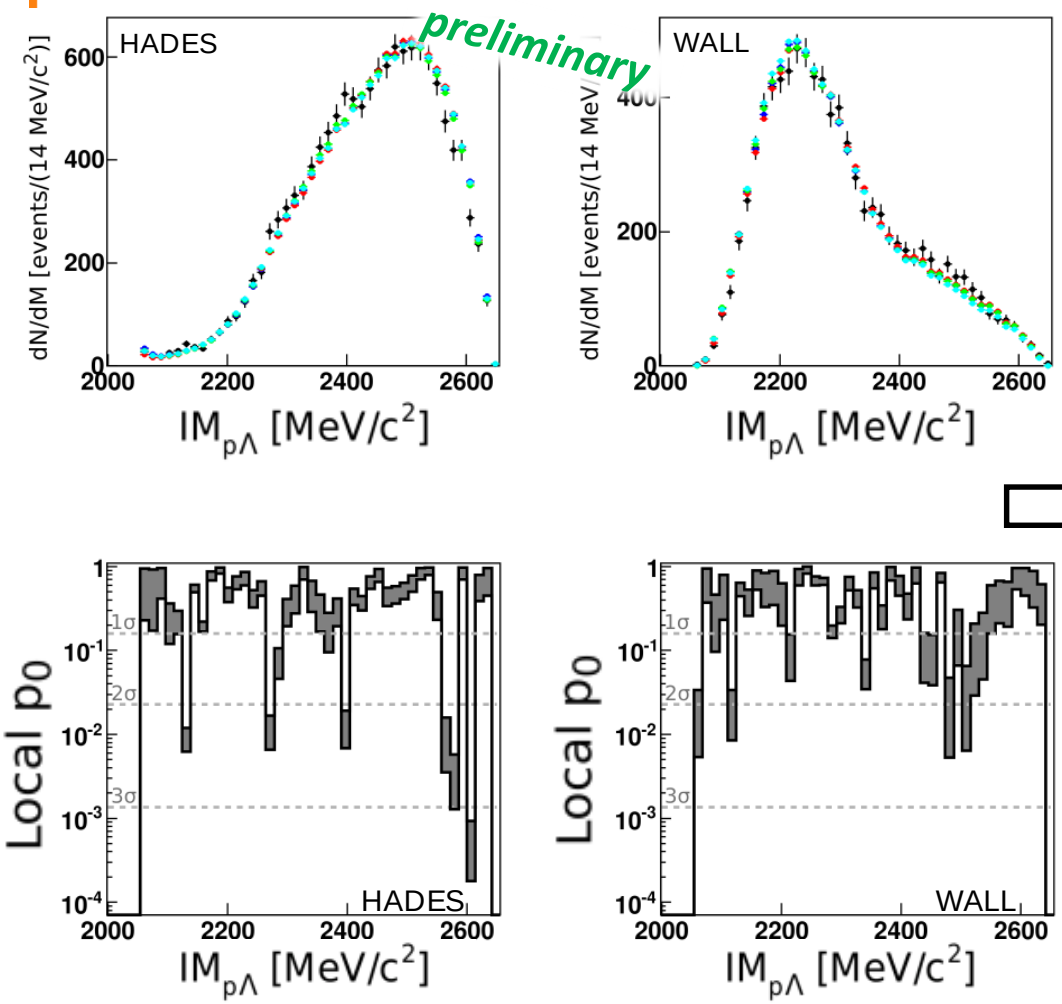

Combined result

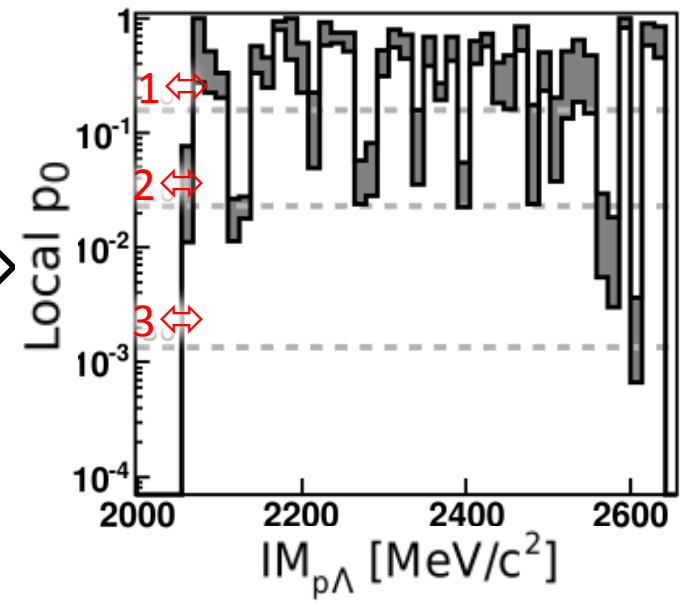

Test of the Null Hypothesis

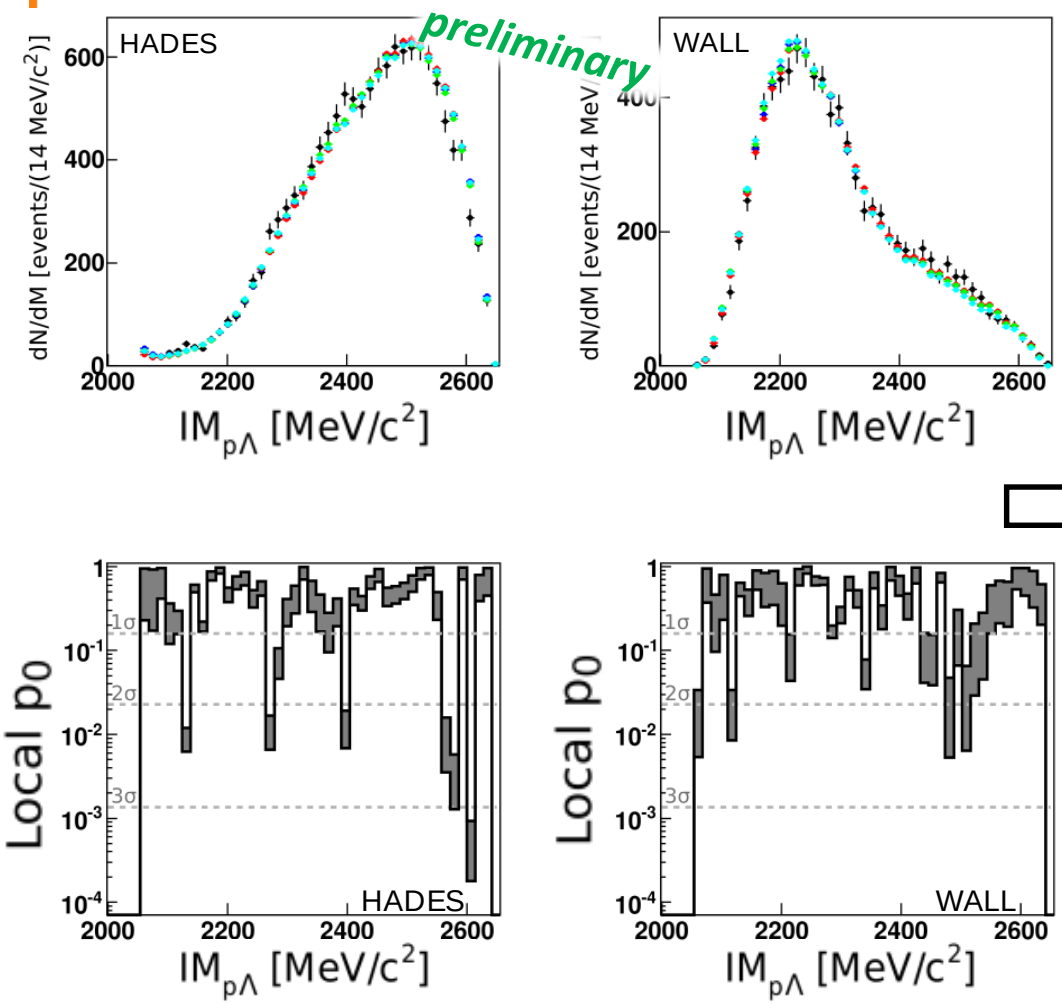

Combined result

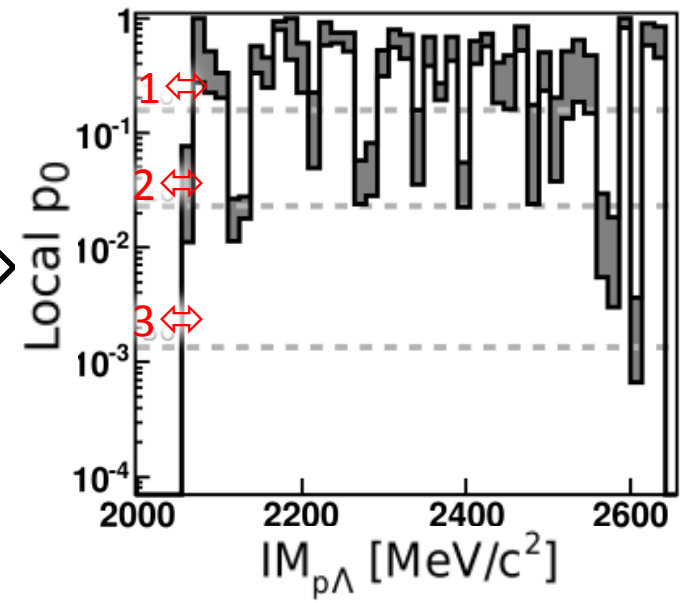

We found no new signal in the data

Test of the Null Hypothesis

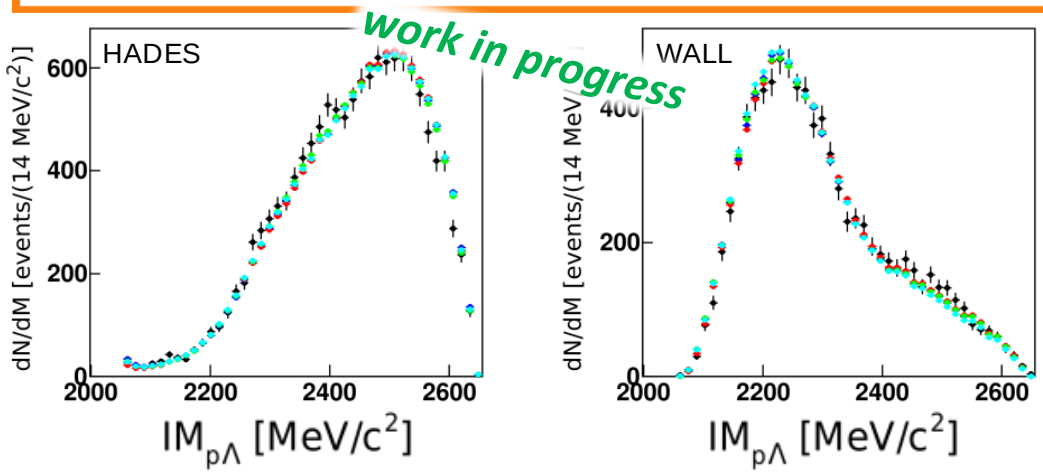

$$\chi^2_P = \frac{(m - \lambda)^2}{\lambda}$$

$$p - value = \int_{\chi^2_{P,d}}^{\infty} P(\chi^2, Ndf) d\chi^2$$

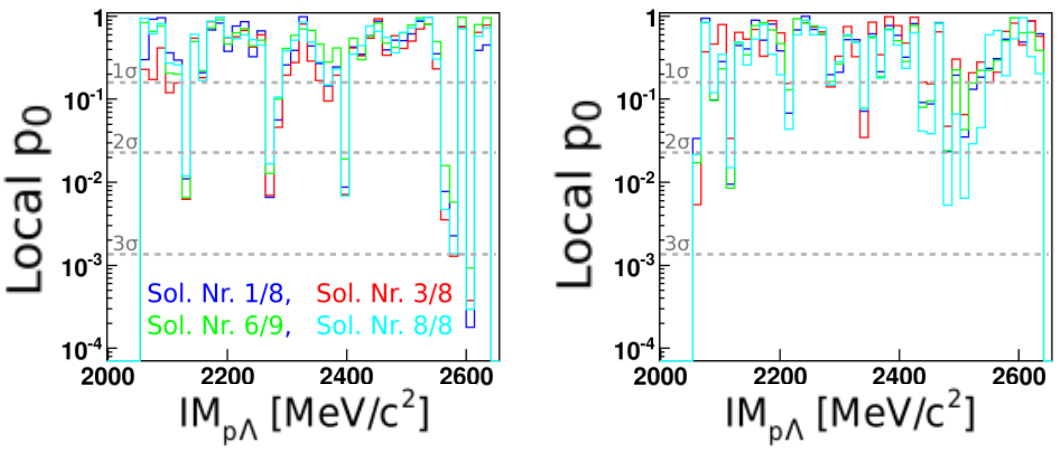

m_i measured events in bin i

λ_i expected events in bin i according to the model

$$\chi^2_P = \frac{(m - \lambda)^2}{\lambda} \Rightarrow \chi^2_P = \sum_{i=1}^{N_b} \frac{(m_i - \lambda_i)^2}{\lambda_i}$$

Combined result

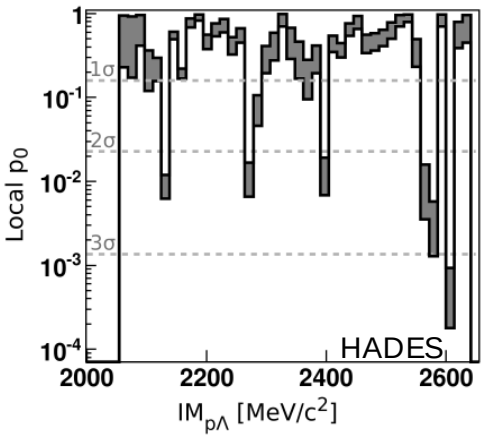

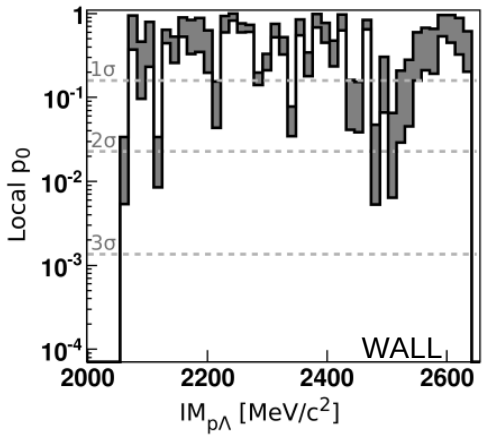

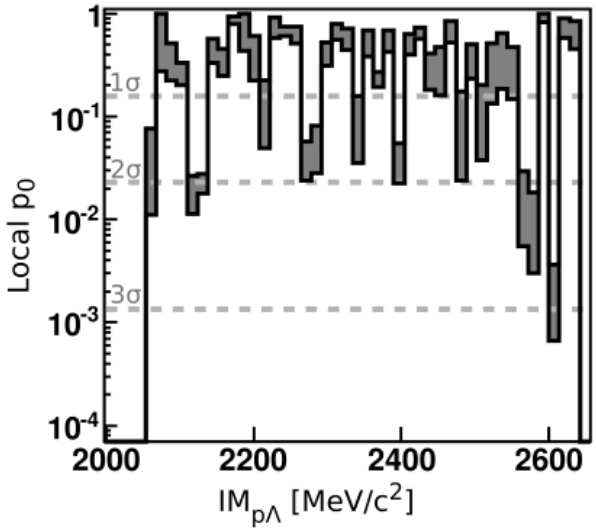

Test of the Signal Hypothesis

Inclusion of a new State

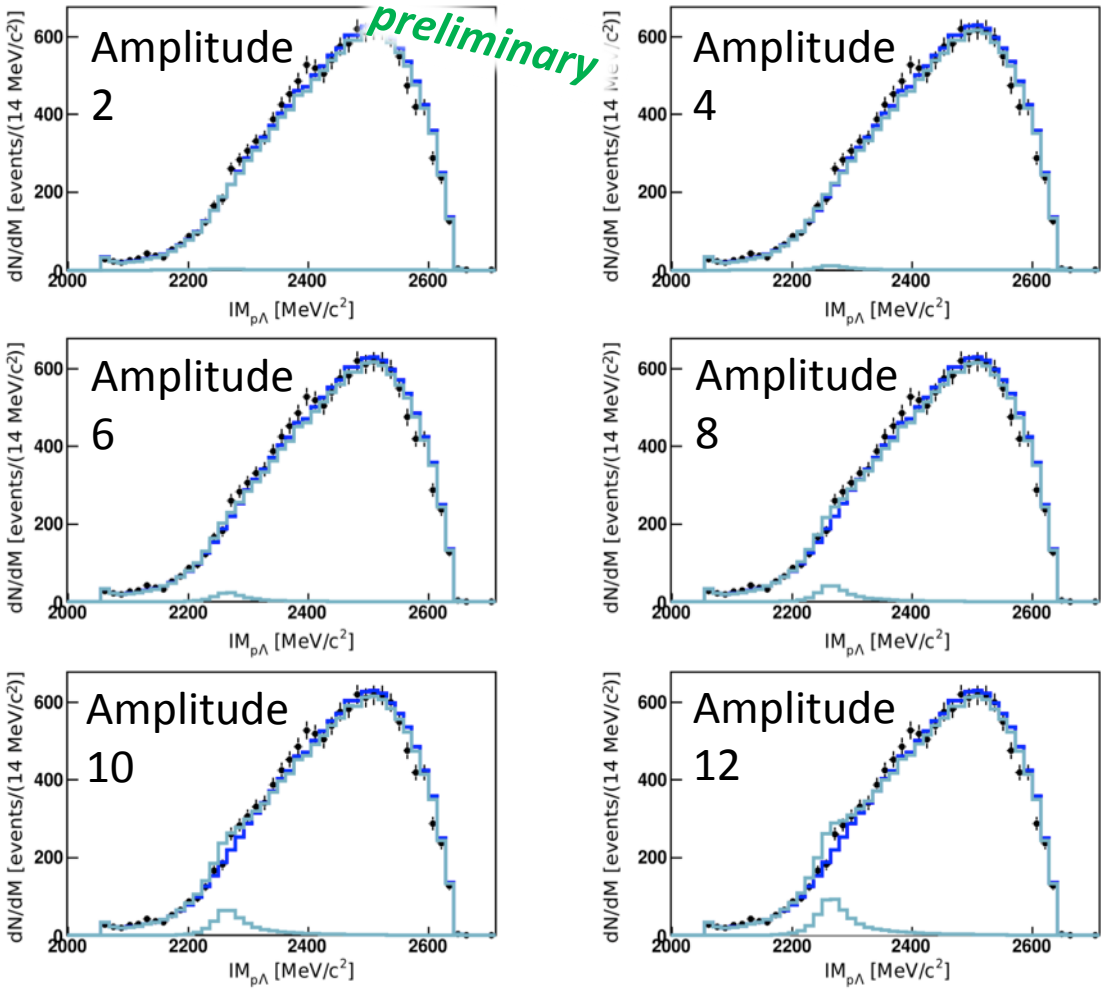

Data Points

Null Hypothesis

Hypothesis with ppK-

Feature of a PWA

… Interferences

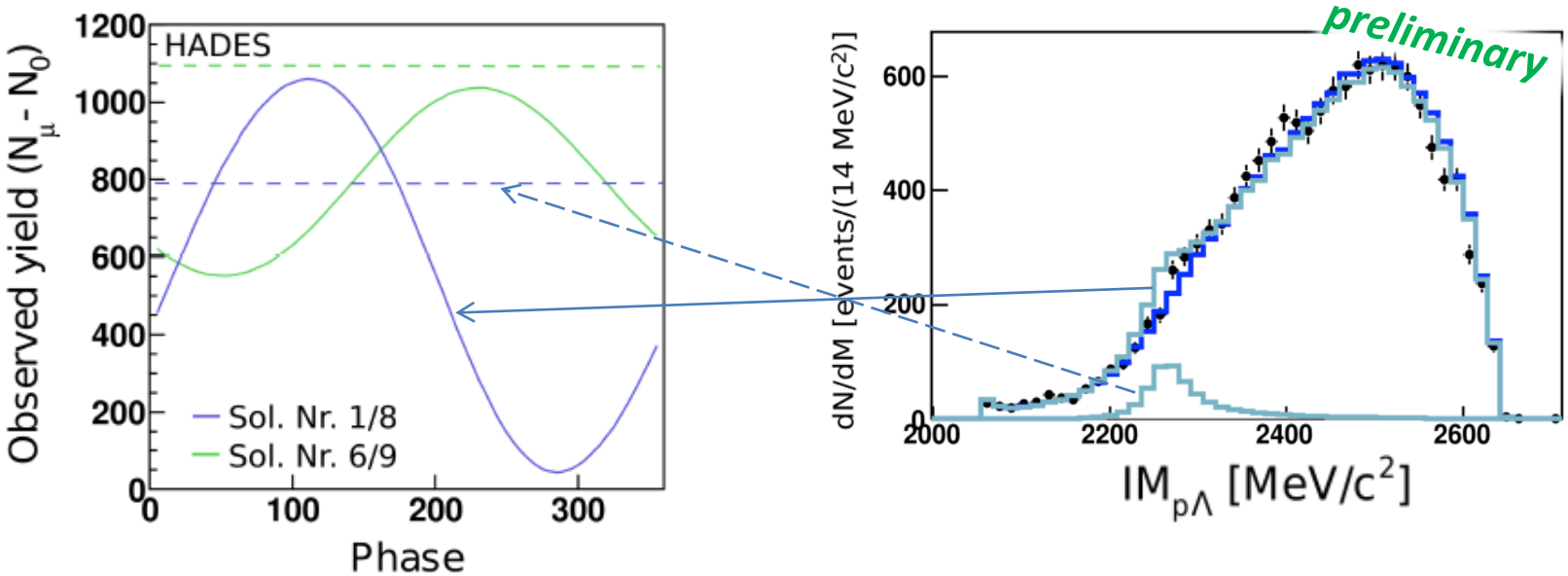

The minimum has to be found by the fit

Upper limit at CL_s 95%

These waves are included into the four best solutions of the PWA

$$^{2S+1}L_J$$

$$Wave A: \; ^{'}p + p^{'} \; ^{1}S_0 \rightarrow \; ^{'}ppK(2250) - K^{'} \; ^{1}S_0$$

$$Wave B: \; ^{'}p + p^{'} \; ^{3}P_1 \rightarrow \; ^{'}ppK(2250) - K^{'} \; ^{1}P_1$$

$$Wave C: \; ^{'}p + p^{'} \; ^{1}D_2 \rightarrow \; ^{'}ppK(2250) - K^{'} \; ^{1}D_2$$

Scanned masses:
2220 – 2370 MeV/c^2 (in steps of 10 MeV/c^2)
Scanned widths:
30 MeV, 50 MeV, and 70 MeV

Thanks to the HADES Collaboration

Jörn Adamczewski-Musch, Geydar Agakishiev, Claudia Behnke, Alexander Belyaev, **Jia-Chii Berger-Chen**, Alberto Blanco, Christoph Blume, Michael Böhmer, Pablo Cabanelas, Nuno Carolino, Sergey Chernenko, Jose Díaz, Adrian Dybczak, **Eliane Epple**, **Laura Fabbietti**, Oleg Fateev, Paulo Fonte, Jürgen Friese, Ingo Fröhlich, Tetyana Galatyuk, Juan A. Garzón, Roman Gernhäuser, Alejandro Gil, Marina Golubeva, Fedor Guber, Malgorzata Gumberidze, Szymon Harabasz, Klaus Heidel, Thorsten Heinz, Thierry Hennino, Romain Holzmann, Jochen Hutsch, Claudia Höhne, Alexander Ierusalimov, Alexander Ivashkin, Burkhard Kämpfer, Marcin Kajetanowicz, Tatiana Karavicheva, Vladimir Khomyakov, Ilse Koenig, Wolfgang Koenig, Burkhard W. Kolb, Vladimir Kolganov, Grzegorz Korcyl, Georgy Kornakov, Roland Kotte, Erik Krebs, Hubert Kuc, Wolfgang Kühn, Andrej Kugler, Alexei Kurepin, Alexei Kurilkin, Pavel Kurilkin, Vladimir Ladygin, **Rafal Lalik**, **Kirill Lapidus**, Alexander Lebedev, Ming Liu, Luís Lopes, Manuel Lorenz, Gennady Lykasov, Ludwig Maier, Alexander Malakhov, Alessio Mangiarotti, Jochen Markert, Volker Metag, Jan Michel, Christian Müntz, **Rober Münzer**, Lothar Naumann, Marek Palka, Vladimir Pechenov, Olga Pechenova, Americo Pereira, Jerzy Pietraszko, Witold Przygoda, Nicolay Rabin, Béatrice Ramstein, Andrei Reshetin, Laura Rehnisch, Philippe Rosier, Anar Rustamov, Alexander Sadovsky, Piotr Salabura, Timo Scheib, Alexander Schmah, Heidi Schuldes, Erwin Schwab, **Johannes Siebenson**, Vladimir Smolyankin, Manfred Sobiella, Yuri Sobolev, Stefano Spataro, Herbert Ströbele, Joachim Stroth, Christian Sturm, Khaled Teilab, Vladimir Tiflov, Pavel Tlusty, Michael Traxler, Alexander Troyan, Haralabos Tsertos, Evgeny Usenko, Taras Vasiliev, Vladimir Wagner, Christian Wendisch, Jörn Wüstenfeld, Yuri Zanevsky

References for the Calculations

[AY02] Yoshinori Akaishi and Toshimitsu Yamazaki. Nuclear anti-K bound states in light nuclei. *Phys.Rev.*, C65:044005, 2002.

[BGL12] N. Barnea, A. Gal, and E.Z. Liverts. Realistic calculations of $\bar{K}NN$, $\bar{K}NNN$, and $\bar{K}\bar{K}NN$ quasibound states. *Phys.Lett.*, B712:132–137, 2012.

[BO12a] M. Bayar and E. Oset. $\bar{K}NN$ Absorption within the Framework of the Fixed Center Approximation to Faddeev equations. 2012.

[BO12b] M. Bayar and E. Oset. Improved Fixed Center Approximation of the Faddeev equations for the $\bar{K}NN$ system with S=0. *Nucl.Phys.*, A883:57–68, 2012.

[DHW08] Akinobu Dote, Tetsuo Hyodo, and Wolfram Weise. K^-pp system with chiral SU(3) effective interaction. *Nucl.Phys.*, A804:197–206, 2008.

[DHW09] Akinobu Dote, Tetsuo Hyodo, and Wolfram Weise. Variational calculation of the ppK^-system based on chiral SU(3) dynamics. *Phys.Rev.*, C79:014003, 2009.

[FIK+11] M. Faber, A.N. Ivanov, P. Kienle, J. Marton, and M. Pitschmann. Molecule model for kaonic nuclear cluster $\bar{K}NN$. *Int.J.Mod.Phys.*, E20:1477–1490, 2011.

[IKS10] Yoichi Ikeda, Hiroyuki Kamano, and Toru Sato. Energy dependence of $\bar{K}N$ interactions and resonance pole of strange dibaryons. *Prog.Theor.Phys.*, 124:533–539, 2010.

[IS07] Y. Ikeda and T. Sato. Strange dibaryon resonance in the $\bar{K}$NN - πYN system. *Phys.Rev.*, C76:035203, 2007.

[IS09] Yoichi Ikeda and Toru Sato. On the resonance energy of the $\bar{K}$NN - πYN system. *Phys.Rev.*, C79:035201, 2009.

[RS14] J. Revai and N.V. Shevchenko. Faddeev calculations of the $\bar{K}NN$ system with chirally-motivated $\bar{K}N$ interaction. II. The K^-pp quasi-bound state. 2014.

[SGM07] N.V. Shevchenko, A. Gal, and J. Mares. Faddeev calculation of a K^-pp quasi-bound state. *Phys.Rev.Lett.*, 98:082301, 2007.

[SGMR07] N.V. Shevchenko, A. Gal, J. Mares, and J. Revai. $\bar{K}NN$ quasi-bound state and the $\bar{K}N$ interaction: Coupled-channel Faddeev calculations of the $\bar{K}NN$-$\pi\Sigma N$ system. *Phys.Rev.*, C76:044004, 2007.

[WG09] S. Wycech and A. M. Green. Variational calculations for $\bar{K}$–few-nucleon systems. *Phys. Rev. C*, 79:014001, 2009.

[YA02] T. Yamazaki and Y. Akaishi. (K^-,π^-) production of nuclear $\bar{K}$ bound states in proton-rich systems via Λ^* doorways. *Phys.Lett.*, B535:70–76, 2002.

N* resonances

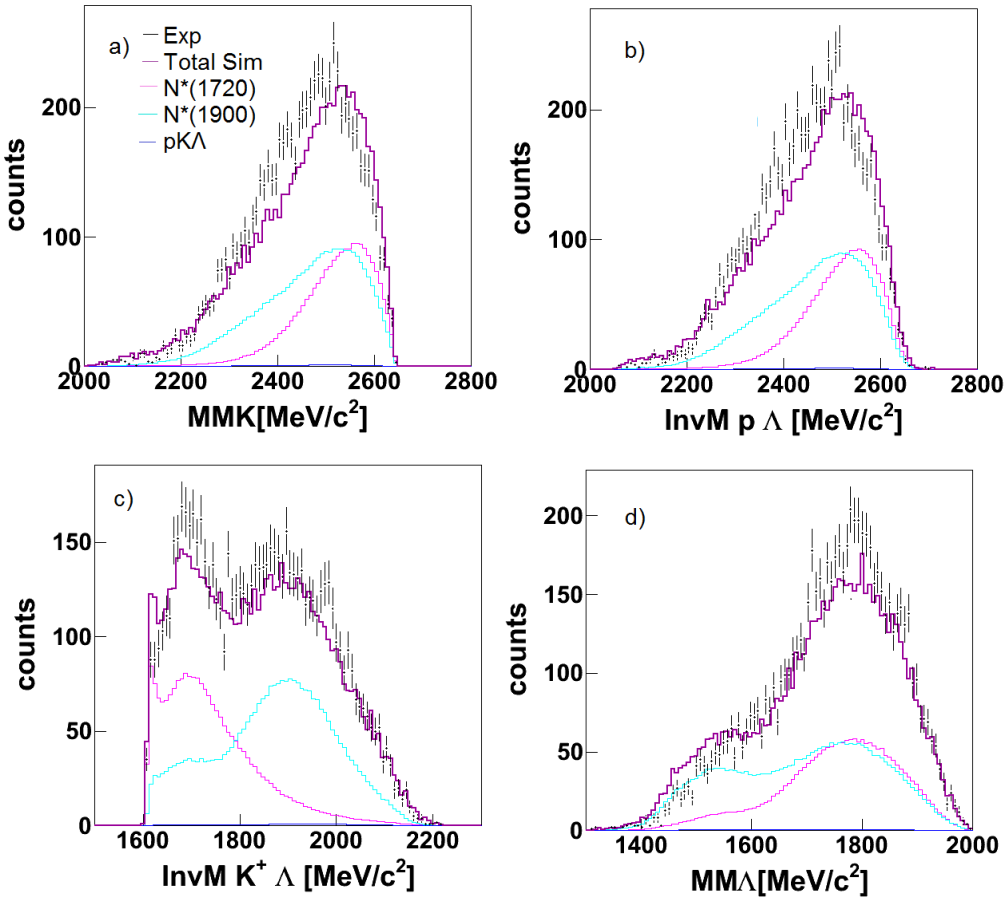

Figure 6.10: a) $IM_{K^+\Lambda}$, b) $IM_{p\Lambda}$,c) MM_{K^+} and d) MM_{Λ} fitted with the sum of the four N^{*+}-resonances from table 6.2 and the simulation of a direct $pK^+\Lambda$ production.

Master Thesis A. Solaguren-Beascoa Negre

Upper Limit

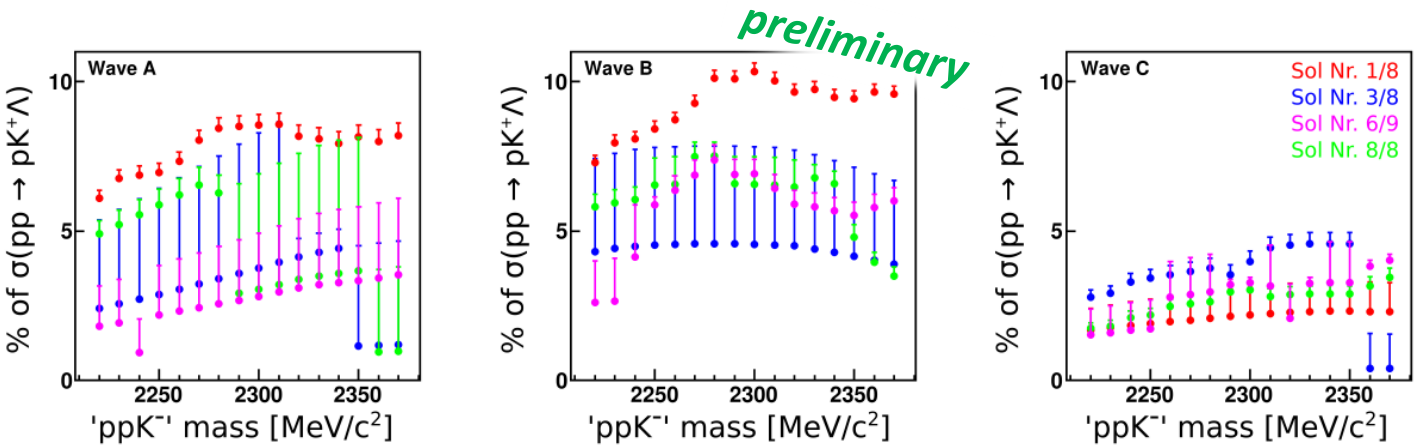

$\Gamma(ppK^-)$=50 MeV

Dalitz Plots

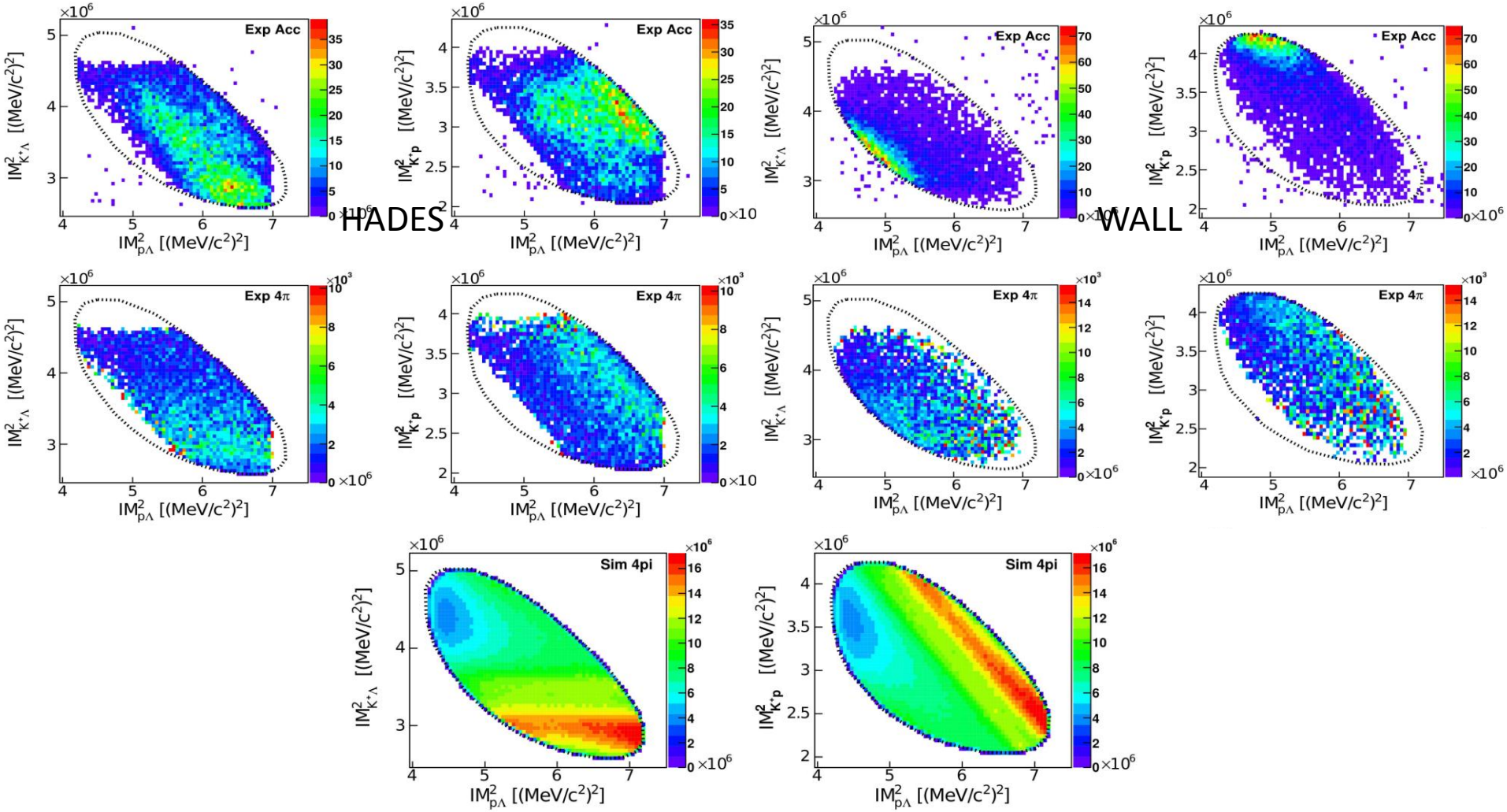

Cross Section

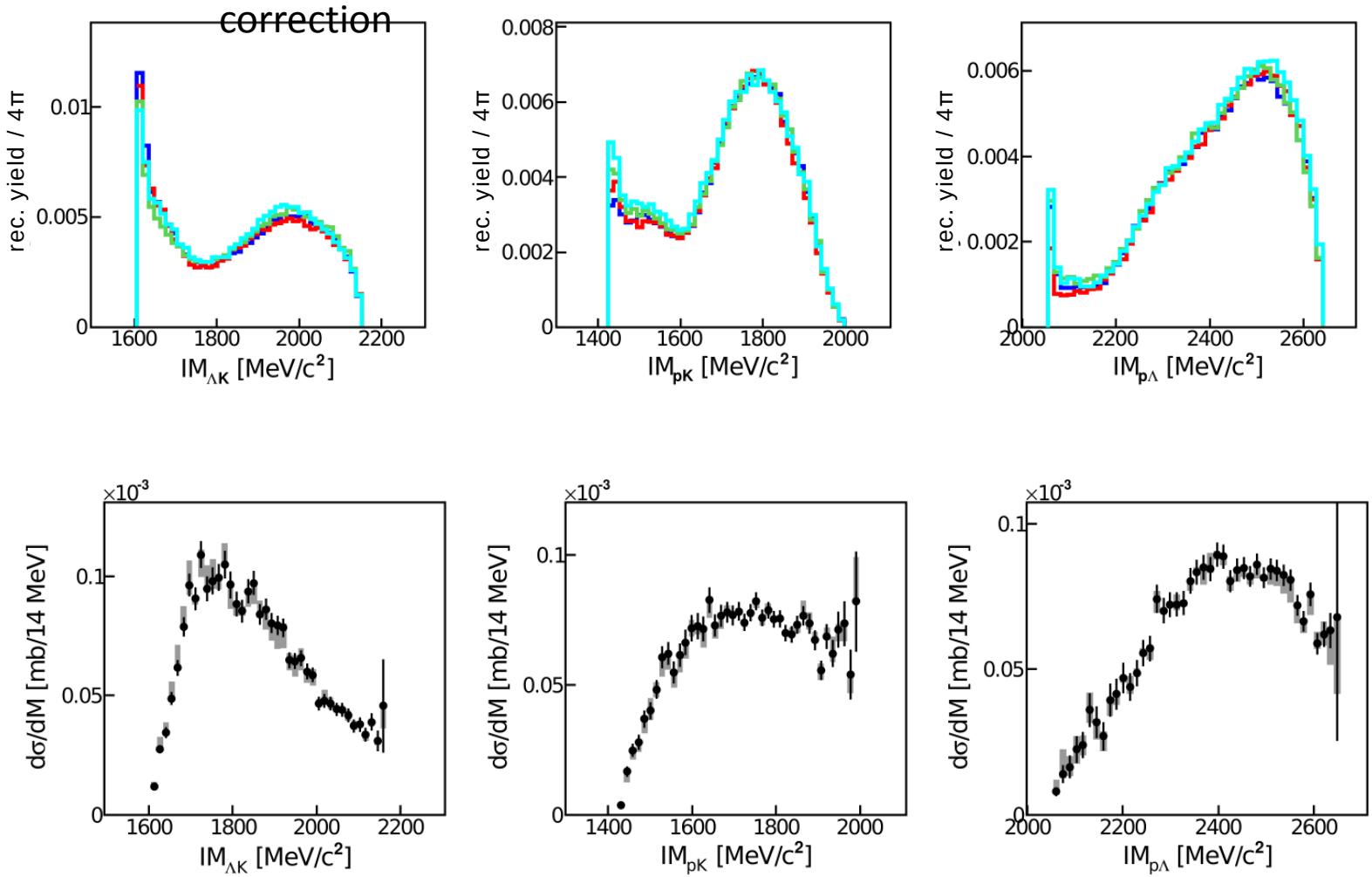

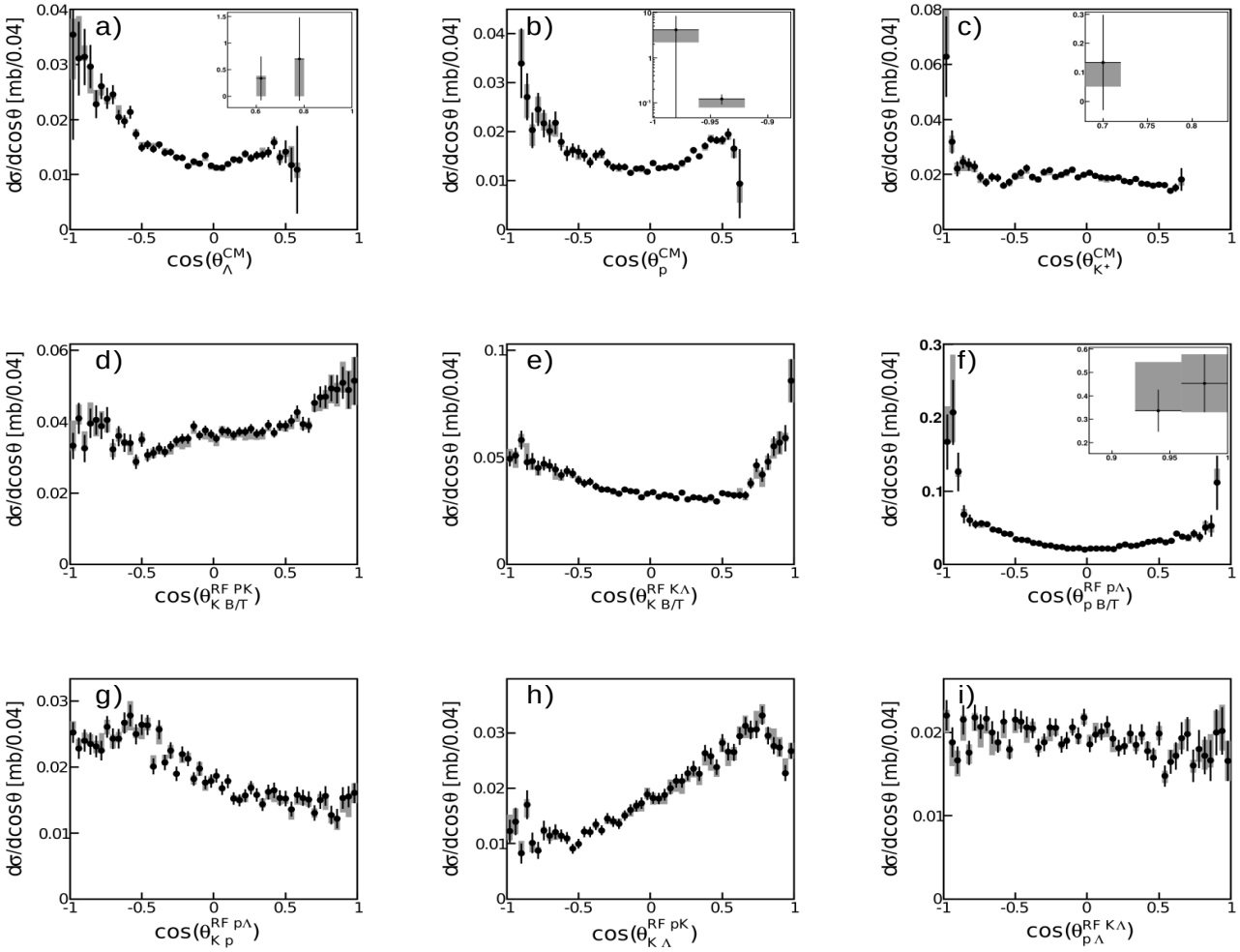
a)
b)
c)
d)
e)
f)
g)
h)
i)
dσ/dcosθ [mb/0.04]
cos(θ^CM_Λ)
cos(θ^CM_p)
cos(θ^CM_K+)
cos(θ^RF pK_K B/T)
cos(θ^RF KΛ_K B/T)
cos(θ^RF pΛ_p B/T)
cos(θ^RF pΛ_K p)
cos(θ^RF pK_K Λ)
cos(θ^RF KΛ_p Λ)

Multi PWA

Combined Analysis of HADES and FOPI

4 Best HADES Solutions
HADES-only
1_8 (s=-0.27 10^4)
8_8 (s=-0.27 10^4)
3_8 (s=-0.27 10^4)
6_9 (s=-0.27 10^4)

→

4 Best HADES Solutions
HADES+FOPI
1_8 (s=-0.83 10^5)
8_8 (s=-0.82 10^5)
3_8 (s=-0.98 10^5)
6_9 (s=-0.78 10^5)

s : - (Log Likely hood) of PWA

Energy dependent coefficient =0

Results of 3_8

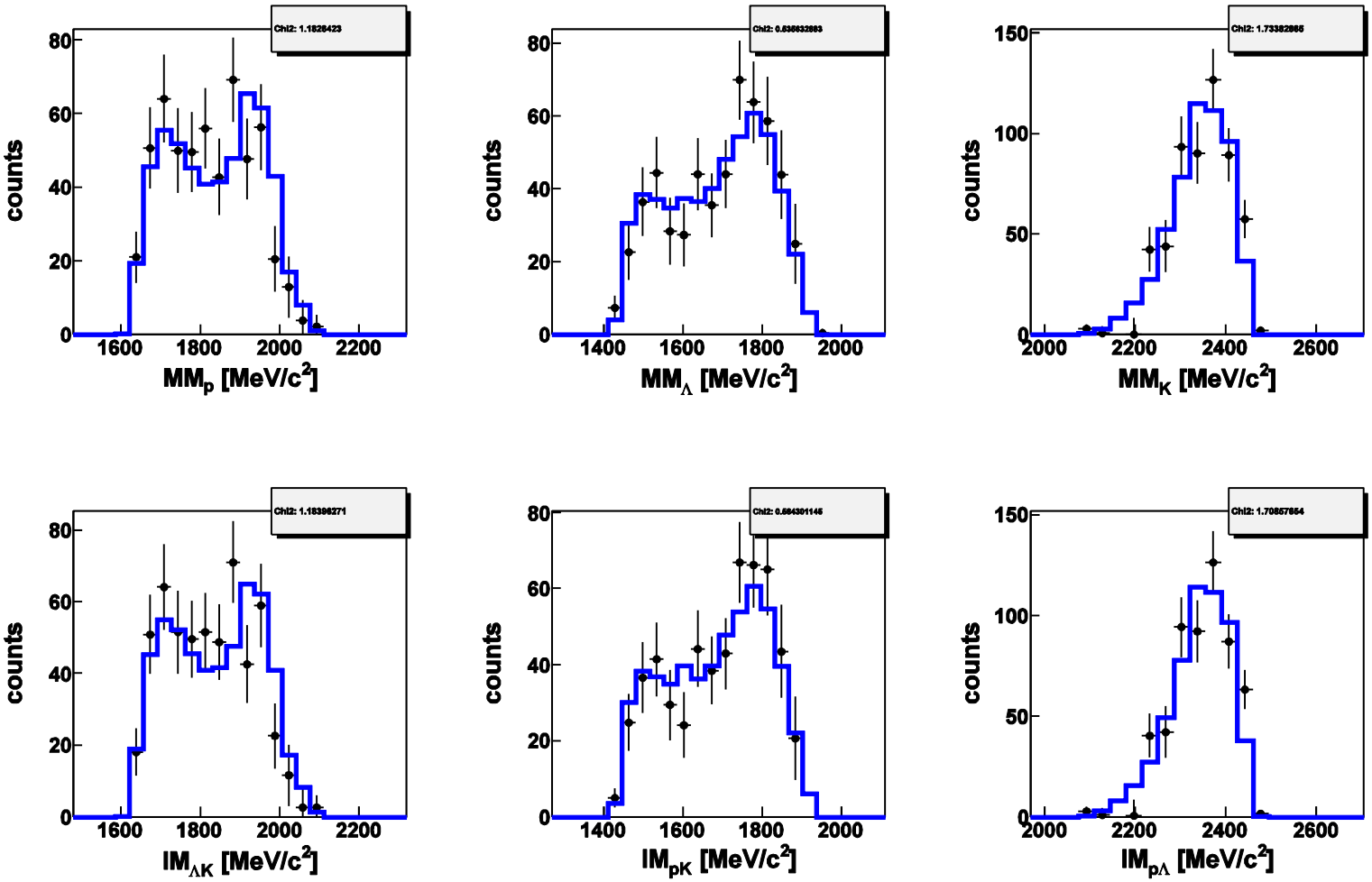

Results of 3_8

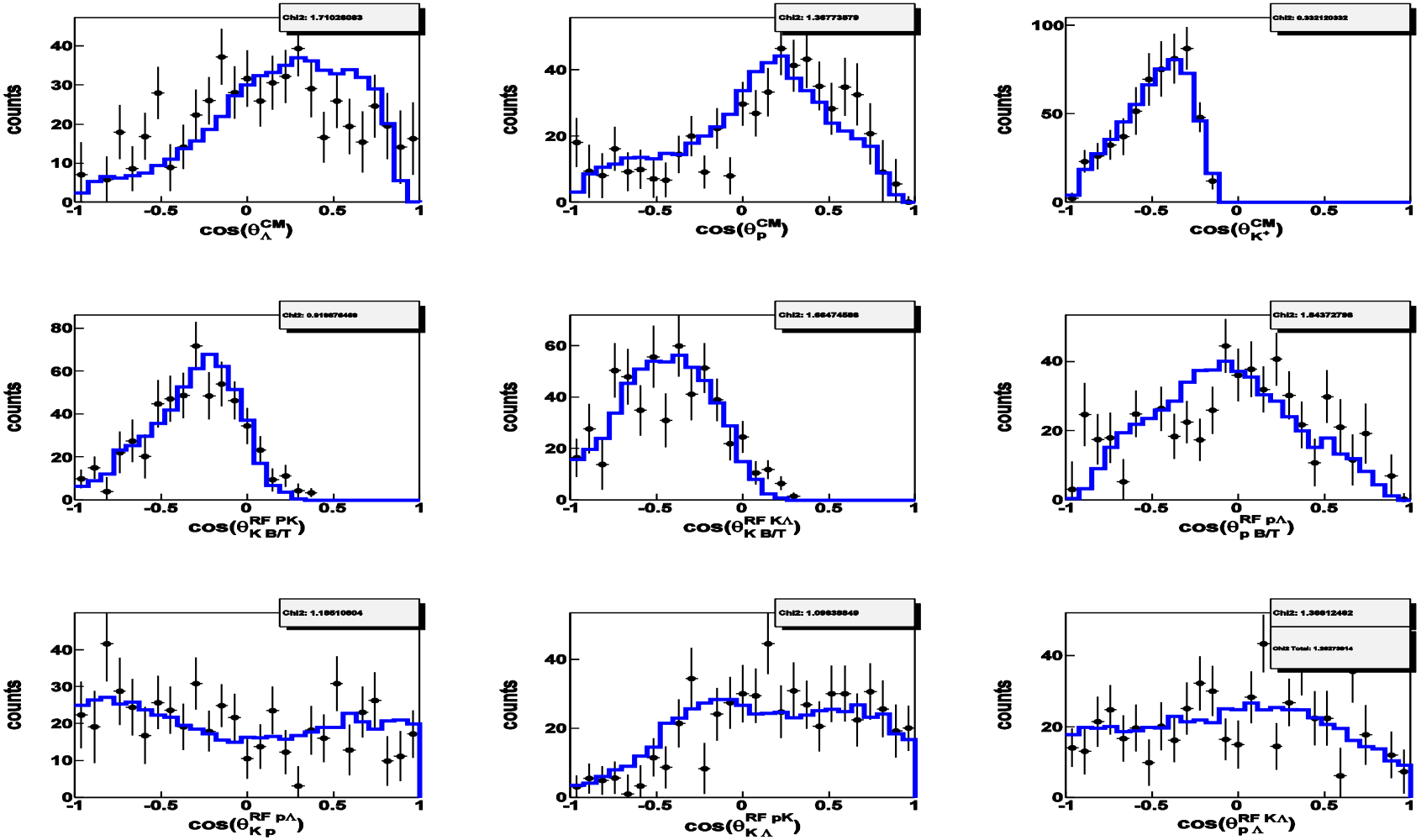

Results of 3_8

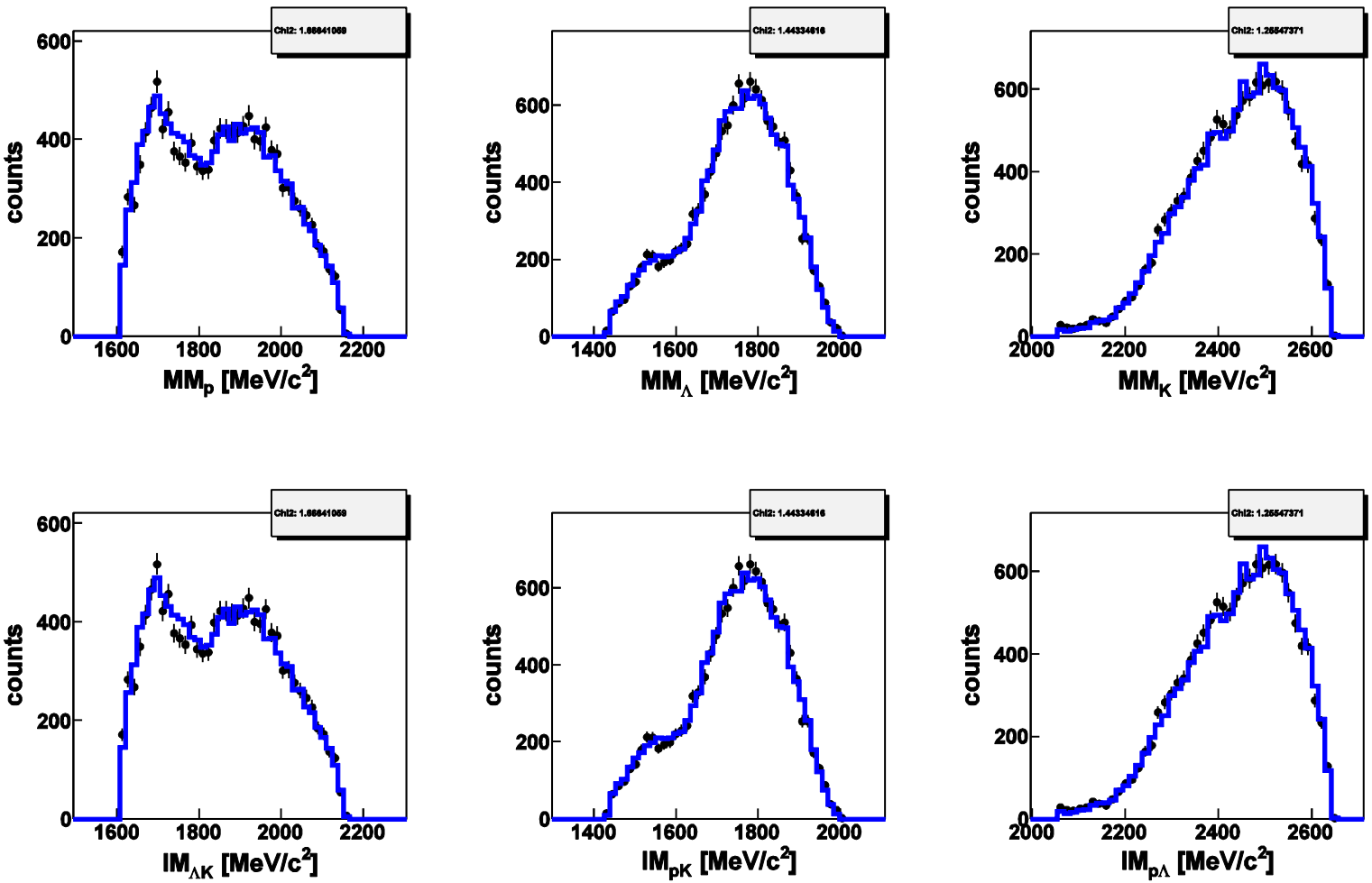

Results of 3_8

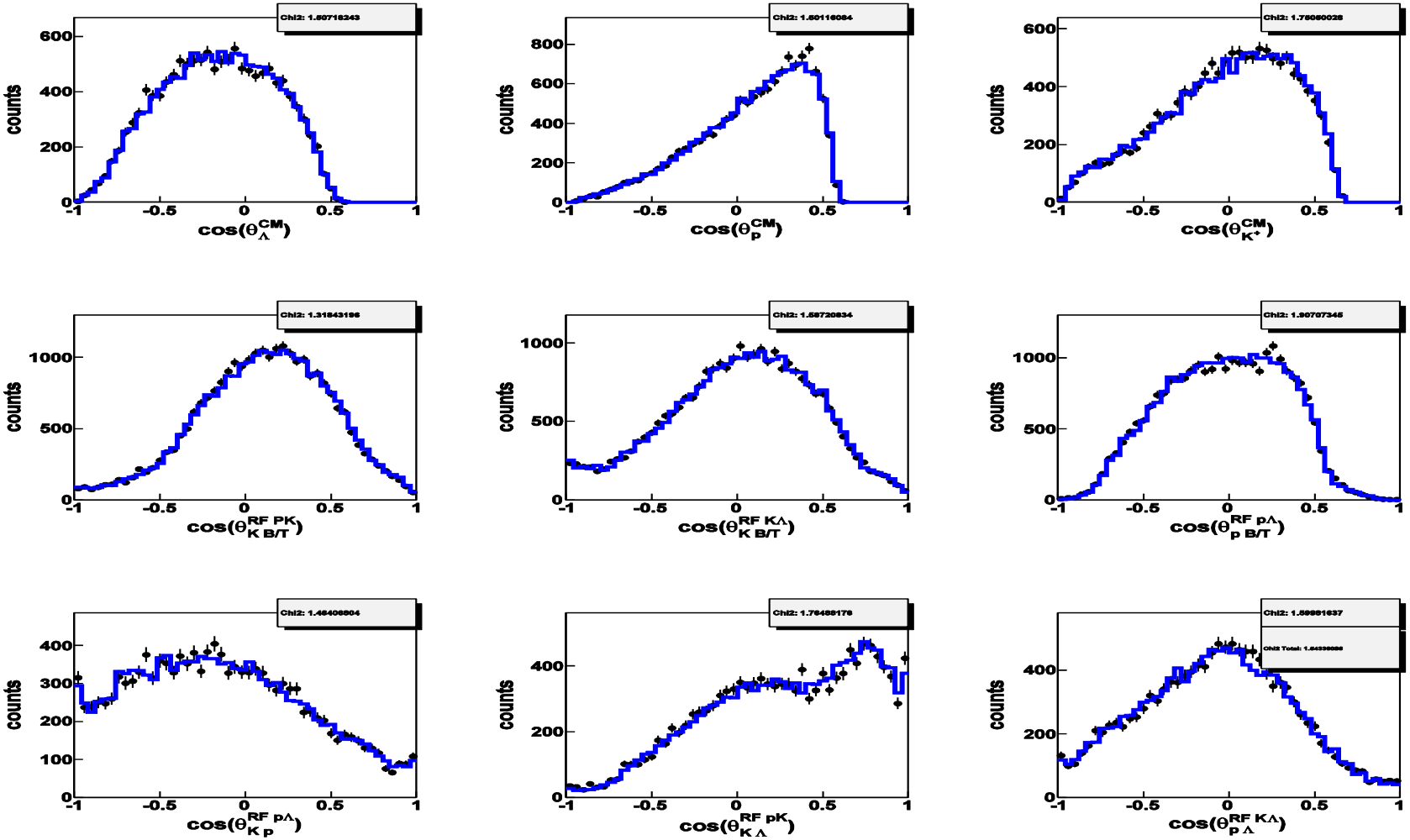

Combined Analysis of HADES and FOPI

4 Best HADES Solutions
HADES-FOPI (ene-fix)
1_8 (s=-0.83 10^5)
8_8 (s=-0.82 10^5)
3_8 (s=-0.98 10^5)
6_9 (s=-0.78 10^5)

→

4 Best HADES Solutions
HADES+FOPI (ene_dep)
1_8 (s=-0.73 10^5)
8_8 (s=-0.76 10^5)
3_8 (s=-0.70 10^5)
6_9 (s=-0.62 10^5)

s : - (Log Likely hood) of PWA

Energy dependent coefficient fitted

Results HADES

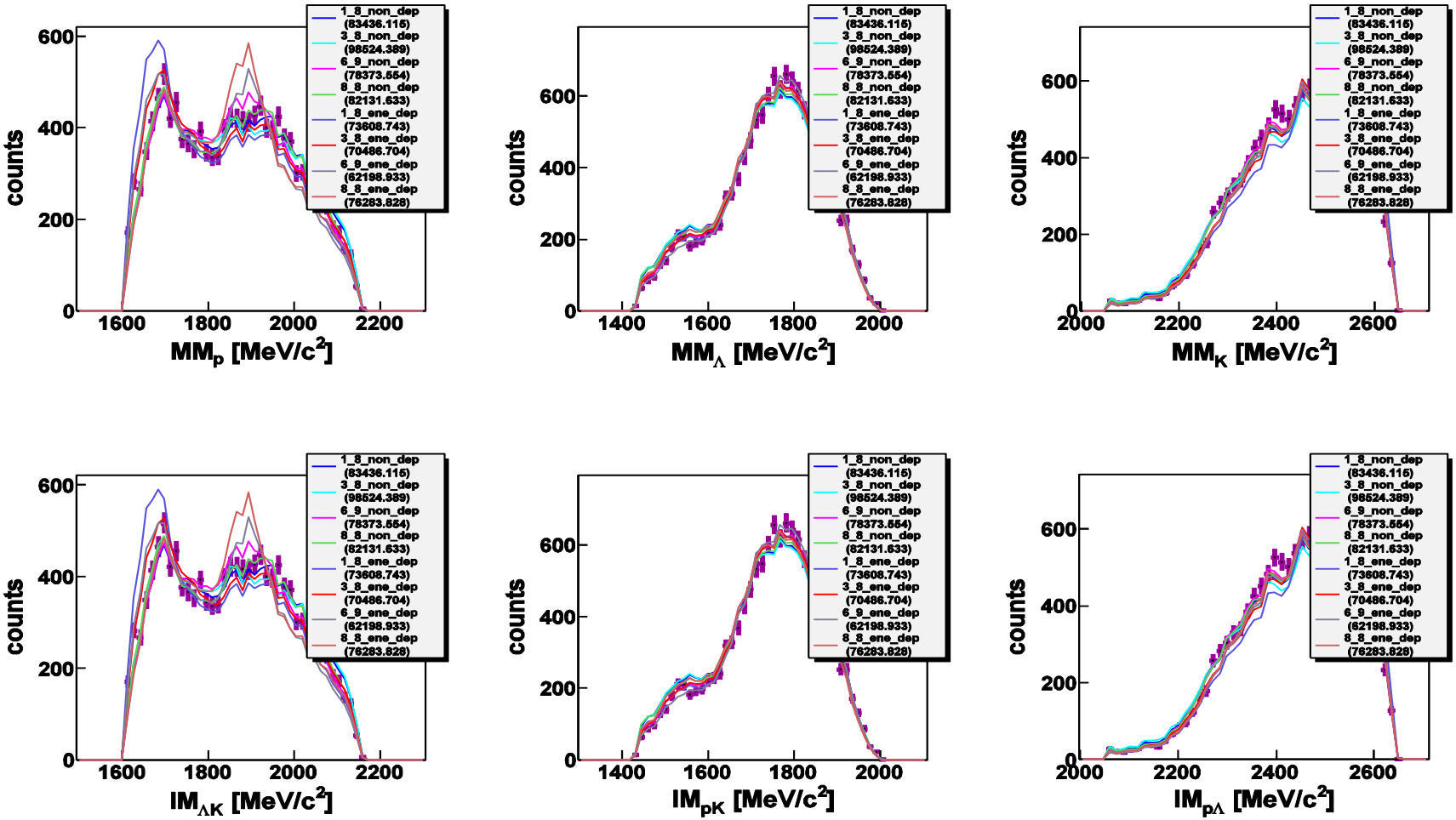

Results HADES

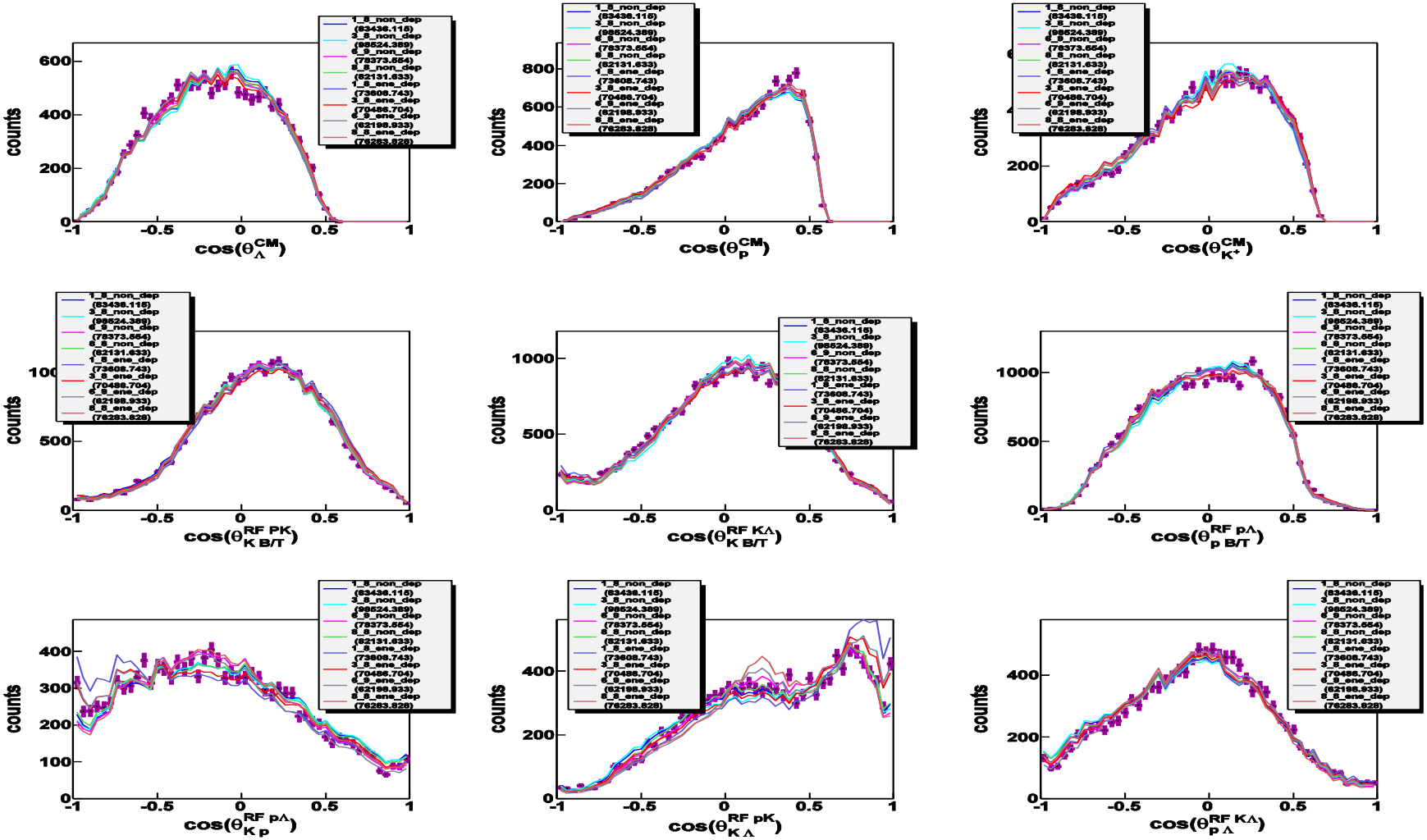

Results WALL

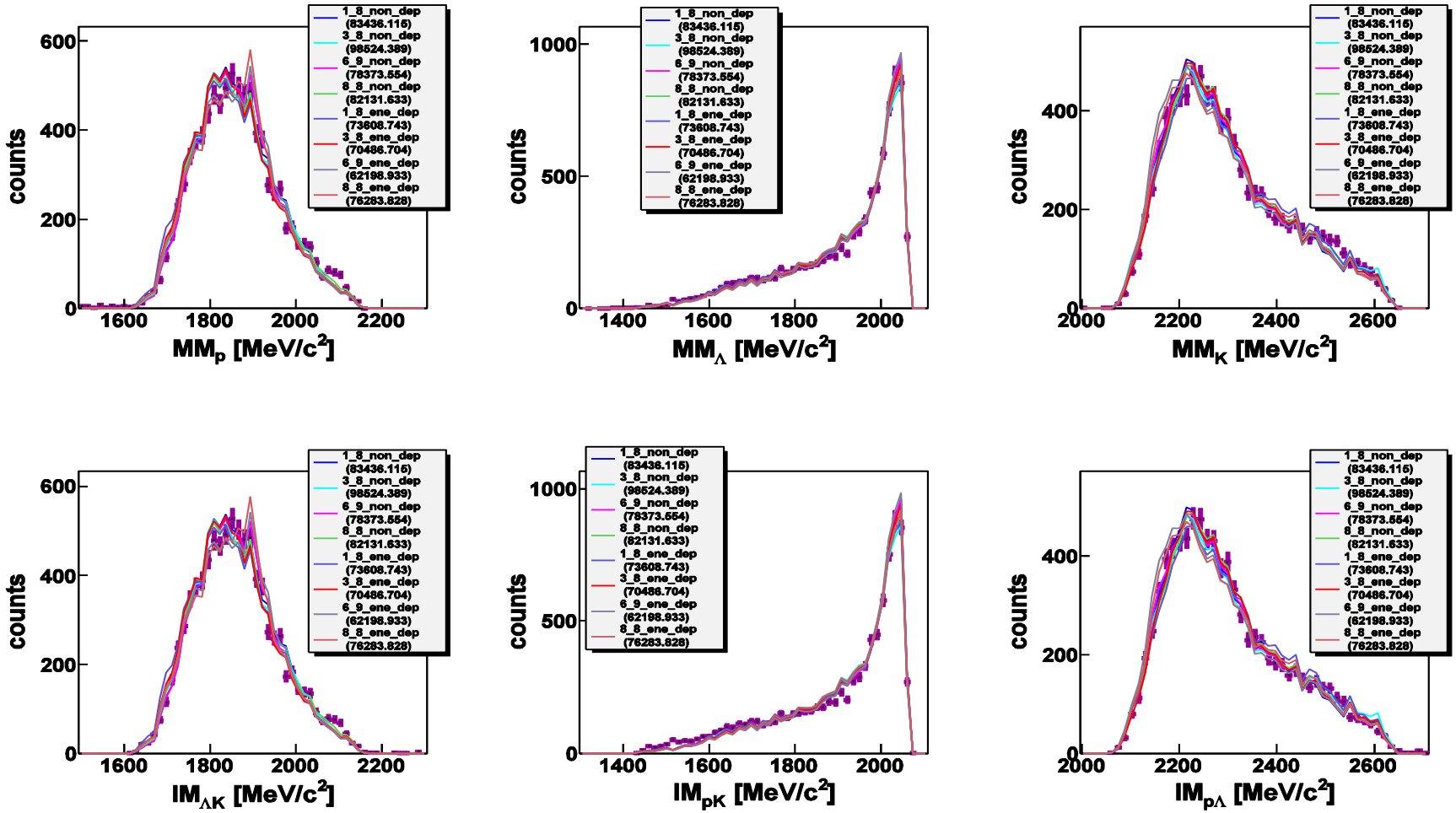

Results WALL

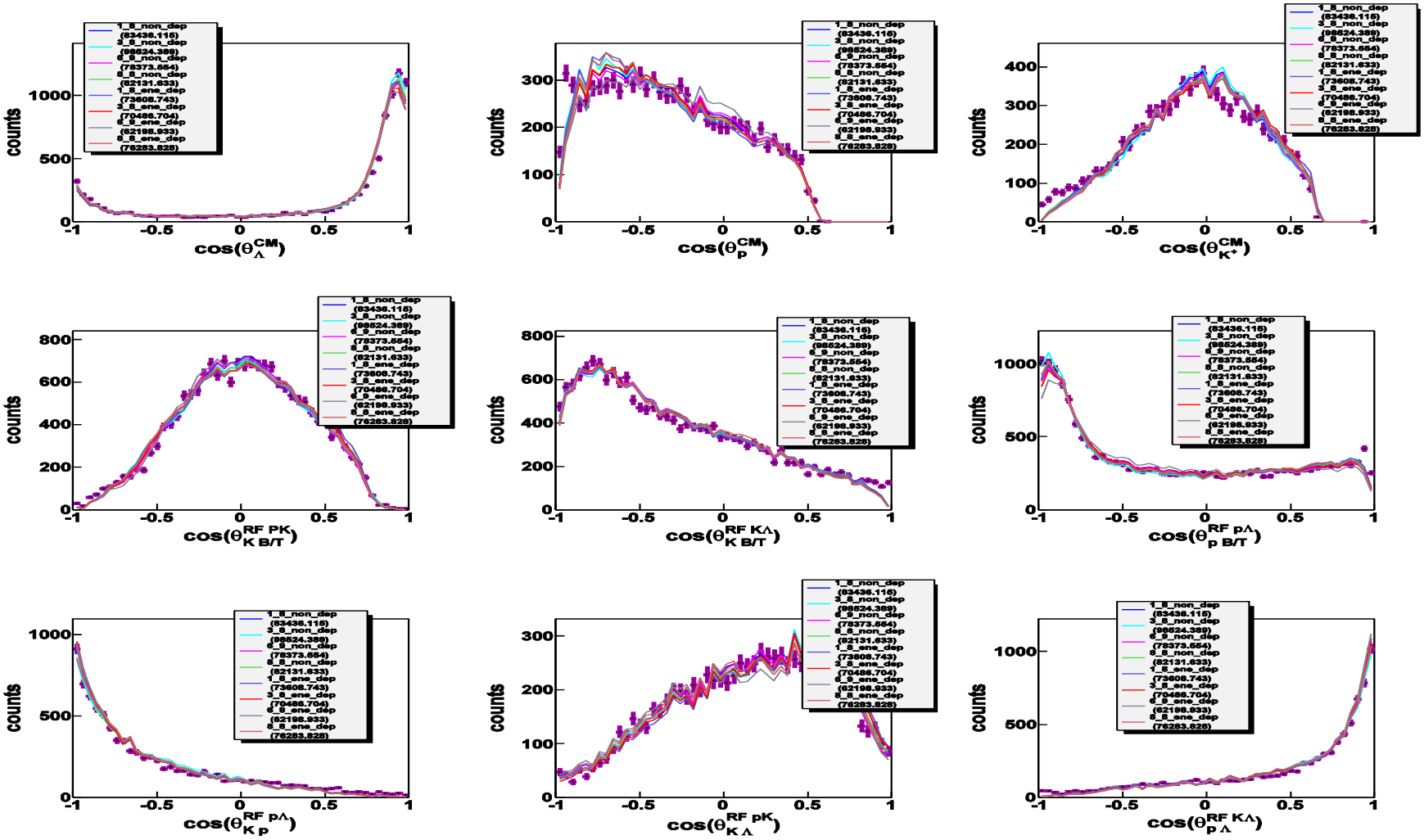

Results FOPI

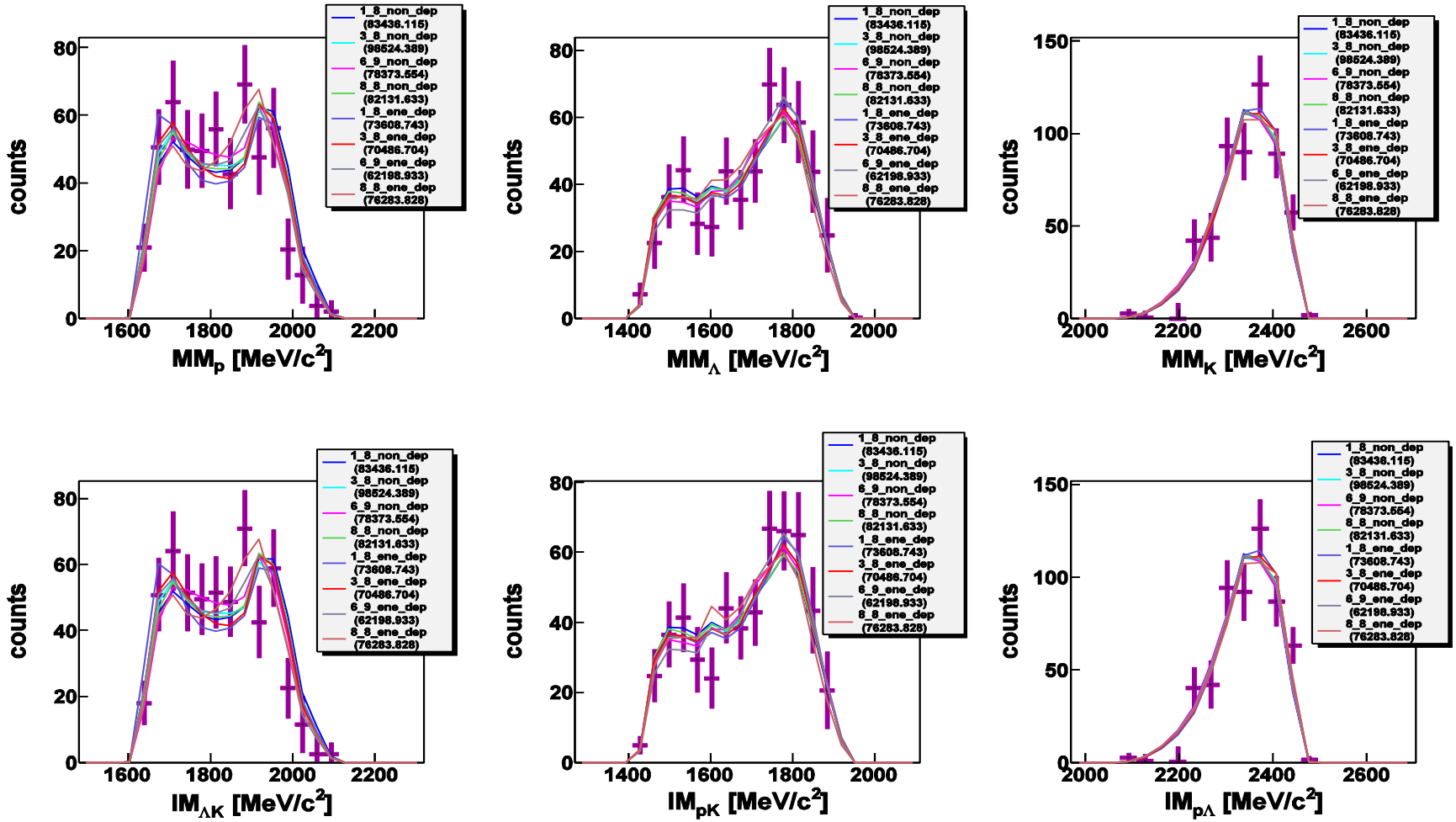

Results FOPI

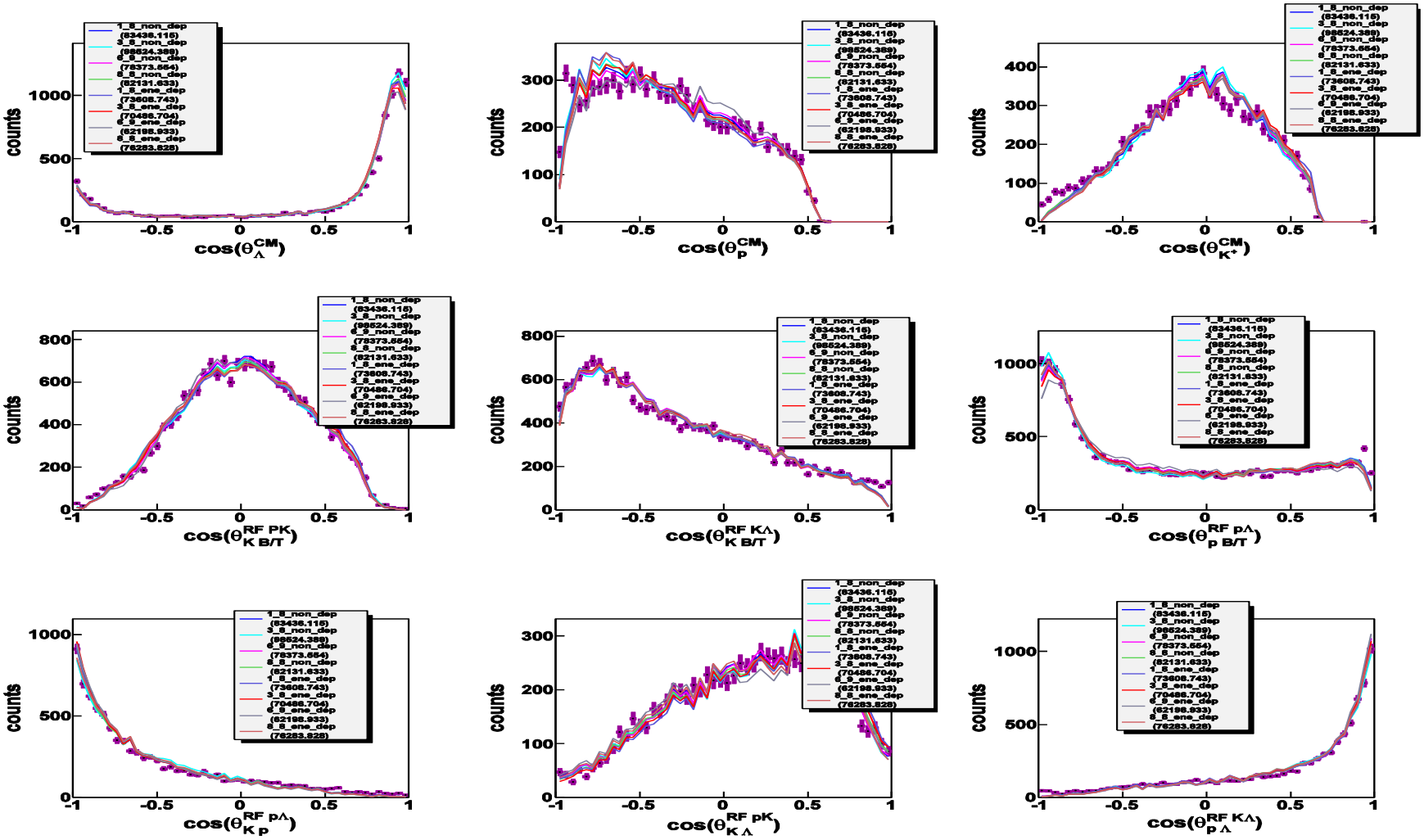

4 PI – param_3_8_ene_dep

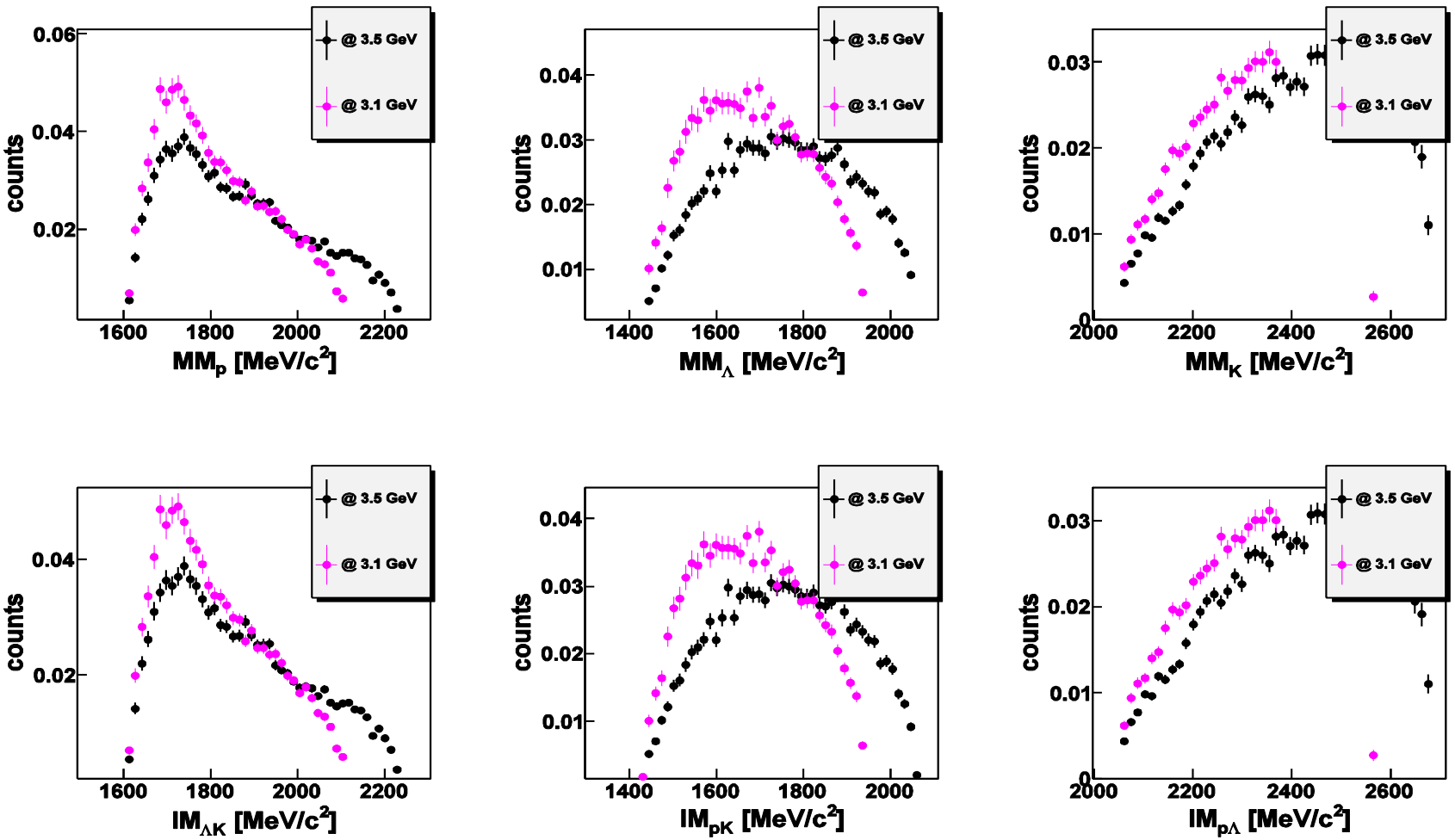

4 PI - param_3_8_ene_dep

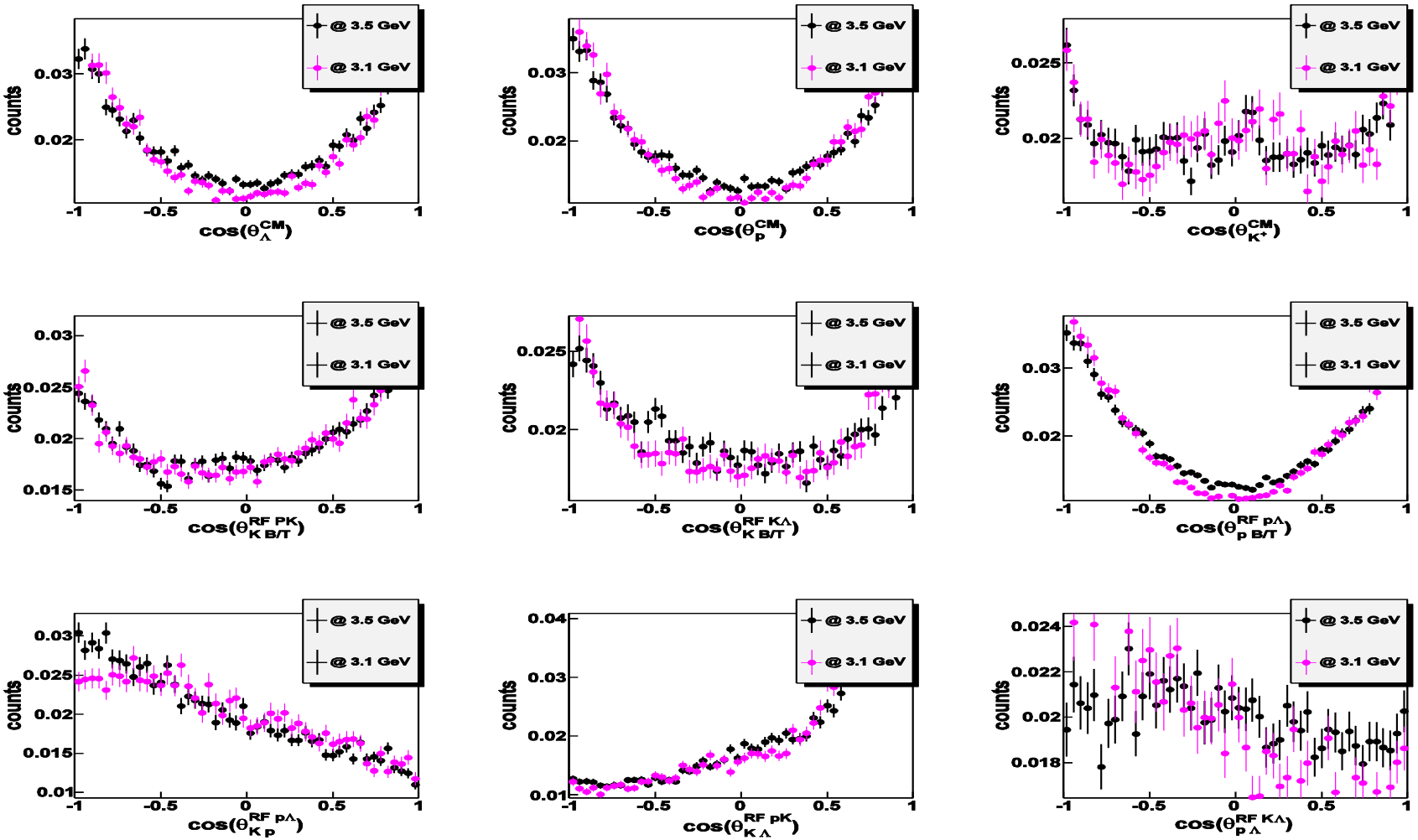

Legendre Fits

Mean of all solutions

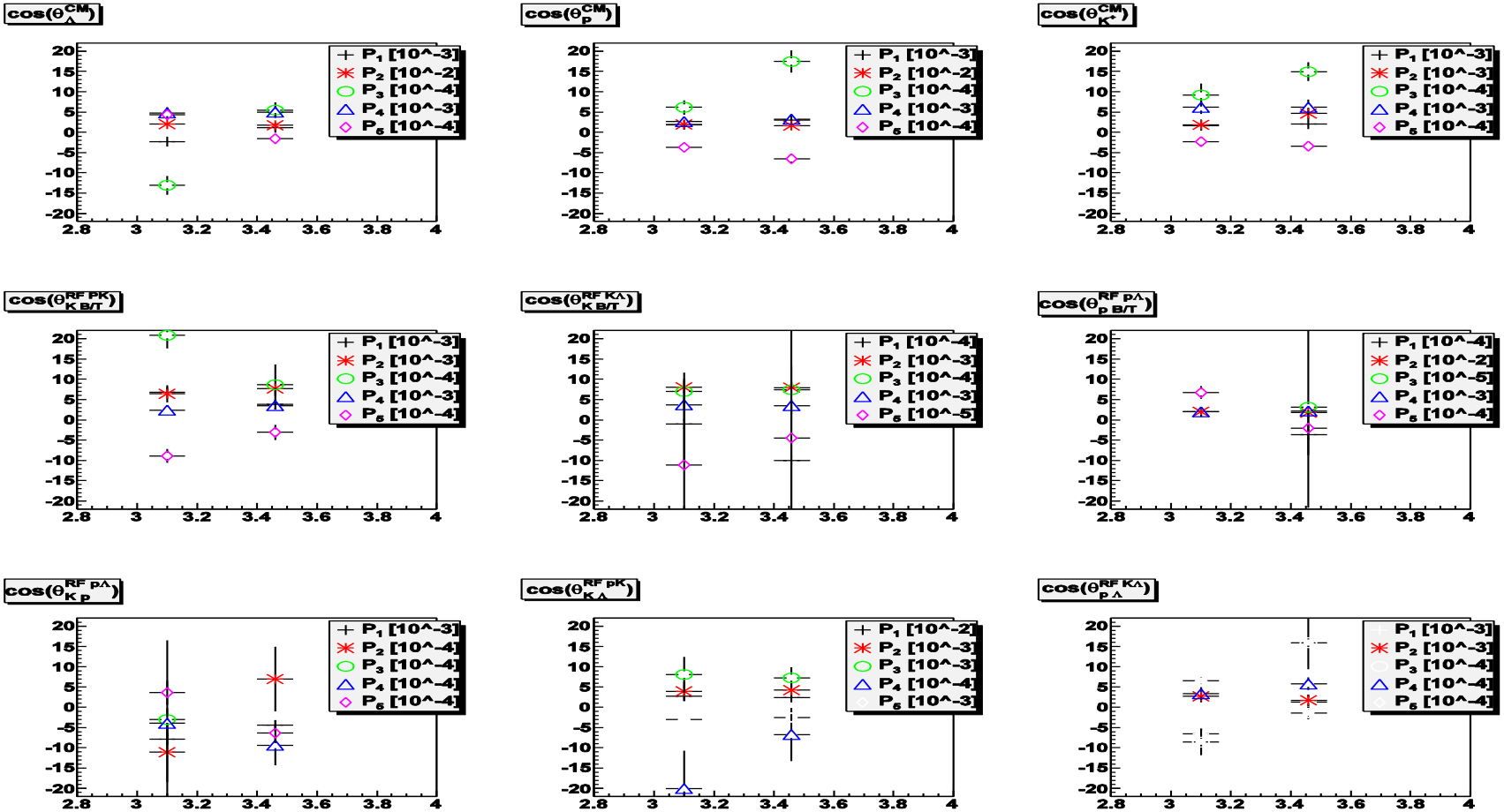

Contributions

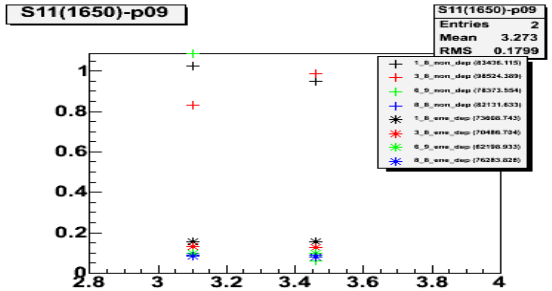

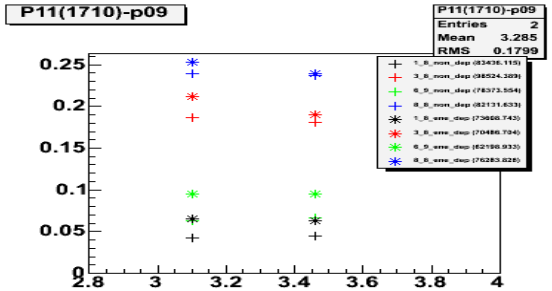

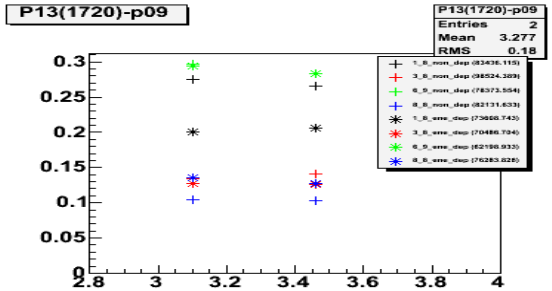

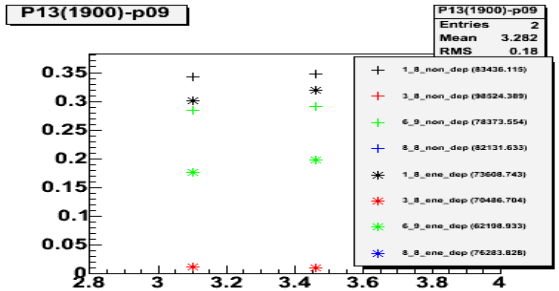

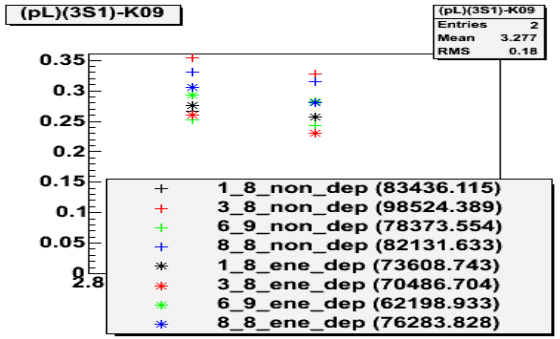

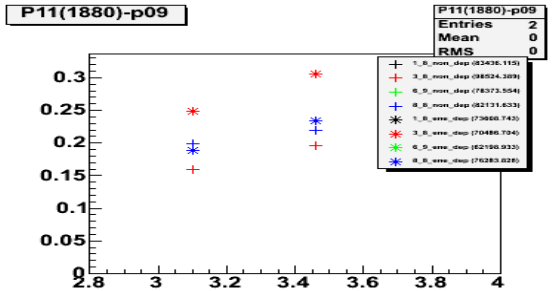

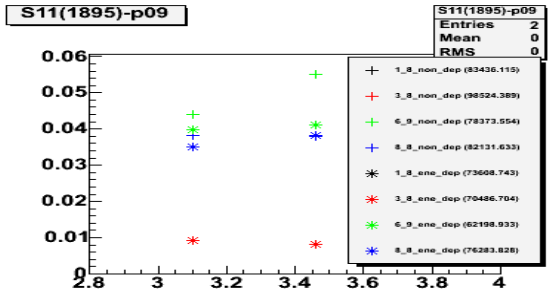

PWA without Interference

Combined Analysis of HADES and FOPI

With Interference:

1. cfgg = Σ cp * tensor
2. Cross section = Σ cfgg * cfgg^{+}

→

Without Interference:

1. cfgg = Σ (cp * tensor) * (cp * tensor)$^{+}$
2. Cross section = Σ cfgg

Results of 3_8_wo_int (not fitted)

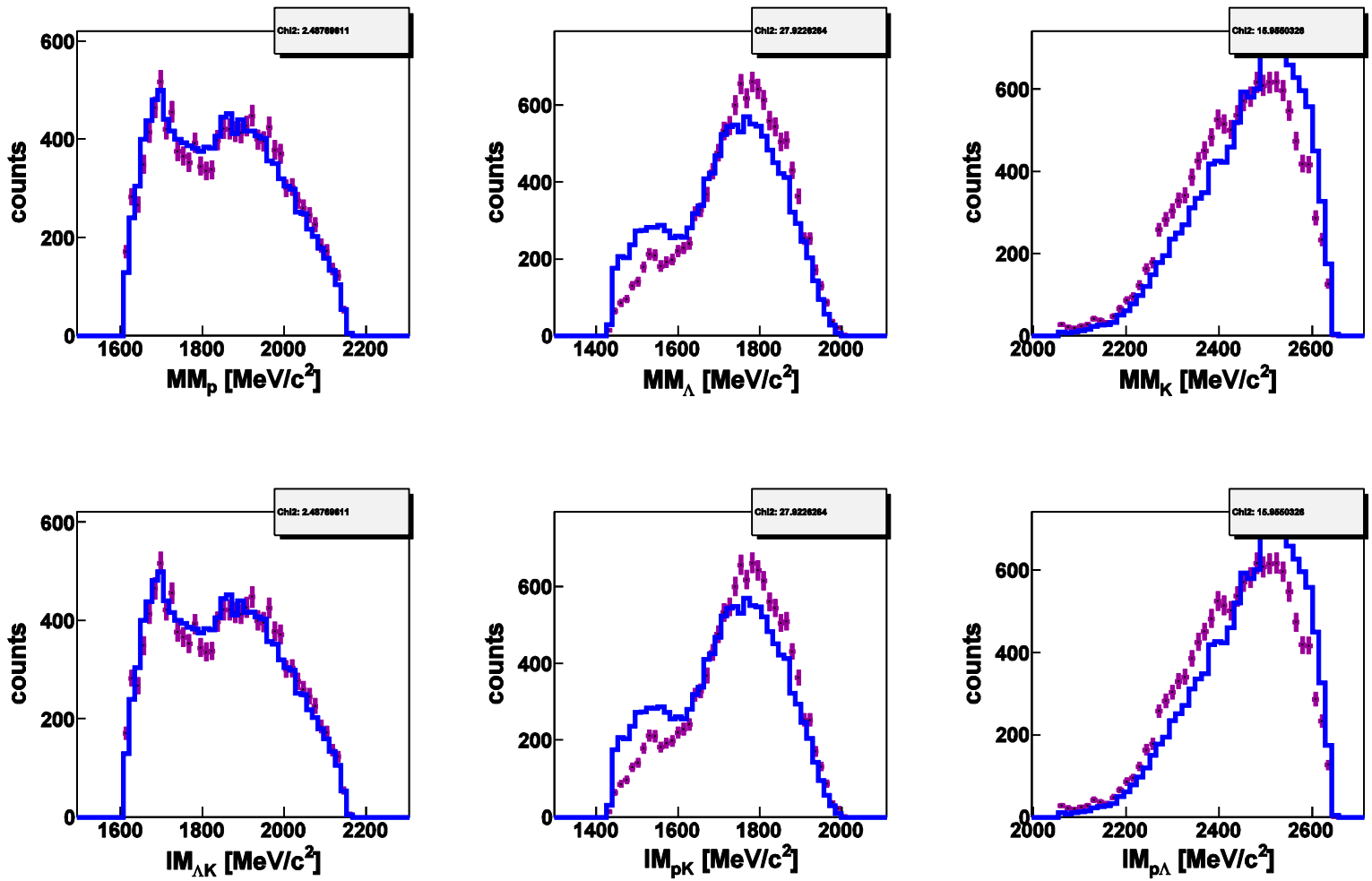

Results of 3_8_wo_int (not fitted)

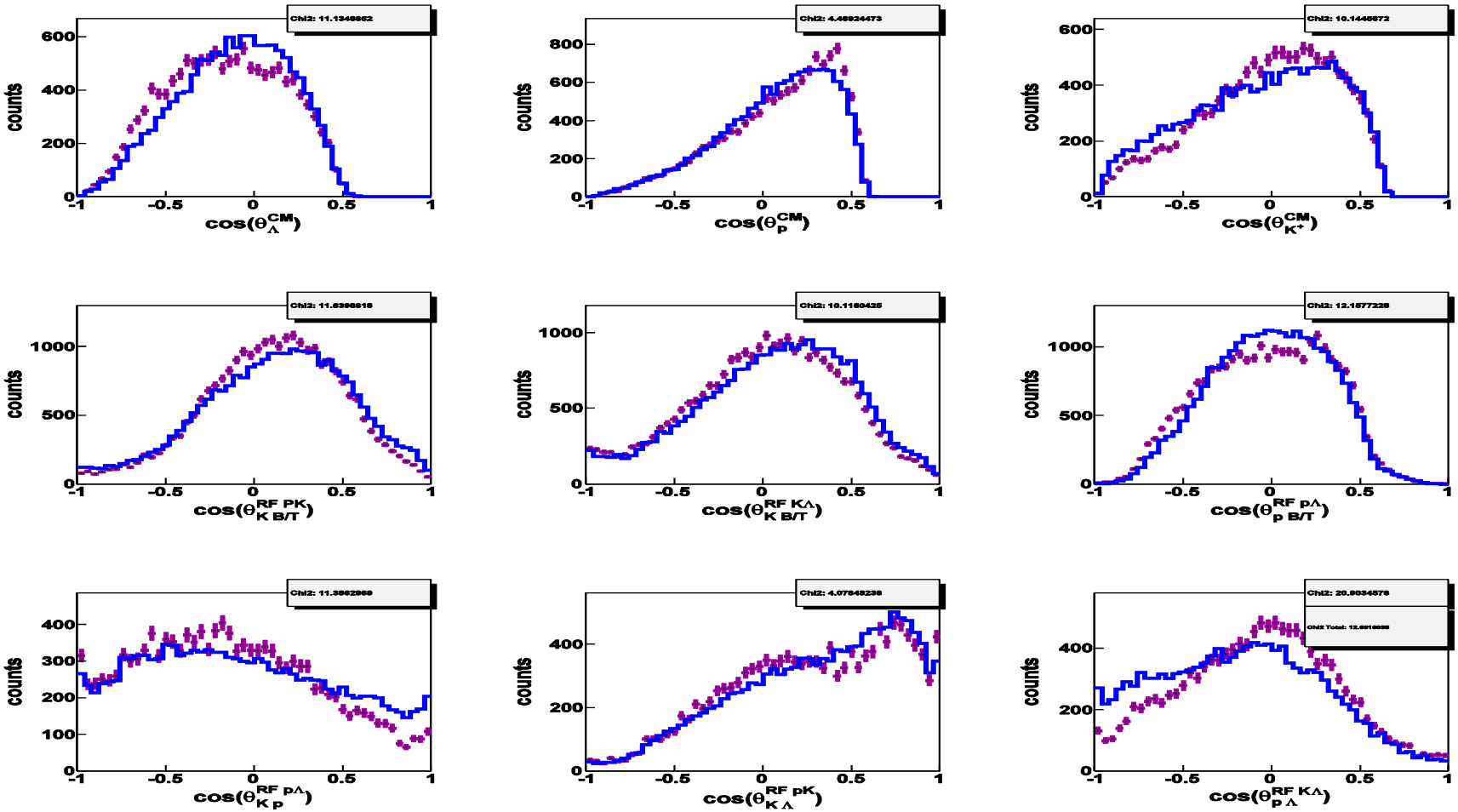

Results of 3_8_wo_int (100 iter)

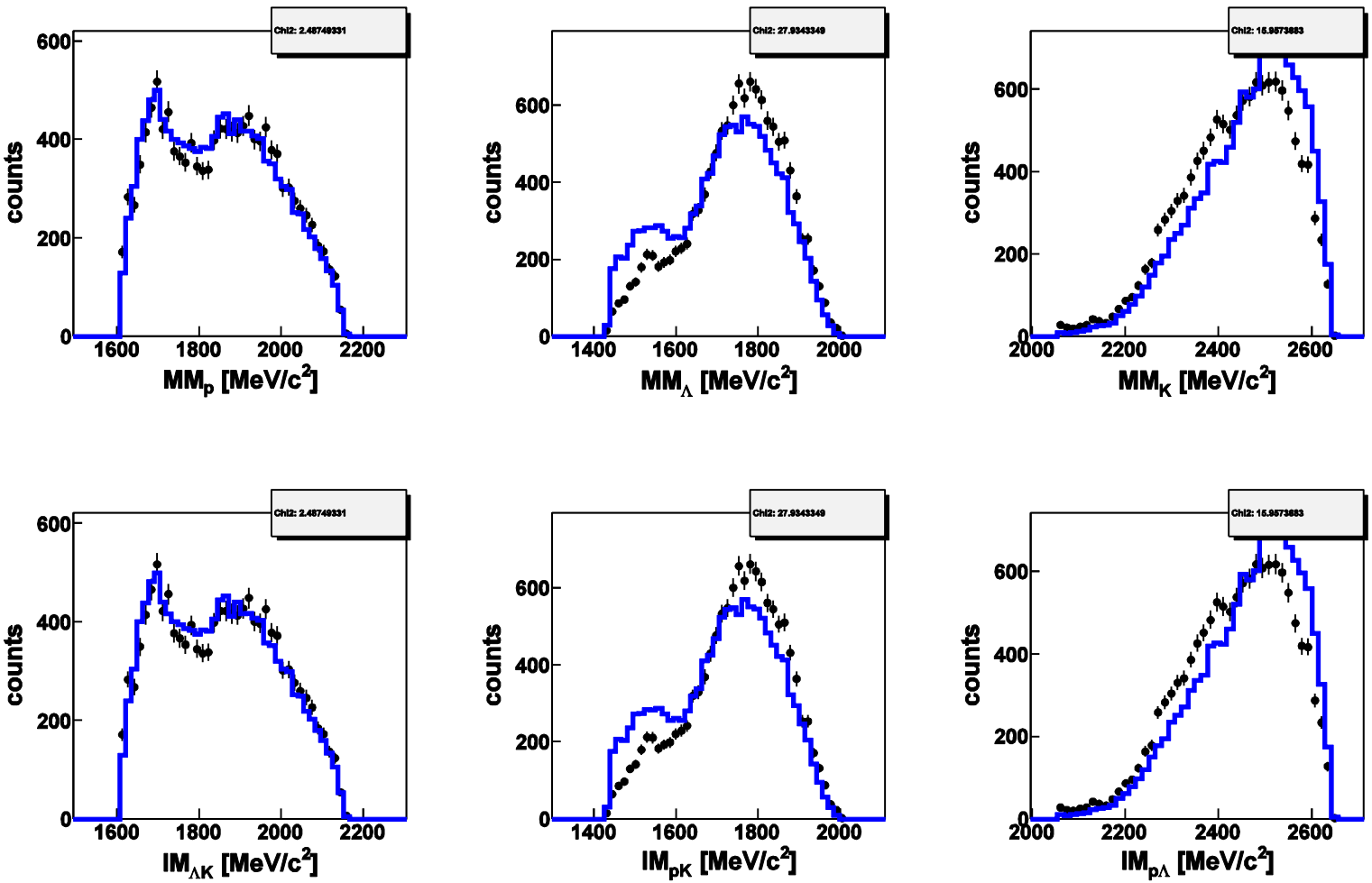

Results of 3_8_wo_int (100 iter)